European School of Molecular Medicine
Sede di Napoli

TELETHON INSTITUTE OF GENETICS AND MEDICINE

EUROPEAN SCHOOL OF MOLECULAR MEDICINE

SEDE DI NAPOLI

UNIVERSITA' DEGLI STUDI DI NAPOLI "FEDERICO II"

Ph.D. in Molecular Medicine – Ciclo IV/XXII

Curricula Human Genetics

A medaka model to study the the molecular basis of Microphthalmia with Linear Skin defects (MLS) syndrome

Tutor:
Prof. Brunella Franco

Internal Supervisor:
Prof. Sandro Banfi

External Supervisor:
Prof. Paola Bovolenta

Coordinator:
Prof. Francesco Salvatore

Ph.D. student:
Dr. Alessia Indrieri

Academic Year: 2009-2010

TABLE OF CONTENTS

LIST OF ABBREVIATIONS

AIF	Apoptosis-Inducing Factor
APAF1	Apoptotic Protease Activating Factor 1
BCL-2	B Cell Lymphoma 2
BCOR	BCL6 corepressor
BMP	Bone Morphogenetic Protein
CHX10	Ceh10 Homeodomain-contain homolog
CMZ	Ciliary Margin Zone
CNS	Central Nervous System
COX	Cytochrome c Oxidase
Cyt c	Cytochrome c
EGF	Epidermal Growth Factor
FADD	FAS-Associated Death Domain protein
FGF	Fibroblast Growth Factor
GCL	Ganglion Cell Layer
GFP	Green Fluorescent Protein
HCCS	holocytochrome c–type synthase
IHC	Immunohistochemistry
ILF	Leukemia Inhibitor Factor
IMS	Mitochondrial Intermembrane Space
INL	Inner Nuclear Layer
ISH	*In Situ* Hybridization
LHON	Leber Hereditary Optic Neuropathy
MAPK	Mitogen-Activated Protein Kinase
MEF	Mouse Embryonic Fibroblasts
MIDAS	Microphthalmia, Dermal Aplasia and Sclerocornea
MITF	Microphtalmia transcriptor-associated factor
MLS	Microphtalmia with Linear Skin lesion
MO	Morpholinos
MOMP	Mitochondrial Outer Membrane Permeabilization
NR	Neural Retina
OFCD	Oculofaciocardiodental
OMIM	On-line Mendelian Inheritance in Man
ONL	Outer Nuclear Layer

OTX2	Orthodenticle homeobox 2
OXPHOS	Oxidative Phosphorylation
pHH3	Phosphorylated Histone-H3
PI	Propidium Iodide
RFP	RedFluorescent Protein
RhoGAP	Rho GTPase–Activating Protein
ROS	Reactive Oxygen Species
RPE	Retinal Pigment Epithelium
TEM	Transmission electron microscopy
TGF	Transforming Growth Factor
TNF	Tumor Necrosis Factor
TRAIL	TNF-Related Apoptosis Inducing Ligand
TRX	thioredoxin
TUNEL	deoxynucleotidyl transferase-mediated dUTP nick-end labeling
VDAC	outer mitochondrial membrane channel
XIAP	X-linked Inhibitor of Apoptosis Protein
Δψm	inner mitochondrial membrane potential

TABLE OF FIGURES

ABSTRACT

The Microphthalmia with linear skin defects (MLS) syndrome is an X- linked dominant male-lethal neuro-developmental disorder associated to mutations in the holocytochrome c-type synthetase (HCCS) transcript. Female patients display unilateral or bilateral microphthalmia and linear skin defects, additional features include central nervous system (CNS) malformation and mental retardation. *HCCS* codifies a mitochondrial protein that catalyzes the attachment of heme to both apocytochrome c and c1, necessary for proper functioning of the mitochondrial respiratory chain. Although mutation analysis clearly indicates a role for HCCS in the pathogenesis of this genetic condition, the molecular mechanisms underlying the developmental anomalies in the presence of HCCS dysfunction are still unknown. Previous studies demonstrated the early lethality of mouse embryonic Hccs knock-out stem cells. To overcome the problem of the possible embryonic lethality, we decided to generate an animal model for MLS syndrome in the medaka fish (Oryzia latipes) using a morpholino-based technology. Fish models (zebrafish and medaka) are considered good models to study developmental biology processes and in particular eye developmental defects.

Three specific morpholinos directed against different portions of the ol*hccs* transcript have been designed and injected and our data indicated that all morpholinos effectively downregulate the expression of the ol*hccs* gene. The injection of the three different morpholinos resulted in a pathological phenotype, which resembles the human condition. Morphants displayed microphthalmia, coloboma, and microcephaly associated to a severe cardiac pathology. To date, this is the only animal model that recapitulates the phenotype observed in MLS syndrome. Analysis with markers for specific retinal cell types showed defects in

differentiation of the ventral neural retina. Characterization of morphants revealed that *hccs* down-regulation results in impairment of mitochondrial functions, overproduction of reactive oxygen species (ROS) and a strong increase of apoptosis mediated by activation of the mitochondrial-dependent cell death pathway in the CNS and in the eyes. Our results clearly indicate that HCCS plays a critical role in mitochondria and imply that MLS should be considered a mitochondrial disease.

It is well established that the intrinsic mitochondrial dependent apoptotic pathway rely on the formation of apoptosomes, which require the presence and/or the activity of cytochrome c, Apaf1, and caspase 9. Detailed studies of the mechanisms that underlie intrinsic apoptosis have shown that the heme group of cytochrome c is necessary for Apaf1 activation, apoptosome formation and activation of caspase 9. Interestingly, our data indicate that, in our model, the mitochondrial dependent apoptosis is triggered by caspase 9 activation and occur in a Bcl-dependent but apoptosome-independent manner suggesting that at least in some tissues the apoptosis can occur in a non-canonical way. Our data support the evidence of an apoptosome-indipendent activation of caspase 9 and suggest the possibility that this event might be tissue specific. Our study shed new light into the functional role of HCCS in the mitochondria. In addition, we provide strong evidences that mitochondrial mediated apoptotic events underlie microphtalmia providing new insights into the mechanisms of this developmental defect.

1. INTRODUCTION

1.1 The vertebrate eye development.

The eye is a bilateral organ that originates from a single field positioned in the anterior portion of the neural plate. This undifferentiated primordium reaches its final complexity through a series of inductive and morphogenetic events that are coordinated by specific genetic programs, which, by enlarge, are conserved among different vertebrate species. A schematic representation of the main events underlying a correct development of the eye is depicted in Figure 1.

The basic components of the complex optic system are derived from four embryonic sources: forebrain neuroectoderm, intercalating mesoderm, surface ectoderm, and neural crest. The neuroectoderm differentiates into the retina, iris, and optic nerve; the surface ectoderm gives rise to lens and corneal epithelium; the mesoderm differentiates into the extraocular muscles and the fibrous and vascular coats of the eye; and neural crest cells become the corneal stroma sclera and corneal endothelium.. During neurulation, eye progenitor cells converge medially and are surrounded rostrally and laterally by telencephalic precursors and caudally and medially by cells that will form the diencephalon. The first morphological sign of eye development in vertebrates is the bilateral evagination of anterior diencephalon in the early neurula after the formation and differentiation of the neural tube. In mammals, this is marked by the appearance of the optic pit, whereas in fish and amphibians a bulging of the optic primordia is observed (Chow and Lang, 2001). Continued evagination of the optic primordial leads to the formation of the optic vesicles connected to the diencephalon by a small canal, the optic stalk (Figure 1 A). These extend towards the overlying, non-neural surface ectoderm that will ultimately give rise to the lens and cornea. Mesenchyme between the optic vesicle and the surface ectoderm (apparent in mammals and chick) is displaced as the two tissues come into close physical contact (Figure 1

B). This is a critical period in eye development during which inductive signals between the optic vesicle and the surface ectoderm are thought to exchange. At this stage, the presumptive lens also shows the first morphological signs of development. This is characterized by formation of the lens placode, a thickening of the surface ectoderm that comes into contact with the optic vesicle (Chow and Lang, 2001). Molecularly, lens placode formation coincides with the onset of crystalline expression. These protein families are expressed at high levels in a lens preferential manner and are required for generating and maintaining lens transparency (Cvekl and Piatigorsky, 1996; Graw, 1996; Wistow and Piatigorsky, 1988; Wride, 1996).

Coordinated invagination of the lens placode and the optic vesicle results in the formation of the lens vesicle and a double-layered optic cup and provides the first indication of the final shape of the eye (Figure 1 C). The inner layer of the optic cup (facing the lens) forms the neural retina (NR), while the outer layer of the optic cup gives rise to the retinal pigment epithelium (RPE) which will be formed of a single layer of cells containing melanin (Figure 1 D).

At the ventral extremity of the optic vesicle, the process of invagination forms a groove that runs continuously from the ventral-most region of the NR and along the ventral aspect of the optic stalk to the junction with the neural tube.

The point at which the laterally growing edges of the optic cup fuse is known as the choroidal (or optic) fissure. This structure provides a channel for blood vessels within the eye and an exit route for projecting axons. Normally, the optic fissure closes during development: its failure to close leads to a pathological condition called coloboma.

Development of the cornea from the surface ectoderm overlying the lens and from migrating neural crest–derived mesenchyme, is a highly coordinated multistep process. Briefly, it first involves the secretion of a collagen-rich extracellular matrix

by the corneal epithelium (ectoderm overlying the lens). This primary stroma attracts a wave of neural crest–derived mesenchymal cells from the region surrounding the eye that coincides with its hydration and the migration of a second wave of neural crest–derived mesenchymal cells. Eventually, an increased level of thyroxine triggers the dehydration and compaction of the posterior stroma that ultimately leads to the formation of the mature, transparent cornea (Chow and Lang, 2001).

The remaining parts of the adult eye, such as the ciliary body and iris are derived from the distal tip of the optic cup at the point where the inner and outer optic cup layers meet (Beebe, 1986) (Figure 1 C).

In vertebrates, the cells that compose the optic vesicle neuroepithelium are initially morphologically and molecularly indistinguishable and therefore are all potentially competent to originate the different retinal cells type, the optic stalk or the RPE. They reach their final complexity through a series of inductive and morphogenetic events. Information, in the form of signaling molecules, derived from the surrounding tissues and the neuroepithelium itself, modulate and restrict the expression of different transcription factors and can drive the differentiation towards a specific cell type (Figure 2). For example extracellular signals, derived from the surface ectoderm in contact with the prospective NR or from the periocular mesenchyme surrounding the presumptive RPE, pattern the distal optic vesicle. The surface ectoderm secretes high levels of two members of Fibroblast Growth Factor (FGF) signaling molecules family, FGF1 and FGF2, (Nguyen and Arnheiter, 2000) while members of the Transforming Growth Factor-β (TGF-β) signaling molecules superfamily, such as activins or the related Bone Morphogenetic Proteins (Bmp) - Bmp4 and Bmp7 - are expressed in the surrounding mesenchyme and/or the presumptive RPE itself (Fuhrmann et al., 2000). FGF and TGF-β/BMP signaling act antagonistically on the specification of

RPE and NR precursors. The first activates NR specification but inhibits RPE formation by activation of the mitogen-activated protein kinase (MAPK) cascade which, in turn, promote the expression of Ceh10 homeodomain-contain homolog (*Chx10*), the best candidate to impose a NR character to the native optic vesicle cells, and reduce the expression of Orthodenticle homeobox 2 (*Otx2*) and Microphtalmia transcriptor-associated factor (*MITF*), transcription factors crucial for the RPE identity. In contrast the induction of TGFβ/BMP signaling by extraocular mesenchyme is essential for the activation of the RPE molecular markers such as *MITF*, and has an inhibitory effect on the *Chx10*.

At the end of the differentiation process, in the adult vertebrate NR there are six types of neurons and one type of glial cells (Müller glial cells), which constitute three cellular layers: rod and cone photoreceptors in the outer nuclear layer (ONL), horizontal, bipolar, and amacrine interneurons and Müller glial cells in the inner nuclear layer (INL), and ganglion and displaced amacrine cells in the ganglion cell layer (GCL) (Figure 3 A). These seven types of cells are differentiated from common progenitors in a temporal order widely conserved during evolution from fish to mammals: ganglion cells first, followed by horizontal cells, cones and amacrine cells, and rods and bipolar cells and Müller glial cells last (Belecky-Adams et al., 1996; Carter-Dawson and LaVail, 1979; Cepko et al., 1996; Hu and Easter, 1999; La Vail et al., 1991; Stiemke and Hollyfield, 1995; Young, 1985) (Figure 3 B). Although there is an exact temporal order, the differentiation stage of each cell type is in part contemporaneous with the differentiation stage of the preceding cell type (Figure 3 B). Thus, retinal development consists of three successive processes: (i) proliferation of progenitors, (ii) neurogenesis, and (iii) gliogenesis. According to the model of "competence", the different retinal cell types derived from a single common progenitor which change competency over time under the control of extrinsic (such as neurotrophic factors) and intrinsic

regulators (such as transcription factors) (Austin et al., 1995; Belliveau and Cepko, 1999; Belliveau et al., 2000; Harris, 1997; Holt et al., 1988; Livesey and Cepko, 2001; Marquardt and Gruss, 2002; Turner and Cepko, 1987; Turner et al., 1990). Thus, in this model progenitors pass through intrinsically determined competence states, during which they are capable of giving rise to a limited subset of cell types under the influence of extrinsic signals (Altshuler et al., 1993; Ezzeddine et al., 1997; Furukawa et al., 2000; Guillemot and Cepko, 1992; Kelley et al., 1994; Zhang and Yang, 2001). TGF, EGF (epidermal growth factor) and ILF (leukemia inhibitor factor) are just some examples of extrinsic factors that can stimulate the production of specific retinal cells types, while leading to suppression of other (Lillien and Wancio, 1998).

Indeed genes coding for transcription factors of the family b-helix-loop-helix, as *Ath5*, *mash1*, *NeuroD*, or genes containing a homeodomain such as *Otx2*, *Chx10*, *Pax6*, *Six3* and *Crx* work as intrinsic regulators (Bramblett et al., 2004; Brown et al., 2001; Burmeister et al., 1996; Dyer et al., 2003; Inoue et al., 2002; Li et al., 2004; Marquardt et al., 2001; Mathers et al., 1997; Morrow et al., 1999; Satow et al., 2001; Tomita et al., 2000). These genes are important both for differentiation and maintenance of retinal cell types; in fact many of them are expressed at high levels in specific cellular regions also when the retina is completely differentiated. In contrast, genes involved in proliferation as *c-myc* and *cyclin D1* are expressed in a small number of retinal progenitor cells that remain proliferating in the ciliary margin zone (CMZ). Thus the development of the eye is an highly complex process, and the sequential and coordinated expression of other numerous genes encoding for transcription factors, cofactors, signal transduction molecules, membrane receptors and others, more or less well characterized, play a key role in different stages of eye development and may be responsible for different eye malformations.

1.2 Microphthalmia and anophtalmia: an overview

Eye diseases represent one of the most common groups of genetic disorders in the human population. Over 200 different forms of ocular heritable disorders have been described and it has been estimated that about 27% of the phenotypes described in OMIM (On-line Mendelian Inheritance in Man) affect the eye.

Congenital anophthalmia and microphthalmia are rare defects of the globe resulting from abnormalities in the development of the primary optic vesicle.

Anophthalmia and microphthalmia describe, respectively, the absence of an eye and the presence of a small eye within the orbit. The term anophthalmia is used where there is no visible ocular remnant. However, ultrasound often reveals a buried microphthalmic remnant or cyst. Microphthalmia refers to an eye with reduced volume and is usually defined in terms of corneal diameter and axial length. It may be associated with other eye developmental anomalies including lens and optic nerve abnormalities, orbital cyst and coloboma, which is a more regional eye defect that is caused by defective closure of the embryonic fissure of the optic cup.

The birth prevalence of anophthalmia and microphthalmia has been generally estimated to be 3 and 14 per 100,000 population respectively, although other evidence puts the combined birth prevalence of these malformations at up to 30 per 100,000 population with microphthalmia reported in up to 11% of blind children (Adapted from Morrison et al., 2002; Shaw et al., 2005). High-resolution cranial imaging, post-mortem examination and genetic studies suggest that these conditions represent a phenotypic continuum.

Both anophthalmia and microphthalmia may be unilateral or bilateral and may occur as an isolated clinical sign or as part of a syndrome (in one-third of cases).

Epidemiological studies have predicted both environmental and heritable factors in causing these defects, in fact anophthalmia/microphthalmia have complex aetiology with chromosomal, monogenic and environmental causes identified. Environmental factors playing a contributory role include gestational-acquired infections, maternal vitamin A deficiency, exposure to X-rays, solvent misuse and thalidomide exposure (Verma and Fitzpatrick, 2007). However, evidences for the role of environmental causes are both more circumstantial and accounts for a smaller proportion of cases compared to heritable factors.

Genetic eye disease can be broadly divided into two main categories, degenerative disorders and developmental anomalies. While for the degenerative diseases, molecular genetics studies have been able, in recent years, to shed light on the molecular basis of a significant number of cases (Farrar et al., 2002), the pathogenetic causes of eye developmental anomalies remain very elusive in the majority of conditions. This is particularly true for the anophthalmia/microphthalmia, with the exception of a few instances where chromosomal duplications, deletions and translocations and monogenic mutations have been implicated and are typically associated with characteristic syndromes.

In the majority of known cases these defects are likely to be caused by disturbances of the morphogenetic pathway that controls eye development. Genetic studies demonstrated that mutations in several genes principally involved in ocular development often cause eye malformations such as anophthalmia and microphthalmia and mutations in these transcripts are associated to specific syndromes including eye developmental defects (Table 1).

For example *SOX2*, regulator of retinal neural progenitor competence (Taranova et al., 2006), has to date been identified as a major causative gene for anophthalmia/microphthalmia. Cytogenetic studies placed the locus at 3q26.3, and de novo heterozygous loss-of-function point mutations in this transcript have been

Name of Gene (Inheritance)	*Name of syndrome*	*Ocular manifestations*	*Systemic manifestations*
SOX2 3q26.3-q27 (AD)	SOX2 anophthalmia syndrome, some cases of AEG	Anophthalmia, microphthalmia, dystrophy	Hypothalamic – pituitary abnormalities, growth failure, genital tract malformation, developmental delay, seizures, oesophageal atresia
OTX2 14q21-14q22 (AD)		Anophthalmia, microphthalmia, coloboma, microcornea, cataract, retinal dystrophy, optic nerve hypoplasia	Agenesis of the corpus callosum, developmental delay
PAX2 10q24.3-q25 (AD)	Renal-coloboma or Papillorenal syndrome	Coloboma, microphthalmia	Renal hypoplasia
PAX6 11p13 (AD)		Aniridia, Peters' anomaly, foveal hypoplasia, keratopathy	Abnormalities of pituitary, pancreatic, and brain development
CHD7 8q12.1 (AD)	CHARGE syndrome	Microphthalmia, coloboma	Heart defects, choanal atresia, retarded growth and development, genital hypoplasia, ear anomalies, and deafness
PTCH 9q22.3 (AD)	Basal cell naevus /Gorlin's syndrome	Microphthalmia, coloboma, cyst	Palmer pits, medulloblastoma basal cell carcinoma
SHH 7q36 (AD)	Holoprosencephaly-3 (HPE3)	Cyclopia, coloboma, hypotelorism	Preaxial polydactyly, cleft lip and palate
CHX10 14q24.3 (AR)		Anophthalmia, microphthalmia, coloboma, cataract, iris abnormalities	
FOXC1 6p25 (AD)	Axenfeld–Rieger syndrome	Iris hypoplasia, iridogoniodysgenesis, glaucoma	Dental abnormalities, midface abnormalities
HCCS Xp22 (X-linked)	Microphthalmia with linear skin defects	Microphthalmia, sclerocornea	Linear skin defects, agenesis of corpus callosum
BRIP1 17q22 (AD)	Fanconi anaemia	Microphthalmia	Bone marrow failure, breast cancer, growth retardation, hearing loss, thumb and kidney abnormalities
DPD 1p22 (AR)		Microphthalmia, coloboma, nystagmus	Epilepsy, mental retardation, motor retardation
SIX3 2p21 (AD)	Holoprosencephaly 2	Cyclopia, Microphthalmia, coloboma	hypotelorism, microcephaly, craniofacial anormalities
SIX6 14q23 (AD)		Microphthalmia, cataract, nystagmus	Pituitary abnormalities
PITX2 4p25 (AD)	Rieger syndrome	Iris hypoplasia, iridogoniodysgenesi, glaucoma	Maxillary hypoplasia, dental abnormalities, excess periumbilical skin
POMT1 9q34.1 (AR)	Walker-Warburg syndrome	Microphthalmia, cataract, retinal dysplasia and detachment, coloboma, optic nerve hypoplasia	Developmental delay, muscular dystrophy, hydrocephalus, agyria, epilepsy
BCOR Xq27-q28 (X-linked)	Oculofaciocardiodental syndrome	Microphthalmia, congenital cataract	Mental retardation, heart defects, dental and facial abnormalities
RX 18q21.3 (AD)		Anophthalmia, microphthalmia, sclerocornea	
FRAS1 4q21 (AR)	Fraser Syndrome	Microphthalmia, cryptophthalmos	Genital and kidney abnormalities, finger webbing
FREM2 13q13.3 (AR)	Fraser Syndrome	Microphthalmia, cryptophthalmos	Genital and kidney abnormalities, finger webbing
HESX1 3p21.2-p21.1 (AD)	Septo-optic dysplasia	Optic nerve hypoplasia	Agenesis of the corpus callosum, panhypopituitarism, and absent septum pellucidum
MAF 16q22-q23 (AD)		Cataract, anterior segment dysgenesis, coloboma	Nephritic syndrome
RAB3GAP 2q21.3 (AR)	Warburg Micro Syndrome	Microphthalmia, microcornea, optic atrophy, cataract	Microcephaly, mental retardation, hypoplasia of corpus callosum,

Table 1. Selected genes and syndromes associated with eye malformations. (Adapted from Ragge et al., 2007)

shown to account for 10–20% of severe bilateral anophthalmia/microphthalmia (Morrison et al., 2002; Shaw et al., 2005), the most common phenotype being bilateral anophthalmia.

PAX6, on chromosome 11p13, has been studied more extensively than most other eye genes. In humans, heterozygous loss-of-function mutations typically produce aniridia (OMIM 106210), a congenital pan-ocular malformation associated with severe visual impairment; however *PAX6* was also the first gene implicated in human anophthalmia (Glaser et al., 1994). Although *PAX6* mutations are an extremely rare cause of anophthalmia, there has recently been interest in a possible co-operative role between *PAX6* and *SOX2*. It has been shown that *PAX6* and *SOX2* co-bind to a regulatory element driving lens induction in the chick (Kondoh et al., 2004), which suggests that lens induction failure could be responsible for microphthalmia in patients with mutations in these genes (Fitzpatrick and van Heyningen, 2005). As expected with genes expressed in the developing brain, patients with inherited *PAX6* and *SOX2* mutations exhibit CNS malformations in addition to dominantly inherited anophthalmia/microphthalmia (Fitzpatrick and van Heyningen, 2005; Sisodiya et al., 2006).

Mutations in three genes with retinal expression are associated with anophthalmia/microphthalmia, possibly through failure of retinal differentiation. Heterozygous loss-of-function mutations of *OTX2* (on chromosome 14q22, autosomal dominant inheritance) have been shown to be associated with a wide range of ocular disorders from anophthalmia and microphthalmia to retinal defects. CNS malformations and mental retardation are common in patients with *OTX2* mutations (Ragge et al., 2005). *RAX*, located on chromosome 18q21.32, is linked to about 2% of inherited anophthalmia/microphthalmia (Voronina et al., 2004). Similarly, *CHX10* mutations (chromosome 14q24.3) account for about 2% of isolated microphthalmia (Ferda Percin et al., 2000).

The *SIX3* gene is responsible for several cases of holoprosencephaly but in one patient it has been associated to microphtalmia and coloboma without other classical signs of holoprosencephaly (Wallis et al., 1999). Mutations in the *PAX2* gene, playing an important role in the morphogenesis of the ventral developing eye (Torres et al., 1996), are responsible for the renal-coloboma syndrome, which is also characterized by optic nerve coloboma (Sanyanusin et al., 1995).

Unlike the previous, which are all transcription factors principally involved in ocular development, mutations in gene that are not directly correlated to eye development, such as *RAB3GAP* and *BCOR,* it has been also described. The first, involved in the Warburg Micro Syndrome, encoding for a protein involved in the GTPase signal transduction and regulates neurotransmitter release and synaptic plasticity (Sakane et al., 2006). *BCOR* (BCL6 corepressor) encoding for a protein ubiquitously expressed in human tissues and mutation in its transcript are responsible for oculofaciocardiodental syndrome (OFCD) and Lenz microphthalmia (Ng et al., 2004). The protein encoded by this gene was identified as an interacting corepressor of BCL6, a POZ/zinc finger transcription repressor that is required for germinal center formation and may influence apoptosis (Gearhart et al., 2006).

However, it must be emphasized that eye developmental anomalies, and anophthalmia/microphthalmia in particular, seem to be a very heterogeneous group of disorders with many different genes involved, as suggested by the limited number of mutations so far identified in the patients analyzed.

Numerous genes encoding for transcription factors, cofactors, signal transduction molecules, membrane receptors and others, more or less well characterized, play a key role in different stages of eye development and may be responsible for different eye malformations.

Genetic counselling can be challenging due to the extensive range of genes responsible and wide variation in phenotypic expression. Appropriate counselling is indicated if the mode of inheritance can be identified. Differential diagnoses include cryptophthalmos, cyclopia and synophthalmia, and congenital cystic eye. Patients are often managed within multidisciplinary teams consisting of ophthalmologists, pediatricians and/or clinical geneticists, especially for syndromic cases. Treatment is directed towards maximizing existing vision and improving cosmesis through simultaneous stimulation of both soft tissue and bony orbital growth. Mild to moderate microphthalmia is managed conservatively with conformers. Severe microphthalmia and anophthalmia rely upon additional remodeling strategies of endo-orbital volume replacement (with implants, expanders and dermis-fat grafts) and soft tissue reconstruction. The potential for visual development in microphthalmic patients is dependent upon retinal development and other ocular characteristics.

The aetiology of anophthalmia/microphthalmia underlies the entire developmental biology of ocular formation and remains a field where our knowledge is increasing exponentially. Despite the progresses made, much work is still needed to understand the processes underlying these complex diseases, which are a significant cause of childhood blindness. Even if these processes are elucidated in the future, novel therapeutic approaches to prevent these conditions from occurring could still be precluded by very early ocular development in the fetus.

1.3 The molecular basis of microphtalmia with linear skin lesion (MLS) syndrome

Among the genetic forms of anophthalmia/microphthalmia, Microphthalmia with linear skin lesions syndrome (MLS, OMIM 309801), first described in the 1990 (al-

Gazali et al., 1990), represents one of the most puzzling genetic disorder. The MLS syndrome, also known as MIDAS (microphthalmia, dermal aplasia and sclerocornea), is a rare X-linked dominant condition characterized by unilateral or bilateral microphthalmia and linear skin defects, which are limited to the face and neck, consisting of areas of aplastic skin which heal with age to form hyperpigmented areas, in affected females and in utero lethality for males. Other ocular abnormalities are variable and can include: sclerocornea; orbital cysts; microcornea; eyelid fissures; corneal leukoma; iridocorneal adhesion (Peters anomaly); congenital glaucoma with total/peripheral anterior synechiae; aniridia; cataracts; a remnant of the anterior hyaloid artery; vitreous opacity; and hypopigmented areas of the retinal pigment epithelium (Cape et al., 2004; Kobayashi et al., 1998; Wimplinger et al., 2006). In Figure 4 and Table 2 are depicted and described some of the most typical clinical signs observed in this genetic condition.

Moreover additional features in female patients include central nervous system anomalies (such as agenesis of corpus callosum, ventriculomegaly, microcephaly reported in about 40% of affected individuals), mental retardation (in about 25% of affected individuals) and congenital heart defects (arrhythmias, septum defects, cardiomyopathy) (al-Gazali et al., 1990; Happle et al., 1993; Lindsay et al., 1994; Sharma et al., 2008; Temple et al., 1990; Van den Veyver, 2002; Zvulunov et al., 1998).

In the majority of cases, patients carry deletions or unbalanced translocations involving the Xp22.3 region resulting in segmental monosomy of this chromosome (Morleo et al., 2005). With the exception of eight males that show a 46 XX karyotype and an translocation Xp,Yp (that causes Xp monosomy in one of two X chromosomes) (Kapur et al., 2008; Morleo et al., 2005), MLS patients are all females.

Clinical feature	Occurrence (%)
Cutaneous	
Linear skin defects	92
Nail dystrophy	13
Ear pit	5
Ocular	
Microphthalmia	89
Corneal clouding/opacities	35
Sclerocornea	33
Cataracts	8
Hypopigmentation of the RPE	5
Developmental	
Short stature	74
Developmental delay	37
CNS	
Agenesis of the corpus callosum, Ventriculomegaly, Microcephaly	40
Mental retardation	25
Seizures	3
Cardiac	
Supraventricular tachycardia	13
Atrial/ventricular septal defects	13
Hypertrophic cardiomyopathy	5
Bradycardia	5
A–V block	5

Table 2. Clinical Features Reported in MLS Syndrome (Adapted from Sharma et al., 2008)

An high degree of intra- as well as inter-familial clinical variability has been observed in this condition possibly related to the role of X-inactivation (Franco and Ballabio, 2006; Morleo and Franco, 2008; Van den Veyver, 2001). In fact the manifestations vary among affected individuals and, although most of them display the classic phenotype of MLS syndrome, many have only a subset of characteristic features: some show the characteristic skin defects without ocular abnormalities, whereas others have eye abnormalities without skin defects (Morleo and Franco, 2008). No genotype-phenotype correlations have been observed since the high phenotypic variability is not correlated to the extent of Xp-terminal deletion. An example is a female with a normal phenotype except for typical MLS

syndrome skin defects (Figure 4 C) who had an affected female fetus with anencephaly. Cytogenetic analysis revealed that both mother and fetus had the same Xp22 deletion that was one of the largest Xp deletions described for MLS syndrome (Lindsay et al., 1994).

Skewed X inactivation has been detected in 16 out of the 17 MLS patients analyzed to date (Cain et al., 2007; Ogata et al., 1998; Schluth et al., 2007; Wimplinger et al., 2006; Wimplinger et al., 2007). It has been proposed that the most severe MLS syndrome clinical manifestations are observed in females whose normal X chromosome is inactivated in the affected tissue or at a specific time of embryonic development; conversely, a milder phenotype or the total absence of MLS syndrome clinical manifestations may result from totally skewed X-chromosome inactivation that forces preferential activation of the unaffected X, not only in blood cells, but also in tissues such as the eye and skin (Morleo and Franco, 2008).

The “MLS minimal critical region”, spanning approximately 610 Kb in Xp22.2 region, has been first defined through a combination of cytogenetic analysis and breakpoint mapping on somatic cell hybrids from ten MLS patients with deletions and translocations involving the Xp22 region (Wapenaar et al., 1993; Wapenaar et al., 1994). Three genes are located in the critical interval, including *MID1*, *HCCS*, and *ARHGAP67*. *MID1* is mutated in Opitz G/BBB syndrome (Quaderi et al., 1997; Schaefer et al., 1997); *ARHGAP6* gene codes for a Rho GTPase–activating protein (Rho GAP) that functions as a GAP for the small GTPase RhoA, as well as a protein implicated in reorganization of the actin cytoskeleton (Prakash et al., 2000; Schaefer et al., 1997); *HCCS* encodes a mitochondrial holocytochrome c–type synthase, also known as “heme lyase”, that catalyzes the covalent attachment of heme to both apocytochrome c and c1 (Bernard et al., 2003; Schwarz and Cox, 2002). In the 2002 Prakash and colleagues showed that *in vivo*

generated deletions involving the equivalent critical MLS region in the mouse (MLSΔ), encompassing *Hccs* as well as parts of *Mid1* and *Arhgap6*, lead to lethality of hemizygous, homozygous, and heterozygous embryos early in development. This lethality can be rescued by overexpression of the human *HCCS* gene from a BAC clone, providing the proof that lethality is indeed due to loss of *HCCS* (Prakash et al., 2002) and defining *HCCS* as the most convincing candidate gene for these disease.

After more than 10 years of effort, in 2006, the conclusive evidence that *HCCS* is the gene responsible for MLS syndrome have been found: the group of Prof. Brunella Franco, at the TIGEM of Naples, in collaboration with the group of Prof. Kerstin Kutsche (Hamburg University) identified loss-of-function mutations associated with the MLS phenotype. More in detail, de novo heterozygous point mutations, a missense (p.R217C) and a nonsense mutation (p.R197X), respectively, were identified in *HCCS* in two patients with MLS and a normal karyotype. Functional analysis demonstrate that both mutant proteins (R217C and Δ197-268) were not able to complement a *Saccharomyces cerevisiae* mutant deficient for the *HCCS* orthologue *Cyc3p,* in contrast to *HCCS* wild type (Figure 5). Moreover, ectopically expressed *HCCS* wild type and the R217C mutant protein are targeted to mitochondria in CHO-K1 cells, while the C-terminal truncated Δ197-268 mutant failed to be sorted to mitochondria (Figure 6). In addition, characterization of a familial case revealed the presence of an 8.6-kb deletion comprising *HCCS* exons 1 and 2, the first 83 bp of exon 3, the 5' untranslated exons 1a and 1b of *MID1*, as well as the respective intronic sequences. These results provided strong evidence for the involvement of the holocytochrome c-type synthase in the pathogenesis of this disorder (Wimplinger et al., 2006). In the 2007 a novel missense mutation (p.E159K) has been identified; it leads to loss-of-function of the encoded holocytochrome c-type synthase, in a sporadic female

patient with microphthalmia of both eyes and bilateral sclerocornea without skin lesions, confirming that the phenotypic variability described in MLS cases is not correlated to the extent of Xp-terminal deletion or to the presence or nature of the *HCCS* mutations.

1.4 HCCS and its role in mitochondrial functioning

HCCS encodes a mitochondrial holocytochrome c–type synthase, also known as "heme lyase," composed of 268 aa (Bernard et al., 2003; Schwarz and Cox, 2002) and located on the outer surface of the inner mitochondrial membrane (Schaefer et al., 1996). It is ubiquitously expressed with the strongest expression observed in heart and skeletal muscle (Schaefer et al., 1996; Van den Veyver et al., 1998).

HCCS catalyzes the covalent attachment of heme to both apocytochrome c and c1, the precursor forms, thereby leading to the mature forms, holocytochrome c and c1, which are necessary for proper functioning of the mitochondrial respiratory chain (Bernard et al., 2003; Moraes et al., 2004). In addition to the well-known role of cytochrome c in oxidative phosphorylation (OXPHOS), it is released from mitochondria in response to a variety of intrinsic death-promoting stimuli, which in turn result in caspase-dependent cell death (Jiang X et al., 2004).

In *S. cerevisiae*, two heme lyases exist, the cytochrome c- (Cyc3p) and the cytochrome c1- specific heme lyase (Cyt2p), whereas only a single heme lyase is required for maturation of both cytochrome c and c1 in higher eukaryotes (Bernard et al., 2003; Schaefer et al., 1996). They are located on the outer surface of the inner mitochondrial membrane and defects in either of the yeast heme lyases result in loss of respiratory growth of the respective strain (Dumont et al., 1987).

Cyt2p and Cyc3p proteins have been extensively studied and well characterized, especially together with cytochrome c and its secondary involvement in

programmed cell death (Li et al., 2000; Liu et al., 1996).

HCCS is the first mammalian holocytochrome c-type synthetases to be described in the literature and it is homologous to the class of heme lyase identified first in organisms such *S. cerevisiae*, *N. crassa* and *C. elegans* (Drygas et al., 1989; Dumont et al., 1987; Zollner et al., 1992).

The protein encoded by the human gene identified by Schaefer and colleagues (Schaefer et al., 1996) showed a 35% of identity with the Cyt2p and Cyc3p protein sequences and seems to be the only example in higher eukaryotes. The amino acid sequences of human and murine proteins shows 85% of identity and identical length. Through complementation studies with both CYC3- and CYT2-deficient yeast strains, Cox T. and colleagues demonstrated specific and complete rescue of *CYC3*$^{-}$ growth-deficient phenotype supporting the conclusion that the human protein possesses HCCS activity (Schwarz and Cox, 2002).

The *HCCS* gene covers a genomic segment of 11 kb and is ubiquitously expressed (brain, placenta, kidney, lung, pancreas) with higher levels in heart and skeletal muscle (Schaefer et al., 1996; Van den Veyver et al., 1998). Moreover by RT-PCR analysis, Schwarz and colleagues also detected an abundant *Hccs* expression in adult and fetal mouse eye (Schwarz and Cox, 2002). This data were confirmed by *in situ* hybridization analysis (ISH) on mouse embryos performed in the laboratory of Prof. Brunella Franco (unpublished data) (Figure 7). At E11.5, E13.5 and E18.5 a specific signal in the eyes and in the encephalon is detected.

The absence or insufficiency of the human HCCS enzyme activity could give rise to a nuclear-encoded respiratory chain defect with complications reminiscent of the mitochondrial myopathies (pathologies in those tissues requiring the highest amounts of energy). Consistent with this prediction is the observation that the highest levels of mouse *Hccs* mRNA are found in the adult heart and with the observation of strong *Hccs* expression in ocular tissue, which also has

considerable energy requirements. This expression profile is reminiscent of that seen for other genes whose protein products function in the mitochondrial respiratory chain (Wang et al., 1999). The HCCS haploinsufficiency could explain some of the MLS clinical features such as the cardiomyopathy present in 18% of cases, the dysgenesis of the corpus callosum present in 40% of cases and the neurological problems commonly observed in MLS patients. These phenotypes are in fact consistent with the involvement of a mitochondrial respiratory chain enzyme. Nevertheless unique skin lesions restricted to the head and neck and the microphthalmia are also diagnostic features and perhaps difficult to explain by deficiency of a mitochondrial enzyme. The typical features of mitochondrial diseases, that are a clinically heterogeneous group of disorders arising as a result of dysfunction of the mitochondrial respiratory chain, include neuromuscular hypotonia, ataxia, encephalomyopathy and various myopathies (DiMauro and Moraes, 1993) (Table 3). Interestingly, MLS patients do not display encephalomyopathies or signs of muscle involvement. However, mutations in genes involved in mitochondrial oxidative phosphorylation often cause neurological disorders. An example is represented by *SCO2* and *SURF*, responsible of infantile cardioencephalomyopathy and of Leigh syndrome, respectively. Both these diseases are associated with deficiency of cytochrome c oxidase (COX), that catalyzes the transfer of reducing equivalents from cytochrome c to molecular oxygen (Papadopoulou et al., 1999; Zhu et al., 1998).

Is therefore not difficult to link HCCS to neurological disorders that characterize the MLS syndrome as well as to cardiac defects found in 18% MLS cases. Moreover it is interesting to underlie that some mitochondrial disorders only affect a single organ. In particular the Leber hereditary optic neuropathy (LHON) is an example of mitochondrial diseases with a typical ocular phenotype. LHON disease has been associated with many missense mutations in the mtDNA and presents in

Disorder	Primary Features	Additional Features
Alpers-Huttenlocher syndrome	•Hypotonia •Seizures • Liver failure	• Renal tubulopathy
Chronic progressive external ophthalmoplegia (CPEO)	• External ophthalmoplegia • Bilateral ptosis	• Mild proximal myopathy
Kearns-Sayre syndrome (KSS)	• PEO onset at age <20 years • Pigmentary retinopathy •CSF protein >1g/L, cerebellar ataxia, heart block	• Bilateral deafness • Myopathy • Dysphagia • Diabetes mellitus • Dementia
Pearson syndrome	• Sideroblastic anemia of childhood • Pancytopenia • Exocrine pancreatic failure	• Renal tubular defects
Infantile myopathy and lactic acidosis (fatal and non-fatal forms)	• Hypotonia in 1st year of life • Feeding and respiratory difficulties	• Fatal form may be associated with a cardiomyopathy and/or the Toni-Fanconi-Debre syndrome
Leigh syndrome (LS)	• Subacute relapsing encephalopathy • Cerebellar and brain stem signs • Infantile onset	• Basal ganglia lucencies • Maternal history of neurologic disease or Leigh Sy
Neurogenic weakness with ataxia and retinitis pigmentosa (NARP)	• Late-childhood or adult-onset peripheral neuropathy • Ataxia • Pigmentary retinopathy	• Basal ganglia lucencies • Abnormal electroretinogram • Sensorimotor neuropathy
Mitochondrial encephalomyopathy with lactic acidosis and stroke-like episodes (MELAS)	• Stroke-like episodes at age <40 years • Seizures and/or dementia • Ragged-red fibers and/or lactic acidosis	• Diabetes mellitus • Cardiomyopathy hypertrophic • Bilateral deafness • Pigmentary retinopathy • Cerebellar ataxia
Myoclonic epilepsy myopathy sensory ataxia (MEMSA)	• Myopathy • Seizures • Cerebellar ataxia	• Dementia • Peripheral neuropathy • Spasticity
Myoclonic epilepsy with ragged-red fibers (MERRF)	• Myoclonus • Seizures • Cerebellar ataxia • Myopathy	• Dementia • Optic atrophy • Bilateral deafness • Peripheral neuropathy • Spasticity
Leber hereditary optic neuropathy (LHON)	• Subacute painless bilateral visual failure • Median age of onset 24 years	

Table 3. Clinical Syndromes of Mitochondrial Diseases (Adapted from Chinnery PF. 2010)

mid-life as acute or subacute central vision loss leading to central scotoma and blindness (Yu-Wai-Man et al., 2009).

In addition, although the main function of the mitochondrion is the production of energy in the form of ATP, it is well known its central role in many other metabolic tasks. One of these is the regulation of intrinsic pathway of cell death a key process required for proper development of the CNS (Valenciano et al., 2009). Thus, even if *HCCS* is one of the few genes involved in eye disease that is not directly involved in eye development, it could be play also an important role in apoptosis since it is necessary for the maturation cytochrome c a key regulator of intrinsic cell death pathway (Ow et al., 2008).

1.5 Mitochondrial-mediated apoptosis

Apoptosis is a process of particular importance for the proper development of the CNS and the eye. The regulatory mechanism of survival/death during neuronal development was not yet fully characterize but it is clear that apoptosis plays a key role in the balance between proliferation and differentiation. Apoptosis (derived from a Greek word meaning “falling off”, as leaves from a tree in Autumn) is the main morphological feature of the process of programmed cell death or “cell suicide”. It is a widespread, physiological phenomenon which occurs during the embryonic development of multicellular organisms (Glucksmann, 1965; Oppenheim, 1991) and represents the most common mechanism to regulate the size of cell populations during development, as well as in adult life. In the developing vertebrate nervous system, for example, around half or more of the nerve cells normally die soon after they are born. Deregulated apoptosis has been implicated in diverse pathologies, including cancer and neurodegenerative disease, and it has been considered the final common pathway resulting from a

variety of primary defects (Tait and Green, 2010; Vecino et al., 2004). In vertebrate cells, apoptosis typically proceeds through one of two signalling cascades termed the intrinsic (or mitochondria-dependent) and extrinsic pathways (also known as “death receptor pathway”). Figure 8 illustrates a schematic representation of the extrinsic (death receptor-mediated) and intrinsic (mitochondria-mediated) central apoptotic pathways.

Both the extrinsic and the intrinsic routes to apoptosis ultimately lead to cell shrinkage, chromatin condensation, nuclear fragmentation (which is frequently accompanied by internucleosomal DNA fragmentation), blebbing, and phosphatidylserine exposure on the surface of the plasma membrane (Zamzami et al., 1996)

In the extrinsic pathway, apoptosis is triggered by the ligand-induced activation of death receptors at the cell surface. Death receptors include the tumor necrosis factor (TNF) receptor-1, CD95/Fas (the receptor of CD95L/FasL), as well as the TNF-related apoptosis inducing ligand (TRAIL) receptors-1 and -2.

Death receptor ligation causes the recruitment of adaptor molecules, such as FAS-associated death domain protein (FADD), that bind, dimerize and activate an “initiator” caspase, caspase 8. Active caspase 8 directly cleaves and activates the “executioner” caspases, caspase 3 and caspase 7. The “executioner” caspases through the cleavage of numerous proteins ultimately lead to the phagocytic recognition and engulfment of the dying cell (Debatin and Krammer, 2004).

In the intrinsic pathway, mitochondrial outer membrane permeabilization (MOMP), which leads to the release of proapoptotic proteins from the mitochondrial intermembrane space (IMS), is the crucial event driving initiator caspase activation and apoptosis. Following its release from mitochondria, cytochrome c binds apoptotic protease activating factor 1 (APAF1), inducing its conformational change and oligomerization and leading to the formation of a caspase activation platform

termed the apoptosome. APAF 1 preexists in the cytosol as a monomer, and its activation depends on the presence of cytochrome c (Cyt c) and ATP/dATP (Cain et al., 2002). The apoptosome recruits, dimerizes and activates an initiator caspase, caspase 9, which, in turn, cleaves and activates caspase 3 and caspase 7.

The mitochondrion also releases other pro-apoptotic proteins such as SMAC (also known as DIABLO) and OMI (also known as HTRA2) blocking the X-linked inhibitor of apoptosis protein (XIAP)-mediated inhibition of caspase activity.

MOMP can even commit a cell to die when caspases are not activated. This "caspase-independent death" (Chipuk and Green, 2005) can occur by release of caspase independent death effectors including apoptosis-inducing factor (AIF) (Susin et al., 1999b) and endonuclease G (Li et al., 2001).

The MOMP is a highly regulated process, primarily controlled through interactions between pro- and anti-apoptotic members of the B cell lymphoma 2 (BCL-2) family (Tait and Green, 2010).

Crosstalk between the extrinsic and intrinsic pathways occurs through caspase 8-mediated cleavage of BCL-2 homology 3 (BH3)-interacting domain death agonist (BID; a BH3 domain-only protein), leading to BID activation and MOMP.

While the extrinsic pathway mediates apoptosis through the specialized subset of death signals detected at the plasma membrane, the intrinsic pathway on the other hand transduces a wide variety of extracellular and intracellular stimuli including loss of survival/trophic factors, toxins, radiation, hypoxia, oxidative stress, ischaemia-reperfusion and DNA damage (Foo et al., 2005). Reactive oxygen species (ROS) excessively produced by the respiratory chain can also cause the progressive mitochondrial damage leading to apoptosis (Skulachev, 1997).

During the past decade, it has become obvious that the mitochondria play a critical role in the regulation of cell death, and that MOMP and release of intermembrane

space proteins are important features for this process. Moreover mitochondria are known to modulate and synchronize Calcium signaling which has long been recognized as a participant in apoptotic pathways (Giacomello et al., 2007). Also the fragmentation of the mitochondrial network and remodelling of the mitochondrial cristae are both required processes for the progression of apoptosis (Scorrano et al., 2002); mitochondrial fusion and fission machinery controls mitochondrial shape and physiology including mitochondrial remodeling during apoptosis. Thus mitochondria exert both vital and lethal functions in physiological and pathological scenario: the mitochondrion is not only the cell's powerhouse, it is also its arsenal.

The mitochondrion sequesters a potent cocktail of pro-apoptotic proteins and the most prominent among these is cytochrome c. After release from mitochondria, the biochemistry of how cytochrome c triggers caspase activation is very complex. It was found that cytochrome c can interact with the C-terminal WD40 repeats of Apaf 1 and that this interaction is required for activation of the pathway (Lassus et al., 2002). An *in vitro* de novo reconstitution of apoptosome was achieved by using purified recombinant Apaf 1, procaspase 9, procaspase 3, and highly purified horse cytochrome c. When all the proteins are incubated together in the presence of nucleotide dATP/ATP, caspase 3 is activated. A striking phenomenon observed in this *in vitro* system is that Apaf 1 and cytochrome c are induced into a huge complex in a dATP/ATP-dependent manner to form the apoptosome (Zou et al., 1999) (Figure 9). It has been demonstrated that apocytochrome c (the cytochrome c without the heme group) binds Apaf 1 but that this interaction is insufficient for caspase activation (Martin and Fearnhead, 2002).

Although the biochemistry of apoptosome formation has been reconstituted by using purified components *in vitro*, an understanding of the composition of the native apoptosome in apoptotic cells has emerged only recently. The successful

immunoprecipitation of catalytically active apoptosomes from Jurkat cells has revealed that the native apoptosome (at least in this cell type) contains caspase 3 and XIAP in addition to Apaf 1 and caspase 9 (Hill et al., 2004). This study also intimates that the interaction of XIAP with caspase 9 is necessary for caspase 3 association with the apoptosome. Interestingly, it has been suggested that Smac or Omi/HtrA2, which are coordinately released from the mitochondrial intermembrane space with cytochrome c, may displace XIAP from the apoptosome and thereby increase apoptosomal activity (Twiddy et al., 2004). These findings raise the intriguing possibility that despite its ability to inhibit caspases, XIAP may initially recruit caspase 3 to the apoptosome, with subsequent displacement of XIAP by Smac or Omi leading to full apoptosomal activation.

Despite recent progress in understanding the role of the apoptosome during development, adult tissue homeostasis, and pathogenesis (Schafer and Kornbluth, 2006), a number of questions remain concerning its precise mechanism of activation/formation. For example, we do not yet know the precise binding site of cytochrome c on Apaf 1, nor do we know how dADP is exchanged for dATP after the initial hydrolysis of dATP.

Moreover in the original model, the formation of the apoptosome is assumed to be the only mechanism to convert procaspase 9 to the active form in the cytosol. However, recent data that uncouple cytochrome c, Apaf 1 and caspase 9 activation in numerous cell death models have been reported (Hao et al., 2005; Ho et al., 2004; Ho et al., 2007; Katoh et al., 2008; Mills et al., 2006).

Interesting a model of cytochrome c knock-in mice, engineered to express a mutant allele with a point mutation rendering it unable to activate Apaf 1, but competent for cellular respiration, yielded some data that challenge our current understanding of apoptosome function (Hao et al., 2005). In contrast to fibroblasts,

thymocytes from these animals retain sensitivity to apoptotic stimuli despite the inactivation of cytochrome c. After γ-irradiation, caspase activation occurs in the absence of detectable Apaf 1 oligomerization, but in an Apaf 1-dependent manner. This suggests the presence (at least in certain cell types) of a cytochrome c independent, Apaf 1-dependent mechanism of caspase 9 activation.

Moreover Apaf 1-deficient primary myoblasts but not fibroblast could activate caspase 9, which suggested that coupling of caspase 9 with Apaf 1 is cell type-specific (Ho et al., 2004). A similar observation was made with Drosophila melanogaster lacking ARK, the fly homologue of Apaf 1(Mills et al., 2006).

Interestingly, a population of procaspase 9/caspase 9 and other caspases pre-exist in the intermembrane space of mitochondria and participate in apoptosis (Costantini et al., 2002; Johnson and Jarvis, 2004; Samali et al., 1999; Susin et al., 1999a). Cytosolic translocation of these molecules can be prevented by Bcl-2 (Costantini et al., 2002; Katoh et al., 2004).

In addiction it has been shown that procaspase 9 is able to homo-dimerize to gain its enzyme activity in the absence of Apaf 1 as evidenced by bacterial expression systems, *in vitro* translation and biochemical analyses (Boatright et al., 2003; Pop et al., 2006; Renatus et al., 2001; Sadhukhan et al., 2006; Srinivasula et al., 1998). In particular, procaspase 9 is dimerized by higher concentrations of kosmotropes, salts able to stabilize proteins, such as 1 M citrate (Boatright et al., 2003; Pop et al., 2006). Citric acid is the first product in the Krebs cycle whose reactions are controlled by the electron transfer system maintaining inner membrane potential (Δψm) for ATP synthesis. It has been showed that an hypoactive Δψm, caused by oxidative stress, leads to an accumulation of citrate, probably due to a feedback control of the Krebs cycle by the electron transfer system. The accumulation of citrate could be a cause of intra-mitochondrial caspase 9 activation (Katoh et al., 2008). Thus in this model, depicted in Figure 10, Katoh and colleagues propose

that an Apaf 1-independent mitochondrial *in situ* caspase 9 activation may be caused by the major metabolic reactions (Krebs cycle) in response to physiological stresses, like the ROS overproduction (Katoh et al., 2008).

It is clear that apoptosis-inducing mechanisms distinct from the apoptosome model deserve more extensive investigation by various approaches, and the continued study of apoptosomal formation, function, and regulation may soon make the apoptosome a viable therapeutic target not only for cancer treatment, but also for degenerative and developmental disorders.

1.6 *Oryzias latipes* as a model system to study developmental defects and genetic diseases.

As stated above MLS syndrome is an X-linked dominant male lethal disorders and previous studies demonstrated the early lethality of *Hccs* knock-out mouse embryos (Prakash et al., 2002). Recently a heart-specific conditional *Hccs* knockout mouse was generated. It has been reported that hemizygous males as well as homozygous females die in utero between 10.5 and 12.5 dpc. In contrast heterozygous females appeared normal after birth. Analyses of heterozygous embryos revealed the expected 50:50 ratio of *Hccs* deficient to normal cardiac cells at mid-gestation, as expected for random X-inactivation; however, diseased tissue contributed progressively less over time and by birth represented only 10% of cardiac tissue volume. This change was accounted for by increased proliferation of remaining healthy cardiac cells resulting in a fully functional heart (Drenckhahn et al., 2008).

Although this model can explain the phenotypically variability of cardiac defects in MLS patients, the molecular mechanisms underlying the eye and brain developmental anomalies in the presence of HCCS dysfunction are still unknown.

Towards this aim we thus decided to generate a model for this disease in a simpler vertebrate species, *Oryzias latipes* (Medakafish), where we planned to perform gain and loss of function studies to better define the function of this gene and its role in the pathogenesis of MLS syndrome.

Medakafish is a particularly amenable model system for this kind of analysis since its use is less time and resource consuming, as compared, for instance, with mice (Ishikawa, 2000). In addition, over-expression of mutated and wild-type mRNA or injections of morpholinos allows to test the function of wild type and dominant negative forms of specific gene or to study the functional loss of the same transcript. Moreover this strategy would allow us to overcome the problem of early embryonic lethality since both over-expression of mutated or wild-type mRNAs and injections of morpholinos don't abolish completely the gene function.

Physiology, embryology and genetics of medaka have been widely studied in the past 100 years. Already in 1913, the medaka was used to show Mendelian inheritance in vertebrates (Ishikawa, 1913; Toyama, 1916). Then, genetic studies on medaka, have been focused on the molecular basis of pigmentation and sex determination (Baroiler et al. 1999; Wada et al. 1998; Matsuda et al. 1998, Matsuda et al.1999, Yamamoto T. 1958). In the past few years this model was a very useful tool to identify some important genes involved in the eye development (Fukada et al. 1995: Simeon A. 1998, Zhou et al. 2000; Chaing et al.1996; Macdonald et al.1995; Ekker et al.1995; Mathers et al.2000).

In addition, the complete sequencing of the human genome and other vertebrate species has greatly contributed to the use of this model to study various biological processes underlying the embryonic development. Different comparative studies among vertebrates have demonstrated an highly conservation in terms of genomic sequences and molecular processes, also in model systems such as teleostei (*Danio rerio* / Zebrafish and *Oryzias latipes* / Medaka). Zebrafish and medaka are

very close species: they are separated from their last common ancestor about 110 million years ago. They are both ideal organisms for genetic studies as they display many advantages such as the simple use of different genetic engineering techniques. They have a short generation time (8-10 weeks for Zebrafish and 6-8 weeks for Medaka). Moreover Zebrafish/Medaka biology allows ready access to all developmental stages, and the optical clarity of embryos and larvae allow real-time imaging of developing pathologies.

In particular, unlike other teleostei, medaka has several advantages. Medaka is very hardy and tolerates a wide range of salinities and temperatures (10–40 °C); it is easy to breed and highly resistant to common fish diseases. For all the above-mentioned reasons, thus, medaka is easier to keep and maintain in aquaculture than Zebrafish and it is easier to handle. Early medaka development is rapid; whereas zebrafish larvae hatch after 2–3 days, medaka embryos are enclosed in a tough chorion that protects them in their natural habitat until they hatch as feeding young adults after 8 days. Both zebrafish and medaka are considered an ideal model to study eye development (Wittbrodt et al., 2002). The eye devolpment in medaka start at the end of gastrulation (stage 15) with the determination of the eye field; in the late neurula stage (Stage 18) the formation of the optic bud (rudimentary eye vesicle) occur; at stage 21 the optic vesicles differentiate to form the optic cups and the lenses begin to form; at stage 24 the spherical optic lenses are completed; at stage 30 the retina begins to differentiate and finally, at stage 38 the eye is completely formed (Iwamatsu, 2004). Figure 11 illustrates some stages of medaka development.

From the experimental point of view, however, the two model systems are completely equivalent. In both systems, reverse-genetic analyses are also facilitated by assays of gene function using transient rather than stable misexpression, which is technically easier than in mice. Microinjection of early

embryos with either mRNA or antisense morpholino oligonucleotides results in transient gene overexpression or knockdown, respectively (Wittbrodt et al., 2002). These can be a great advantage in terms of speed and allow studying a highly specific gene function, without any laborious, time and resource consuming techniques.

The identification of thousands of early developmental fish mutants through genetic screens that were carried out in the 1990s, established the fish as a mainstream model in developmental biology. Recently, the same attributes that have propelled the rise of fish in developmental biology research have also prompted the increased use of this organism as a model for several human diseases. Many fish models of monogenic human genetic diseases have already been generated through forward and reverse genetic approaches, allowing an enhanced understanding of the basic cell-biological processes that underlie the disease phenotype of the specific genetic diseases under study beyond that gained from existing models (Lieschke and Currie, 2007; Wittbrodt et al., 2002). For all the above mentioned considerations, we believe that the Medakafish could be a powerful tool to study the function of the *HCCS* gene and to understand the molecular basis of the Microphthalmia with linear skin lesions syndrome.

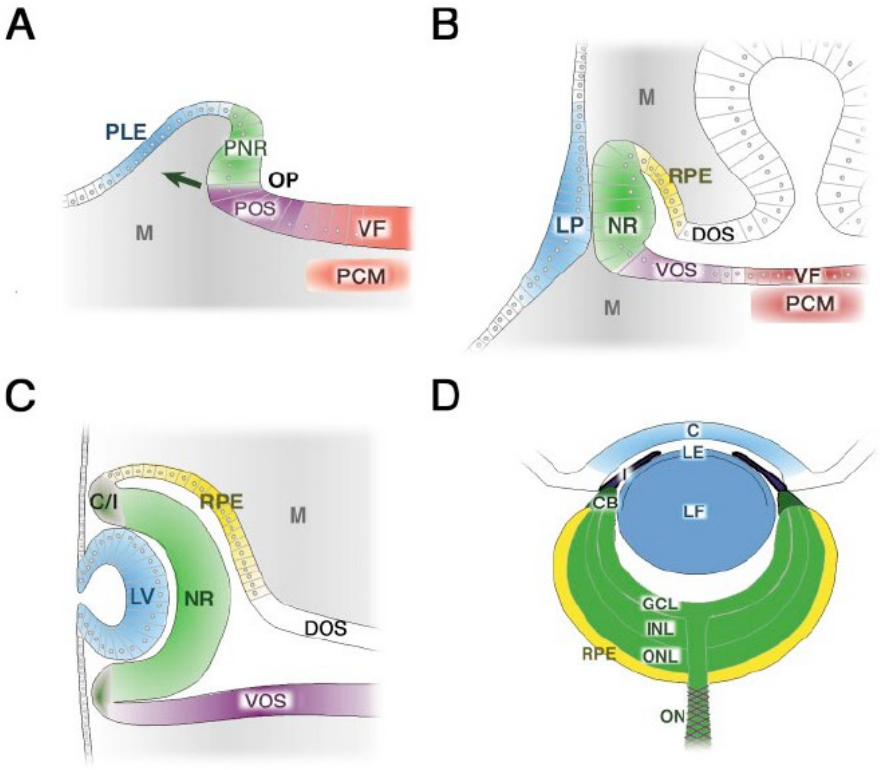

Figure 1. Schematic overview of vertebrate eye development.
In panels A–D, presumptive or differentiated eye tissues are color-coded in the following manner: blue, lens/cornea; green, neural retina; yellow, retinal pigmented epithelium (RPE); purple, optic stalk; red, ventral forebrain/prechordal mesenchyme; grey, mesenchyme.
(A) Formation of the optic vesicle is initiated by an evagination (indicated by arrow) of the presumptive forebrain region resulting in the formation of the optic pit (OP). The optic vesicle region is divided into dorso-distal region (green), which contains the presumpitve neural retina (PNR) and RPE (not shown), and the proximo-ventral region, which gives rise to the presumptive ventral optic stalk (POS); PLE, presumptive lens ectoderm; M, mesenchyme; VF, ventral forebrain; PCM, prechordal mesoderm.
(B) Continued growth of the optic vesicle culminates with a period of close contact between the lens placode (LP) and the presumptive neural retina (NR) during which important inductive signal likely exchange: RPE, presumptive retinal pigmented epithelium; VOS, ventral optic stalk; DOS, dorsal optic stalk.
(C) Invagination of the optic vesicle results in formation of the lens vesicle (LV) and neural retina (NR) and establishes the overall structure of the eye. The point at which the neural retina and RPE meet gives rise to components of the ciliary body and iris (C/I).
(D) Mature eye: C, cornea; LE, lens epithelium; LF, lens fiber cells; I, iris; CB, ciliary body; GCL,ganglion cell layer; INL, inner nuclear layer; ONL, outer nuclear layer; ON, optic nerve. (Adapted from Chaw and Lang 2001)

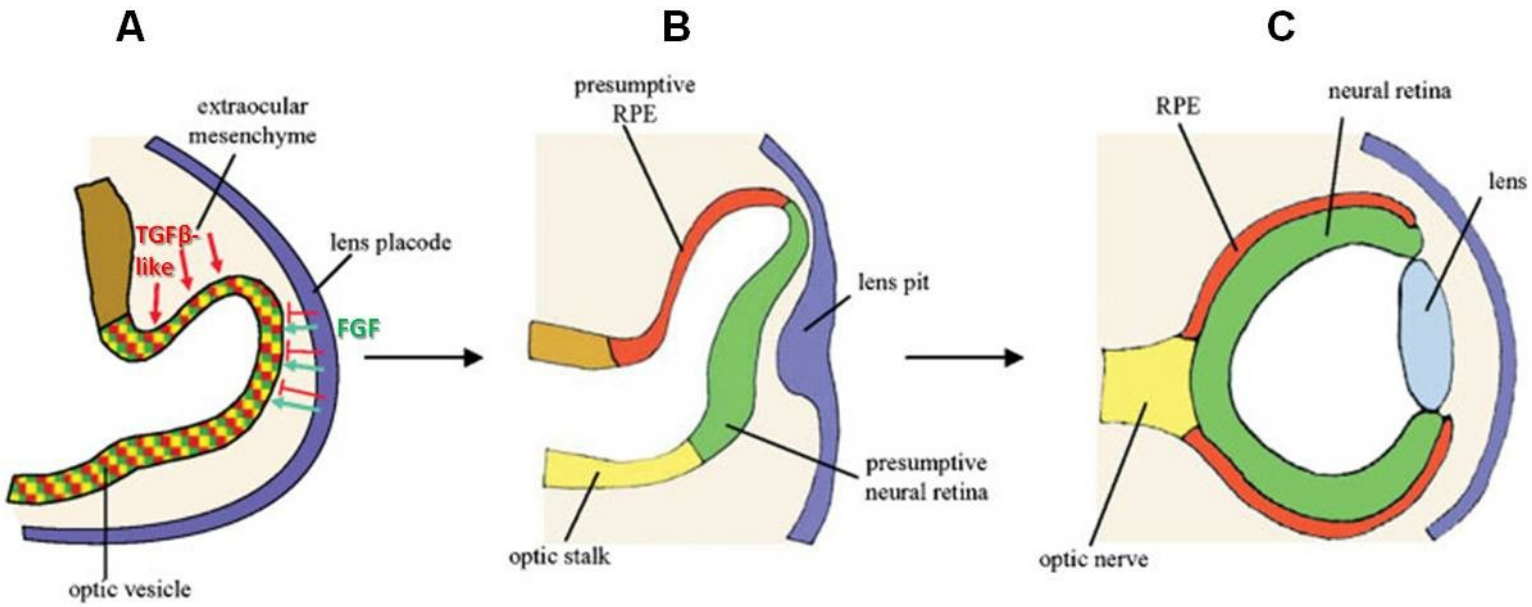

Figure 2. Schematic representation of the optic vesicle patterning. (A) Unpatterned optic vesicle: all the neuroepithelial cells are indistinguishable (mixed colour-code) and express a common set of transcription factors. TGFb-likesignals from the extraocular mesenchyme favour cells of the optic vesicle to become RPE (red arrow), whereas FGF signals from the lens placode repress RPE (red line) and activate neural retina (green arrow) identity. (B) Patterned optic vesicle: different transcriptional regulators become restricted to the presunptive RPE(red) and neural retina (green). (C) Differentiated optic cup. (Adapted from Martinez-Morales et al., 2004)

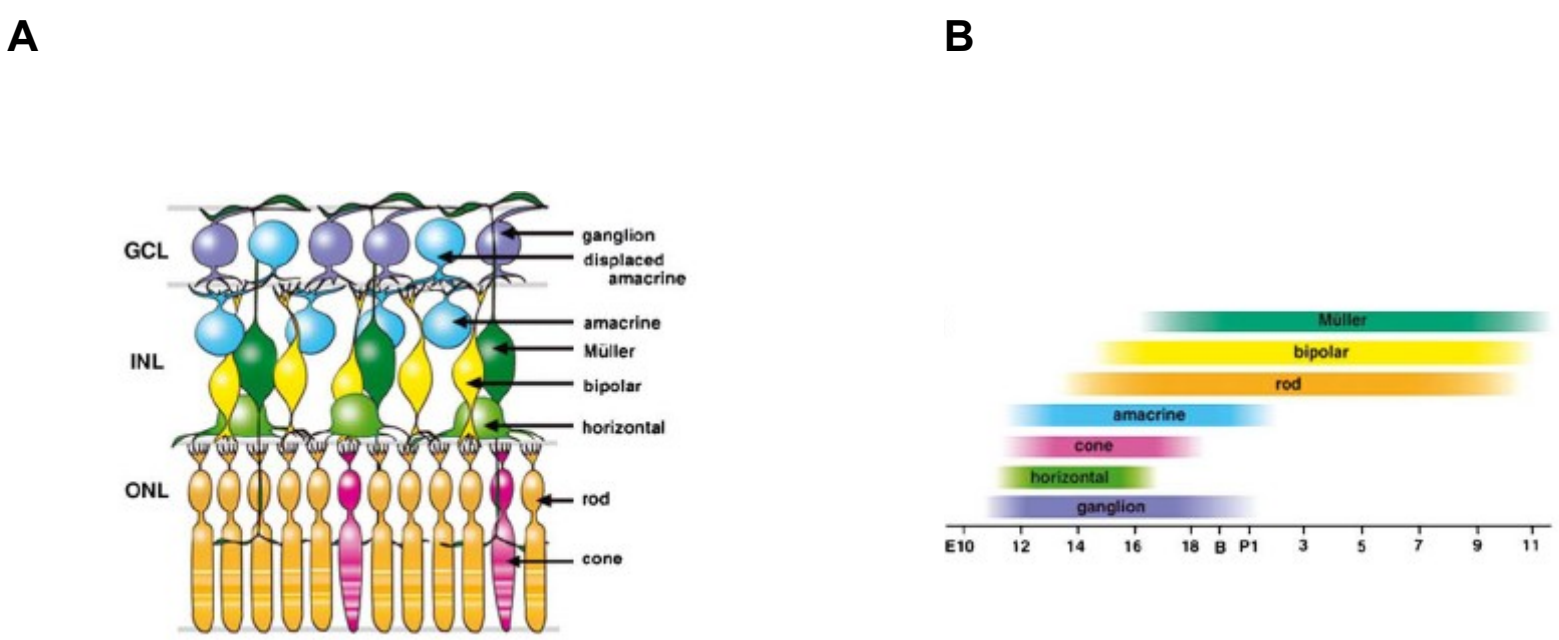

Figure 3. Schematic structure of the neural retina and its differentiation. (A) Vertebrate neural retina composed of seven types of retinal cells which constitute three cellular layers. GCL, ganglion cell layer; INL, inner nuclear layer; ONL, outer nuclear layer. (B) Retinal cells are differentiated in an order conserved among many species: ganglion cells first and Müller glial cells last. (Adapted from Hatakeyama and Kageyama, 2004).

Figure 4. Clinical Features Reported in MLS Syndrome. (A) Microphthalmia. (B) Typical linear skin lesions on the face and neck. (C) Reticulolinear scar lesions on the neck in a patient with one of the largest Xp deletions described for MLS syndrome (Xp22-pter).(Adapted from Lindsay et al., 1994)

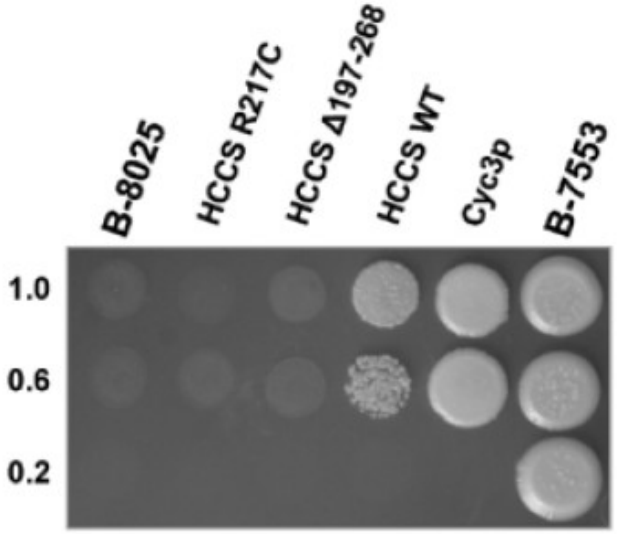

Figure 5. HCCS mutant proteins are not able to complement S. cerevisiae CYC3 deficiency. Functional complementation of the S. cerevisiae strain B-8025 ($Cyc3^{-}$). B-8025 was transformed with human wild-type HCCS (HCCS WT), the mutants Δ197–268 and R217C, or yeast CYC3 (Cyc3p) expression constructs and was grown on minimal medium. Saturated and diluted cultures were spotted on glycerol medium and incubated at 30°C. The top row shows spots of saturated cultures, and the middle and bottom rows show spots of dilutions. Note partial restoration of growth by Cyc3p and wild-type HCCS, whereas no growth was observed for the untransformed strain or that expressing HCCS Δ197–268 or HCCS R217C. Strain B-7553 served as wild-type growth control. (Adapted from Wimplinger et al., 2006)

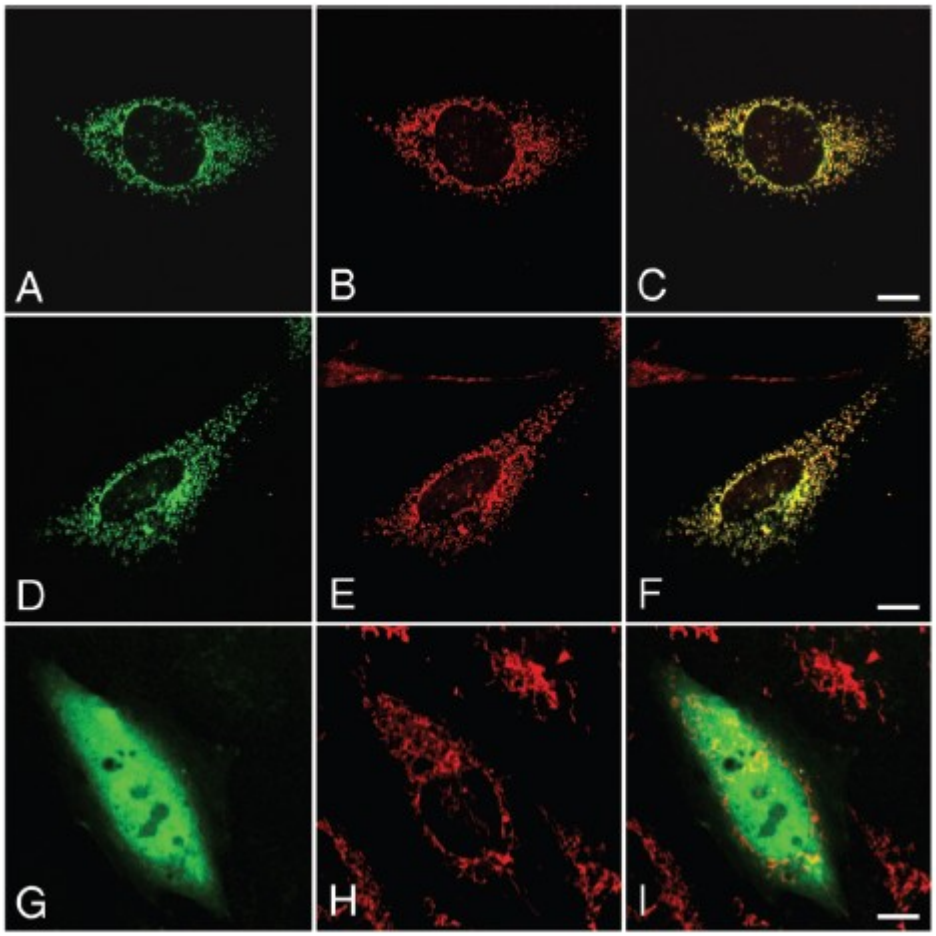

Figure 6. Targeting of ectopically expressed HCCS wild-type and mutant proteins to mitochondria. Subcellular localization of different N-terminally HA-tagged HCCS proteins ectopically expressed in CHO-K1 cells (A, D, and G) and staining of endogenous mitochondria by MitoTracker (B, E, and H) are shown. HA-tagged HCCS wild-type protein (A [green]) is targeted to mitochondria (B [red]), as shown by colocalization with the MitoTracker (C [yellow]). Similarly, HA-tagged HCCS R217C mutant protein (D [green]) shows a mitochondrial (E [red]) distribution (F [yellow]). In contrast, the truncated HCCS Δ197–268 protein is diffusively dispersed in the cell (G), and the two fluorescence patterns (G and H) show no overlap (I). (Adapted from Wimplinger et al., 2006).

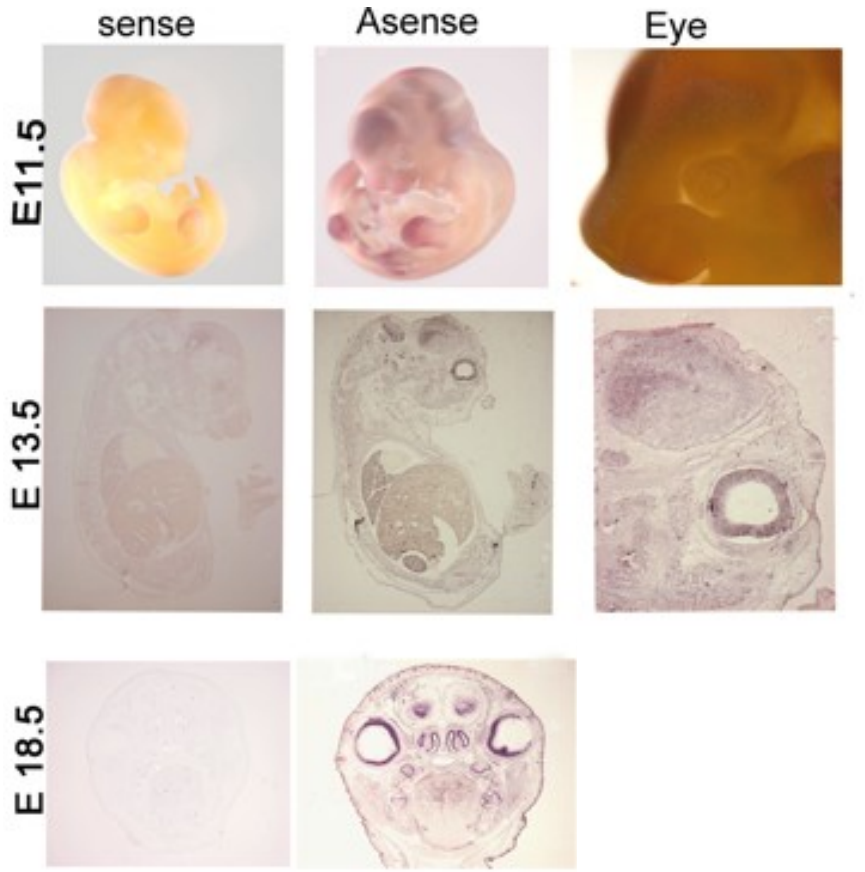

Figure 7. HCCS expression analysis in mouse. *In situ* hybridisation analysis (ISH) on wild type mice at E11.5, E13.5 and E18.5. A specific signal in the eyes and in the encephalon is detected. The first row show images of whole mouse ISH while the other rows illustrates the results of ISH on sagittal and frontal sections. (unpublished data)

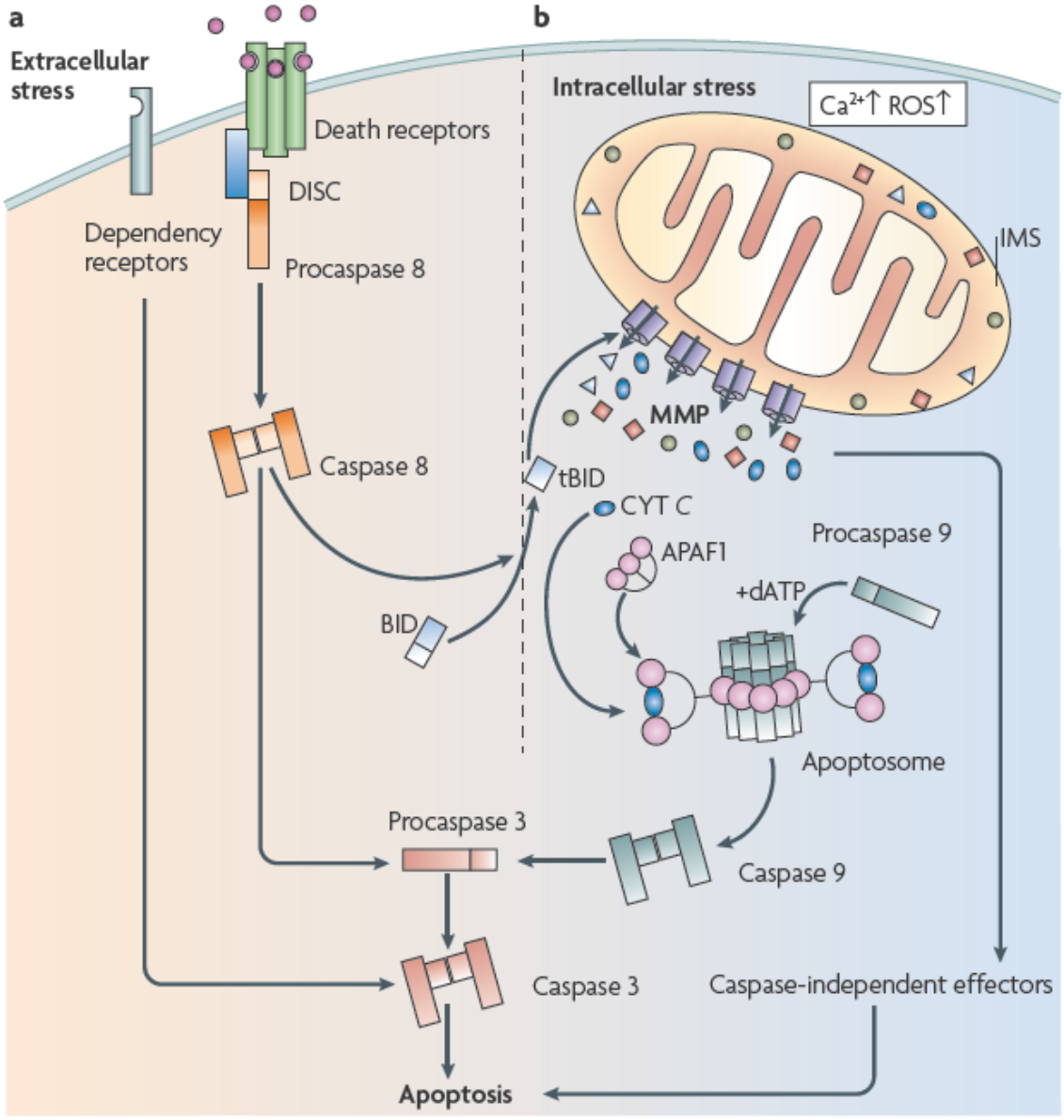

Figure 8. The extrinsic (death receptor-mediated) and intrinsic (mitochondria-mediated) central apoptotic pathways. (Adapted from Galluzzi et al., 2009)

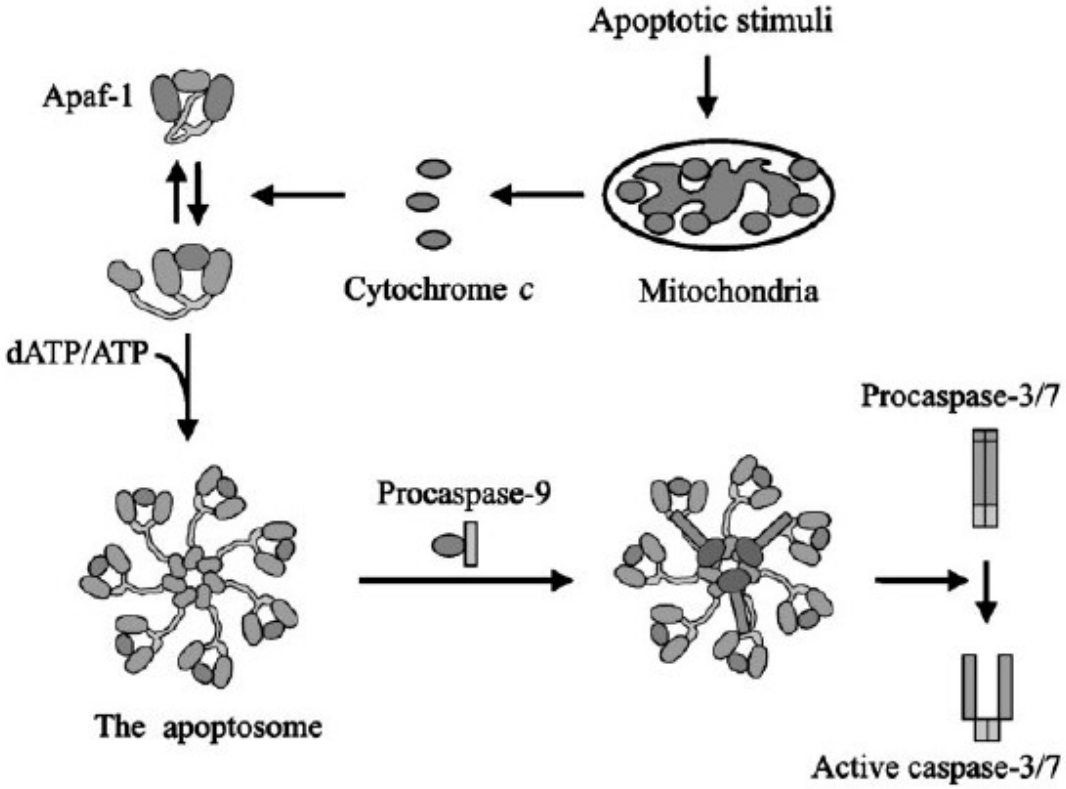

Figure 9. The mechanisms of apoptosome formation and caspase activation initiated by cytochrome c release. (From Jiang and Wang, 2004)

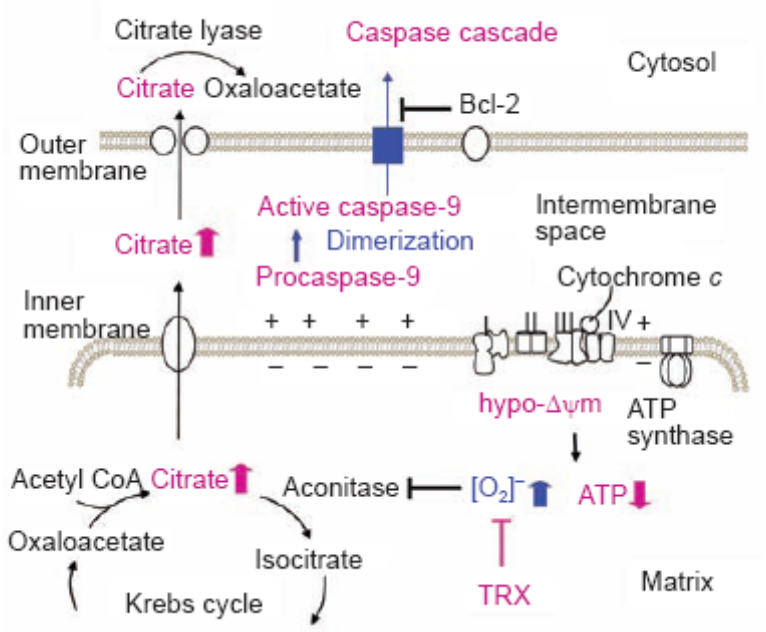

Figure 10 Schematic presentation of the mitochondrial biochemical alterations in the course of Apaf 1-independent caspase 9 activation.
The mitochondrial inner membrane is illustrated with the electron transfer system (complexes I-IV), ATP synthase and citrate transporter (oval). A part of the Krebs cycle in the matrix is depicted. The outer membrane with pores permeable to the metabolites is also shown. Biochemical changes revealed by this study are highlighted in magenta. Bold arrows indicate an increase (upward) or decrease (downward) in each physiological parameter. Bar-headed lines indicate inhibition. The hypo-Δψm condition and the results with thioredoxin (TRX) predict free radical ($[O2]^-$) production by which aconitase is inactivated. Dimerization of procaspase 9 by a topical increase in citrate is hypothesized. Cytosolic translocation of caspase 9 is inhibited by Bcl-2, although the mechanism has not been identified (blue box) (Adapted from Katoh et al., 2008).

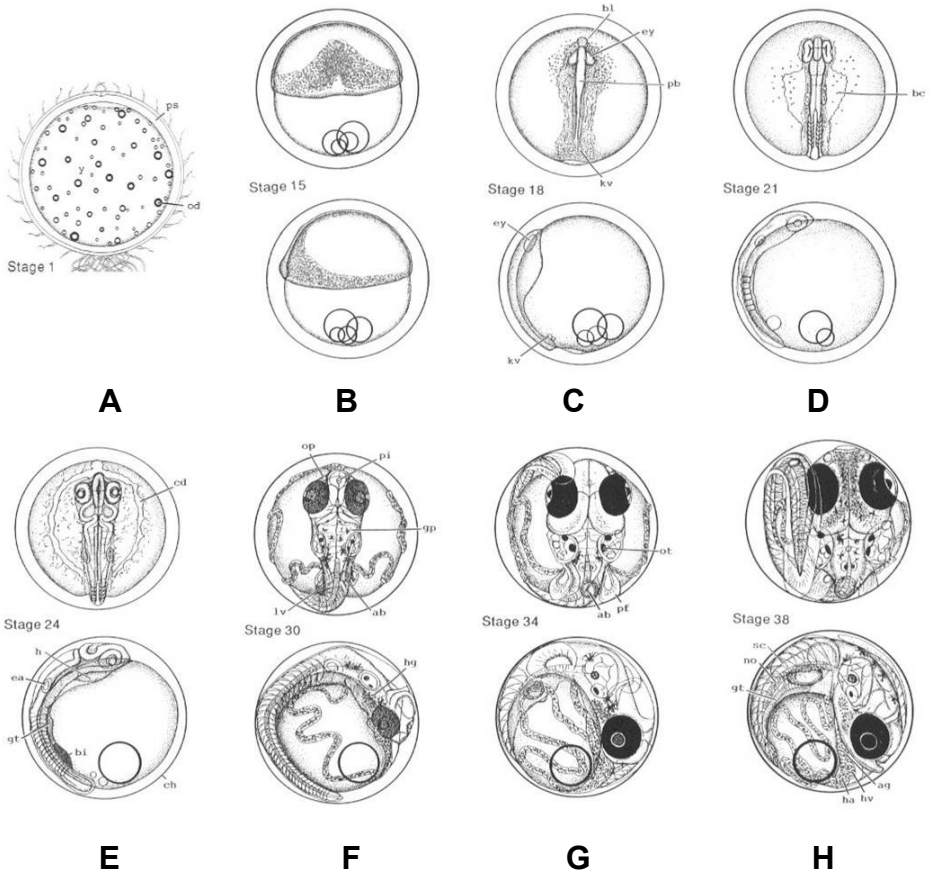

Figure 11. Selected stages of Medaka development. (A) Stage 1, Fertilized eggs; (B) Stege 15, Gastrula stage: (C) Stage 18, Late neurula stage: Optic bud (rudimentary eye vesicle) formation; (D) Stage 21, 6 somite stage: the optic vesicles differentiate to form the optic cups and the lenses begin to form. (E) Stage 24, 16 somite stage: the neurocoele is formed in the fore-, mid- and hind-brains, the spherical optic lenses are completed. (F) Stage 30, 35 somite stage: the retina start to differentiate; in the heart, the sinus venosus, atrium, ventricle and bulbus arteriosus are differentiated. (G) Stage 34 (H) Stage 38 (8 days) Hatching stage. ab, swim (air) bladder; ag, artery globe; bc, body cavity; bl, beak-like mass of cells; cd, Cuvierian duct; ch, chorion; ea: otic (ear) vesicle; ey, optic (eye) vesicle; gp, guanophores; gt, gut tube; h, heart rudiment; ha, atrium of heart; hv, ventricle of heart; kv, Kupffer's vesicle; lv, liver; no, notochord; od, oil droplet; op, olfactory pit; ot, otolith; pb, protobrain; pf, pectoral fin; pi, pineal gland; ps, perivitelline space; sc, spinal cord.(Adapted from Iwamatsu, 2004).

2. MATERIALS AND METHODS

2.1 Medaka Stocks

Wild type Oryzias latipes of the cab strain were maintained in an in-house facility in a constant re-circulating system at 28°C on a 14 hours light/10 hours dark cycle. Embryos were staged according to Iwamatsu 2004 (Iwamatsu, 2004).

2.2 Isolation and characterization of ol*hccs*

To identify the ol*hccs* gene, were performed a BLAST searches with the human HCCS protein sequence (NP_005324 [GenBank]) in the Ensembl madaka database (www.ensembl.org) and identified putative ol*hccs* transcripts. The entire ol*hccs* coding sequence including part of the 5'untranslated region were isolated by RT-PCR amplification from a cDNA derived from a pool of medaka embryos at different stages. Total RNAs were isolated from medaka embryos homogenized in TRIzol reagent (Invitrogen Carlsbad, CA) using a sterile pestle. RNA was isolated by chloroform extraction, isopropanol precipitation, and washed in 75% ethanol. Contaminating genomicDNA was removed with Dnase I (Roche, Basel, Switzerland). RNA was reverse transcribed to cDNA using the Superscript III First Strand Synthesis Kit (Invitrogen). PCR was performed using 2 µl of the reverse transcription reaction as a template with the High Fidelity PCR system (Roche, Basel, Switzerland) and using the following ol*hccs* specific primers:

ol*hccs*aFw 5'- TGCCGGTCGGTGGGTCCTTTG-3'

ol*hccs*aRv 5'- CCAGTCTGCTGAAGCGCTGCAC-3'

ol*hccs*bFw 5'- GATGTCAGTCACCCATCACG-3'

2.3 Morpholinos (MO) and mRNAs injections

ol*hccs* specific morpholinos (MO) (Gene Tools) were designed on the two different 5'UTR region of the transcripts (ol*hccs*a-MO and ol*hccs*b-MO) and on the first common exon-intron splice site (ol*hccs*-MO) as follow:

ol*hccs*a-MO 5'- AGGTGTAGACGCAGAAGCGCCCATC-3'

ol*hccs*b-MO 5'- GACTGACATCCCGATGGAGAGACCA-3'

ol*hccs*-MO 5'-TGAAGTCAGGAACGTACCATGTTAG-3'

The following MO containing five mismatches (ol*hccs*a-mmMO) with respect to the ol*hccs*a-MO sequence was used as control (mismatches are in red):

ol*hccs*a-mmMO 5'-A**T**GTGTA**A**ACGCA**T**AAGC**T**CCCAT**T**

ol*Apaf1* specific MO were also designed on the 5'UTR region of ol*Apaf1:*

ol*Apaf1*-MO 5'- CTTCAGGCAAGTCACCTCCGACCAT-3'

MOs were injected in a range of concentrations (0,03 - 0,4 mM). Their efficiency was measured as the ability of interfering with eGFP expression using a reporter construct. The pCS2/ol*hccs*a-GFP, pCS2/ol*hccs*b-GFP and pCS2/ol*hccs*-GFP reporter plasmids were constructed cloning the complementary region of the MOs in frame with the eGFP coding sequence. MOs were individually co-injected with the different eGFP mRNAs (25 ng/µL) and RFP mRNA (25 ng/µL). The inhibitory efficiency of each MO was measured by quantification of the green/red fluorescence ratio (eGFP/RFP) intensity using Photoshop CS3 software (Adobe)

to measure average pixel intensity of RFP and eGFP, as previously reported (Conte et al., 2010b; Esteve et al., 2004). Selected MO working concentrations was 0,3 mM for ol*hccs*a-MO, 0,1 mM for ol*hccs*b-MO, 0,06 mM for ol*hccs*-MO, 0,1 mM for ol*Apaf1*-MO. MOs were injected into one blastomere of the embryos at the one-two cell stage. Control embryos were always injected with either ol*hccs*a-mmMO or eGFP mRNA to follow the efficiency of the injections as well as for testing possible defects associated with the injection procedures. At least 3 independent experiments were conducted for each marker and condition.

Activation of p53 is an occasional off-targeting effect of MO injections (Robu et al., 2007), and can be counteracted by injection of a p53 Mo (Eisen and Smith, 2008). Thus possible non-specific effects of ol*hccs*a-MO were ruled out by coinjecting it with a Mo designed against medaka p53 (p53MO) (Conte et al., 2010b).

ol*hccs*a mRNA carrying silent mutations at the MO binding site, h*Bcl-xL* mRNA, eGFP mRNA and RFP mRNA were cloned and transcribed out of pCS2+ vector using the SP6 mMessage mMachine kit (Ambion) according to manufacturer instructions. The synthesized mRNAs were quantified and re-suspended in 1x Yamamoto Ringer (Yamamoto and Yamagami, 1975). Rescue experiments were performed by co-injecting ol*hccs*a or h*Bcl-xL* mRNA with ol*hccs*a-MO. ol*hccs* mRNA (200 ng/µL) or h*Bcl-xL* mRNA (200 ng/µL) were co-injected with ol*hccs*a-MO into one blastomere of the embryos at the one-two cell stage. All the injection solutions included 25 ng/µL of eGFP mRNA as a lineage tracer.

2.4 Caspase inhibitors

Caspase inhibitors (CalBiochem) were caspase 1 inhibitor I (Ac-YVAD-CHO), caspase inhibitor I (Z-VAD-FMK), and caspase 9 inhibitor III (Ac-LEHDCMK). Stocks were diluted in DMSO or distilled water. Caspase inhibitors at final

concentration of 5 μM were co-injected with ol*hccs*a-MO as previously reported (Walker and Harland, 2009).

2.5 Whole-Mount *In Situ* Hybridization

Whole-mount *in situ* hybridization was carried out as using digoxygenin-labeled antisense RNA riboprobes as previously described (Loosli et al., 1998). Probes for ol*Otx2*, ol*Pax6*, ol*Bmp4*, ol*Tbx5*, ol*Vax2,* ol*CyclinD1* and ol*Ath5,* have been previously described (Conte et al., 2010a; Del Bene et al., 2007; Ruiz et al., 2009) The cDNA of the ol*hccs*, ol*Islet*2 genes were isolated by RT-PCR amplification with the following specific primers:

ol*hccs*aFw 5'- TGCCGGTCGGTGGGTCCTTTG-3'

ol*hccs*aRv 5'- CCAGTCTGCTGAAGCGCTGCAC-3'

islet2Fw 5'-TCTGTTCTCCCAAGACCCGCTA-3'

islet2Rv 5'-AGGCTGGACAACATCAGACGA-3'

Selected embryos were fixed in 10 ml of 4% paraformaldehyde prepared in 2X in 2X PTW (PBS containing 0.1% Tween) for 1 hour at room temperature and then 12 hours at 4°C. The embryos were dechorionated and washed 4 times with 1X PTW. Finally, embryos were dehydrated in methanol 100% and stored at -20°C (embryos in methanol survive to several months of storage without degeneration). Embryos were gradually rehydrated washing with 75% methanol/PTW, 50% methanol/PTW and 25%methanol/PTW. Than samples, were treated with 10mg/ml proteinase K in PTW for a different amount of time (from 5 to 60 minutes) depending on the specific embryonic stage and washed twice with freshly prepared 2mg/ml glycine in PTW. After the embryos were refixed in 4%

paraformaldehyde/PTW at room temperature for 20 minutes and washed through five changes of PTW. The embryos were pre-hybridized for at least 1 hour at 65°C with hybridization buffer prepared as follow: Formamide 100% 25ml, SSC 20X (pH7.0) 12.5 ml, Heparin (50mg/m) 150 µl, Torula-RNA 250 mg, Tween20 10%. The probes were added and the samples were hybridized overnight at 65°C. After the hybridization step, embryos were washed at 65°C with 50% formammide/2xSSCT, 2xSSCT and 0.2xSSCT. Then the embryos were incubated at room temperature with a blocking solution (5% serum/PTW) for two hours in agitation. The samples were then incubated for 12 hours at 4° with 200 µl of anti-DIG antibody (1:4000 dilution). Then the samples were washed 3 times for 10 minutes with the SB solution (0.1M Tris pH 9.5, 0.1M sodium chloride, 50 mM, Magnesium chloride, 0.1% Tween). Subsequently the embryos were placed in the appropriate colour solution with specific reagents NBT / BCIP (Boehringer).

The reaction was blocked with TE/Tween 0.1% solution, the embryos were again fixed in 4% paraformaldehyde/PTW for 20 minutes, washed with PTW1X and stored in glycerol. The embryos were embedded in a mix of BSA/Gelatine and sectioned with vibratome. Bright-field images were obtained on a Leica DM-6000 microscope. Adobe Photoshop was used to adjust image brightness and contrast. A minimum of 20 embryos, obtained from independent injections, were hybridized for each marker and condition.

2.6 Immunohistochemistry

Embryos at different developmental stages were collected and fixed. The embryos were dechorionated, dehydrated and stored at -20°C in methanol 100% as in 2.5. Embryos were gradually rehydrated washing with 75% methanol/PTW, 50% methanol/PTW and 25%methanol/PTW. The samples, were treated with 10mg/ml

proteinase K in PTW for a different amount of time (from 5 to 60 minutes) depending on the specific embryonic stage and washed twice with freshly prepared 2mg/ml glycine in PTW. The embryos were then refixed 4% paraformaldehyde/PTW at room temperature for 20 minutes and washed through five changes of PBS/ 0,05% TritonX-100. Embryos were placed in the blocking solution (0,1 M phosphate buffer pH 7.2; 1% DMSO; 5% Fetal Bovine Serum FBS; 0,05% TritonX-100). Embryos were stained in toto with anti-Phospho-Histone3 antibodies (1:100) (Cell Signaling), followed by biotinylated-secondary antibodies and peroxidase-coupled streptavidin (ABC-Elite kit, Vector Laboratories). Antigen localization was detected by incubation in PBS containing 30 µg/mL DAB to which 0.003% hydrogen peroxide was added. The embryos were embedded in a mix of BSA/Gelatine and sectioned with vibratome. At least ten retinas were analyzed for each stage. The number of positive cells was normalized to the total area of retina determined with the Image-J analysis software.

For immunofluorescence OCT embedded fixed embryos were cryostat-sectioned. The sections were permeabilized boiling in citrate buffer 1 minute in the microwave. Permeabilized sections were washed with PTW, and blocked in FBS 5% / PTW for 1 hour. Sections were incubated overnight at 4°C with the following primary antibodies: α-active caspase 3 (1:500) (BD Pharmingen™), α-rhodopsin (1:10000; Sigma), α-syntaxin (1:1000; Sigma) and α-GS6 antibodies (1:500; Chemicon). Alexa-488–conjugated goat anti-rabbit or antimouse (1:1,000; Invitrogen) IgGs were used as secondary antibodies. Propidium iodide (PI) (1:1000) was added for nuclear staining. Stained sections were mounted with Vectashield (Vector Laboratories). Microscopy analysis was performed with a Leica DM6000 microscope and with Leica TCS SP2 AOBS confocal microscope. Adobe Photoshop was used to adjust image brightness and contrast. The results were obtained from four independent experiments.

2.7 TUNEL Staining

Embryos at different developmental stages were collected and fixed. The embryos were dechorionated, dehydrated and stored at -20°C in methanol 100% as in 2.5. Embryos were gradually rehydrated washing with 75% methanol/PTW, 50% methanol/PTW and 25%methanol/PTW. The samples, were treated with 10mg/ml proteinase K in PTW for a different amount of time (from 5 to 60 minutes) and washed twice with freshly prepared 2mg/ml glycine in PTW. After the embryos have been refixed 4% paraformaldehyde/PTW and washed through five changes of PBS/0,1% TritonX-100. Then embryos were permeabilized in a 0,1 % NaCitrate/0,1% TritonX-100 in ice for 15 minutes.

Embryos were processed with terminal deoxynucleotidyl transferase-mediated dUTP nick-end labeling (TUNEL) kit (Roche Diagnostics) according to manufacturer's instructions. The embryos were embedded in a mix of BSA/Gelatine and sectioned with vibratome. At least ten embryos were analyzed for each stage.

2.8 Transmission electron microscopy (TEM)

The embryos were fixed overnight at 4°C in 2.5% glutaraldehyde / 2% paraformaldehyde in PTW. The material was then rinsed in buffer and post-fixed in 1% osmium tetroxide in PBS for 1 hour at 4°C. After dehydration in a graded series of ethanol, the material was embedded in an Epon-Araldite mixture. Ultrathin sections, obtained with a Leica Ultracut UCT, were routinely stained (5% uranyl acetate following by 1% lead citrate) and observed with a JEOL-JEM-1011 transmission electron microscope operating at 100 kV.

2.9 Detection of ROS levels

Reactive oxygen species (ROS) accumulation, assessed by the levels of the oxidized form of the cell-permeant ROS indicator acetyl ester of 5- (and 6-) chloromethyl-2',7'-dichlorodihydrofluorescein diacetate (CM-H_2DCFDA) (Invitrogen), was detected in live fish as follows. Injected embryos at stage 24 were *in vivo* dechorionated, several groups of three embryos were put in the wells of a 96-well plate, and excess medium was removed using a fire-polished glass Pasteur pipette. Embryos were incubated in 1 µg/ml CM-H_2DCFDA for up to 2 h, and the fluorescence was measured with the Fluoroscan Ascent FL plate reader (Thermo) (excitation 485 nm, emission 520 nm) after every 10 min. The spontaneous oxidation of CM-H_2DCFDA was monitored in the wells without fish, and the levels were low and did not change with time. H_2O_2 solution served as a positive control.

3. RESULTS

3.1 Identification and characterization of ol*hccs*

To identify the ol*hccs* gene, we performed BLAST searches with the human HCCS protein sequence (NP_005324 [GenBank]) in the Ensembl madaka database and identified putative ol*hccs* transcripts, which were confirmed by PCR cloning and sequence analysis. ol*hccs* encodes for two transcript variants (ol*hccs*a and ol*hccs*b) derived from an alternative splicing; the predicted proteins of 281 aa and 258 aa differ in the N-terminal portion and shown respectively 64% and 69% of identity with the human HCCS protein (Figure 12 and Figure 13 A.). In order to analyzes the expression patter of the gene in medaka we performed an *in situ* hybridization (ISH) analysis using a probe that is able to recognize both transcripts: according with the human and mouse *hccs* expression data (Ramskold et al., 2009; Schaefer et al., 1996; Schwarz and Cox, 2002; Franco, unpublished data), ol*hccs* seems to be ubiquitously expressed but a very strong expression is detectable in muscles, heart, CNS (Figure 13 B-D) and in the eye where the expression is evident from early stages (stage 24) (Figure 13 E). The expression of *olhccs* continued throughout the development and at stage 38, when the retina is fully differentiated, becomes more specific for the ganglion and amacrine cell layers, and for the ciliary marginal zone (CMZ) , although lower level of transcripts are also detectable in other layers (Figure 13 F-H).

3.2 Knockdown of ol*hccs* results in a specific phenotype recapitulating the human MLS condition

To determine and analyze the ol*hccs* function during development we employed antisense morpholinos (MO) to achieve functional gene knockdown. We used three different MOs designed against the 5'UTR of the two transcript variants

ol*hccs*a and ol*hccs*b (ol*hccs*a-MO and ol*hccs*b-MO) and against the first common splice donor site (ol*hccs*-MO). The olhccs-MO is predicted to downregulate both transcripts. These MOs were independently injected at 1–2 cell stage and then the embryos were phenotypically analyzed.

Injection of ol*hccs*-MO resulted in a very severe phenotype and about the 80% of fish die before the gastrulation stage. Injection of both ol*hccs*a-MO and ol*hccs*b-MO induce in the fish defects that resemble the human MLS condition: the embryos show a severe ocular phenotype with microphtalmia, alteration of RPE, and coloboma in 50% of cases (Figure 14 A-C, I). In particular reduction in eye size was evident starting from stage 24 and the eyes treated with ol*hccs*a-MO showed a reduction in size of about 50% compared with the size of the eyes of the uninjected controls at stage 38 (Figure 14 G). These defects are associated also with microcephaly and a cardiovascular pathology consisted of significant pericardial edema, bradycardia (reduced heart rate), ventricular asystole (failure to contract), and failure to develop into a loop (red arrows in Figure 14 H-I). These defects were progressive, eventually leading to death after stage 38.

Of note, injection of ol*hccs*a-MO and ol*hccs*b-MO yielded indistinguishable phenotypes. The ol*hccs*a-MO was thus used for analysis and quantization in all subsequent experiments, with all phenotypic observations additionally verified using the ol*hccs*b-MO. To ensure the specificity of the ol*hccs*a-MO, we performed all the appropriate control experiments (Eisen and Smith, 2008). We were able to rescue the phenotype by coinjecting the MO with the wt ol*hccs* mRNA and this experiment demonstrate that all the defects observed in the injected embryos are due to specific downregulation of ol*hccs* (Figure 14 D). In addition, a mismatch MO with five base substitutions in its sequence (ol*hccs*a-mmMO) did not show any phenotype at an equivalent dose (Figure 14 E).

Finally, it has been proposed that an activation of p53 could represent a non specific off-target effect of some MOs (Robu et al., 2007). In this case the phenotype can be rescued by co-injection of the morpholino against the sequence under study and that of p53 (Eisen and Smith, 2008). We thus co-injected ol*hccs*a-MO with p53-MO (Conte et al., 2010b) and no amelioration of the phenotype was observed (Figure 14 F) indicating that in this case the activation of p53 is not involved in the observed phenotype.

To further ensure that ol*hccs*a-MO was blocking the translation of ol*hccs*, we constructed and coinjected with the ol*hccs*a-MO a GFP reporter, where the coding region of the GFP was fused to the 5'UTR of ol*hccs*a (ol*hccs*a-GFP) (Figure 15 A). If the ol*hccs*a-MO binds the target sequence and represses translation of the GFP, the embryo would lack green fluorescence. To obtain a quantitative measurement of the repression of GFP by the MO, RNA coding for RFP was also coinjected and the green/red fluorescence ratio was quantified as previously described (Conte et al., 2010b; Esteve et al., 2004). As illustrated in figure 15 C a reporter GFP fused to the 5'UTR of ol*hccs*a, was translationally repressed when coinjected with ol*hccs*a-MO. However, when the same GFP construct was coinjected with ol*hccs*a-mmMO, it was not able to repress the translation of the GFP (Figure 15 D) further supporting the specificity and quality of our controls.

Together, these results demonstrate that ol*hccs*a-MO is specifically able to inhibit translation and therefore abolish the function of ol*hccs*a *in vivo*, and that this leads to the induction of a specific phenotype resembling the human MLS condition.

3.3 Knockdown of ol*hccs* leads to an increase of apoptosis.

The microphthamia is a one of most common defects associated with *HCCS* mutations (Sharma et al., 2008; Wimplinger et al., 2006; Wimplinger et al., 2007).

In order to understand the molecular basis leading to a microphthalmic phenotype in the absence of HCCS, we start to analyze the different processes that could be involved in the onset of this ocular defect.

The hypothesis would be that the size of the eye may be affected either by a decrease in cell proliferation or by an increase in apoptosis. Analysis at stages 24 and 30 of phosphorylated histone-H3 (pHH3), a marker of dividing cells (Saka and Smith, 2001), showed no significant difference between the ol*hccs*a-MO-injected and the control embryos in the number of proliferating cells in the eye (Figure 16 A-E). At stage 38 the proliferation rate is even increased in the ventral portion of the retina as showed by pHH3 immunohistochemistry (IHC) and *in situ* hybridization (ISH) analysis of markers of proliferation cyclin D1 and Ath5 (Figure 16 F-K).

In contrast, the analysis of cell death by TUNEL staining clearly demonstrated that apoptosis was significantly increased in the eye of ol*hccs*a knockdown embryos (Figure 17). Furthermore, the increase in apoptosis due to ol*hccs*a knockdown is evident from early stages (stage 24), and interestingly worsen during the development of the fish along with the worsening of the microphthalmic phenotype observed. The microphthalmia become very dramatic at stage 38 when the retina is fully differentiated and no apoptosis could be observed in control embryos as by this stage the differention of the retina is complete (Figure 17 A-F,I).

In order to confirm this data we performed an immunofluorescence analysis with an antibody able to recognize the active form of caspase 3. The “executioner” caspase 3 is a key member of most apoptotic pathways and its activation leads to the cleavege of a variety of substrates, including DNA fragmentation factors and cytoskeletal elements, resulting in the ordered destruction of the cell. As depicted in Figure 17 H a great numbers of caspase-3-active positive cells are observed in

the retina of morphant embryos, confirming that an increase of apoptosis is associated to hccs deficiency.

Moreover these results indicate that ol*hccs* inactivation is associated to caspase-dependent increased cell death and suggest that the microphthalmic phenotype observed in ol*hccs*a knockdown embryos could be due to an increase of apoptosis rather than a decrease in cell proliferation.

Notably, no apoptotic cells were detected in the heart of ol*hccs*a-MO-injected embryos (Figure 18). These results are in accordance to what previously reported in a heart-specific conditional knockout mouse model of *Hccs* (Drenckhahn et al., 2008) and in a zebrafish model of OXPHOS deficiency (Baden et al., 2007), suggesting that the cardiac phenotype observed in ol*hccs*a-MO-injected embryos could be due to an energy failure and not to pathological changes caused by cell death.

3.4 The microphthalmic phenotype is caused by activation of Mitochondrial-Dependent cell death pathway

Apoptosis is strictly connected to the pathogenesis of many human diseases, including developmental, neurodegenerative or cardiovascular diseases.

To test whether the increase in apoptosis is the main cause of the microphthalmia observed in our model, we coinjected a general Caspase inhibitor (Z-VAD-FMK) with ol*hccs*a-MO and analyzed the effect on the size of the eye. Notably, the ZVAD-FMK was able to fully rescue the microphthalmic phenotype. In addition, TUNEL assay showed no significant difference in the number of apoptotic cells between the embryos coinjected with Z-VAD-FMK and ol*hccs*a-MO, and the control embryos (Figure 19 A,C,F). This data clearly demonstrate that a caspase-

dependent cell death pathway is responsible for the microphthalmic phenotype observed in our model.

In order to elucidate which pathway was involved in the activation of the caspase cascade, we tested two different specific Caspase inhibitors (Caspase 1 and Caspase 9) for their ability to rescue the apoptotic phenotype in morphant embryos. While the inhibitor of caspase 1 did not display any effect, the Caspase 9-specific inhibitor, Ac-LEHD-CMK, was able to fully rescue the microphthalmia (Figure 19).

The initiator caspase 9 is one of the most important members of the mitochondria-mediated cell death pathway and its activation in response to *hccs* knock-down strongly suggested the involvement of the "intrinsic pathway" in the onset of microphtalmia. To test this hypothesis we tried to rescue the phenotype by the over-expression of the anti-apoptotic gene *Bcl*-xL. The protein encoded by this transcript belongs to the BCL-2 protein family and is located at the outer mitochondrial membrane where regulates the opening of the outer mitochondrial membrane channel (VDAC). As expected, the over-expression of *Bcl*-xL was also able to rescue the microphthalmia confirming an activation of the intrinsic cell-death pathway (Figure 20).

Together these results clearly indicate the involvement of Mitochondrial-Dependent cell death pathway in the onset of the microphthalmic phenotype associated to ol*hccs* down-regulation.

3.5 ol*hccs* down-regulation leads to activation of caspase 9 in an apopotosoma-independent manner.

Our data demonstrated that the downregulation of ol*hccs* leads to an increase of Mitochondrial mediated apoptosis which is responsible for the onset of the

microphtalmic phenotype. In particular we showed that an activation of “initiator” caspase 9 underlie this process.

Detailed studies of the mechanisms underlying intrinsic apoptosis have shown that the heme group of cytochrome c is necessary for Apaf1 activation, apoptosome formation and caspase 9 activation (Martin and Fearnhead, 2002). However, as described in the introduction, recent models propose that the activation of caspase 9 can occur in a apoptosome-indipendent manner. We thus decided to test if in our model an apoptosoma-independent caspase 9 activation can occur by looking at the effects of *Apaf1* down-regulation in ol*hccs*a-MO injected embryos.

To achieve a functional gene knockdown we designed morpholinos against the ol*Apaf*1 5’UTR (ol*Apaf*1-MO). ol*Apaf*1-MO and ol*hccs*a-MO were coinjected at 1–2 cell stage and then embryos were analyzed by TUNEL assay.

Interestingly, our results showed that *Apaf*1 down-regulation was not able to block the apoptotic cascade and to rescue the microphtalmic phenotype (Figure 21), thus indicating that in our model the activation of cell death is mediated by an apoptosome-independent caspase 9 activation.

3.6 Impairment of mitochondrial function and overproduction of reactive oxygen species (ROS) in ol*hccs* knockdown embryos.

Mitochondria have long been known to be critical for cell survival due to their role in energy metabolism and for their pivotal role in progression through apoptotic pathways. HCCS acts binding heme to cytochrome c and c1 (Bernard et al., 2003; Schwarz and Cox, 2002) and the holo-form of proteins are necessary for their activity. We thus, analyzed the effect of HCCS deficiency on mitochondrial functions.

For this purpose in collaboration with Dr. I. Ferrero and Dr. P. Goffrini (University of Parma) we performed HCCS complementation studies in yeast.

We used a strain, of *Saccharomyces cerevisiae* mutant deficient for the *HCCS* orthologue *Cyc3* which is not able to grow on non-fermentable carbon sources like glycine. In this condition, the cell can't use glycolysis but needs mitochondrial oxidative phosphorylation to produce ATP. The respiratory growth can then be restored transforming the yeast with *Cyc3* or *HCCS* (Bernard et al., 2003; Schwarz and Cox, 2002; Wimplinger et al., 2006) (Figure 22 A).

The analysis of the cytochromes absorption spectra shows that both cytochromes c and b, and $a+a_3$ (component respectively of Complex III or Complex IV of mitochondrial respiratory chain) were reduced, indicating a block at the distal end of the respiratory chain (Figure 22 B).

Analysis of OXPHOS complexes activity in *hccs*-deficient medaka embryos are still in progress in collaboration with Prof. M. Zeviani at Carlo Besta Institute of Neurology, Milan. Nevertheless, as expected from an OXPHOS-deficient tissue, Transmission Electron Microscopy (TEM) analysis on morphants retina shows the presence of abnormal mitochondria, with internal disorganization of the cristae (Figure 23). This result further supports the key role of *hccs* in the physiology of fish mitochondria.

It has been demonstrated that when the respiratory chain is inhibited downstream of complex III, electrons coming from succinate oxidation could also lead to superoxide anion generation by reverse electron transport from Complex II to Complex I (Lambert and Brand, 2004; St-Pierre et al., 2002). Moreover ROS production increases when electron transport is reduced, which occurs at low respiratory rates (Korshunov et al., 1997) or in pathological situations (Wallace, 2005). We thus checked the production of ROS in hccs-deficient embryos and, as expected, ol*hccs* morphants showed increased levels of ROS, as detected by

accumulation of oxidized CM-H_2DCFDA probe *in vivo* (Figure 24). Intracellular oxidation of CM-H_2DCFDA can be caused by various reactive species, including H_2O_2, peroxy products, peroxyl radicals, and singlet oxygen. Excessive ROS production can lead to oxidation of macromolecules and has been implicated in mtDNA mutations, ageing, and cell death (Ott et al., 2007). Interestingly, in agreement with a recent model depicted in Figure 10 (Katoh et al., 2008), the overproduction of ROS could be directly responsible for the Apaf 1-independent caspase-9 activation observed in ol*hccs* knock-down embryos.

3.7 Analysis of retinogenesis in presence of hccs dysfunction

Programmed cell death is a process of particular importance for the proper development of the CNS and the eye. Our data showed that high level of apoptosis occur in crucial stages of retina development. We thus investigated if downregulation of *hccs* can influence the proper retinogenesis and the differentiation of specific retinal cell types during eye development.

ISH and immunofluorescence analyses on differentiated retina using retinal cell type specific markers (see below) showed the presence of all the seven types of retinal cells indicating that the increased apoptosis is not specific for a particular cell type (Figure 25). We looked at the following markers: *otx2 (*marker of bipolar cells), *islet2* (marker of ganglion cells), rhodopsin (marker of photoreceptor cells), α-syntaxin (marker of connection between ganglion and amacrine cells) and GS6 (marker of Müller cells). As depicted in Figure 25 the same analysis showed that the signal for all these markers is present in the dorsal part of the retina while is absent in the ventral retina where ISH of *Ath5* and *Cyc D1* and IHC with α-pHH3 indicated an increase of cell proliferation (Figure 16 F-K). Taken together these

data demontrate that morphants display a differentiation defect of the ventral retina, although all retinal cell types seem to be present.

Our data indicated that the increased apoptosis due to *hccs* down-regulation is not specific for the ventral part of the retina. Thus, in order to understand the differentiation problem of the ventral retina, we also analyzed the expression of genes involved in dorsal-ventral pattern specification. However, ISH analysis on stage 24 embryos using specific probes for *Pax6*, *Vax2*, *Tbx5*, and *Bmp4*, gene involved in specification of dorsal-ventral pattern, do not show changes in the their expression (Figure 26). These data suggest that in ol*hccs*-deficient embryos the dorsal-ventral pattern is not affected and further experiments will be necessary to explain the phenotype observed in the ventral retina.

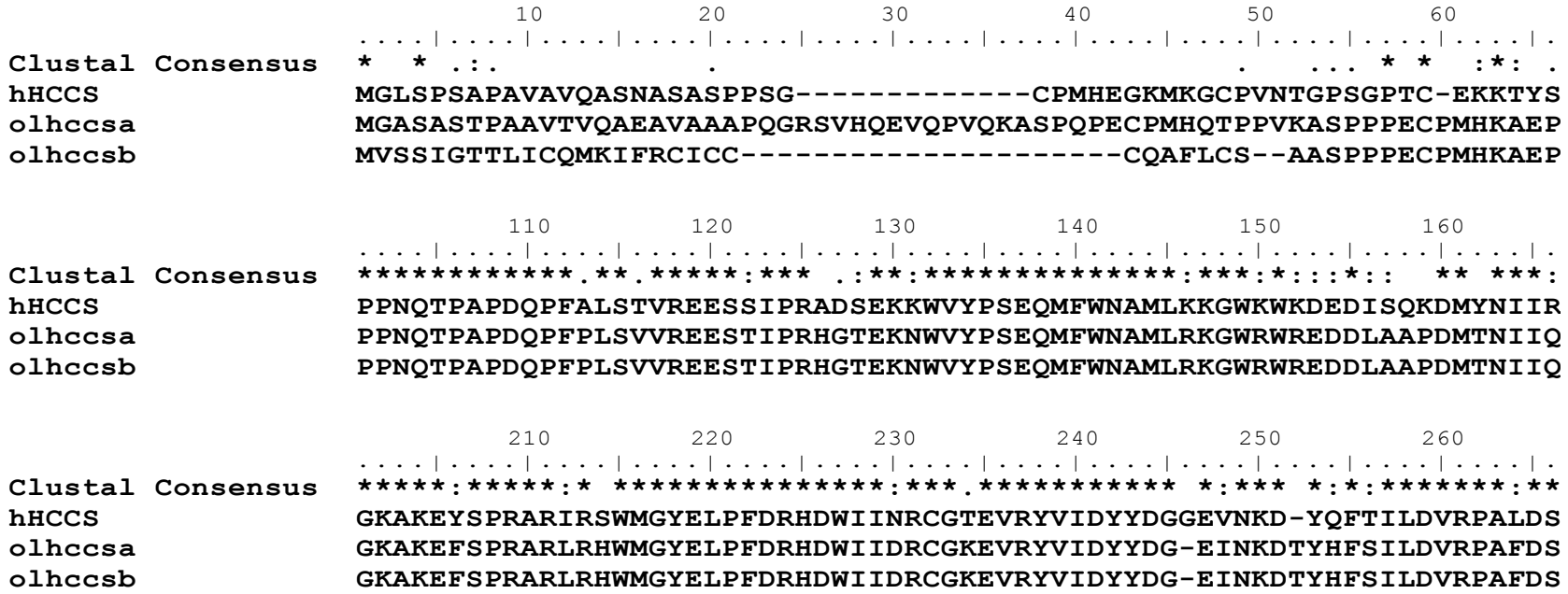

Figure 12. ClustalW multiple alignment of the human (hHCCS) and the two medaka (olhccsa and olhccsb) HCCS amino acid sequences.

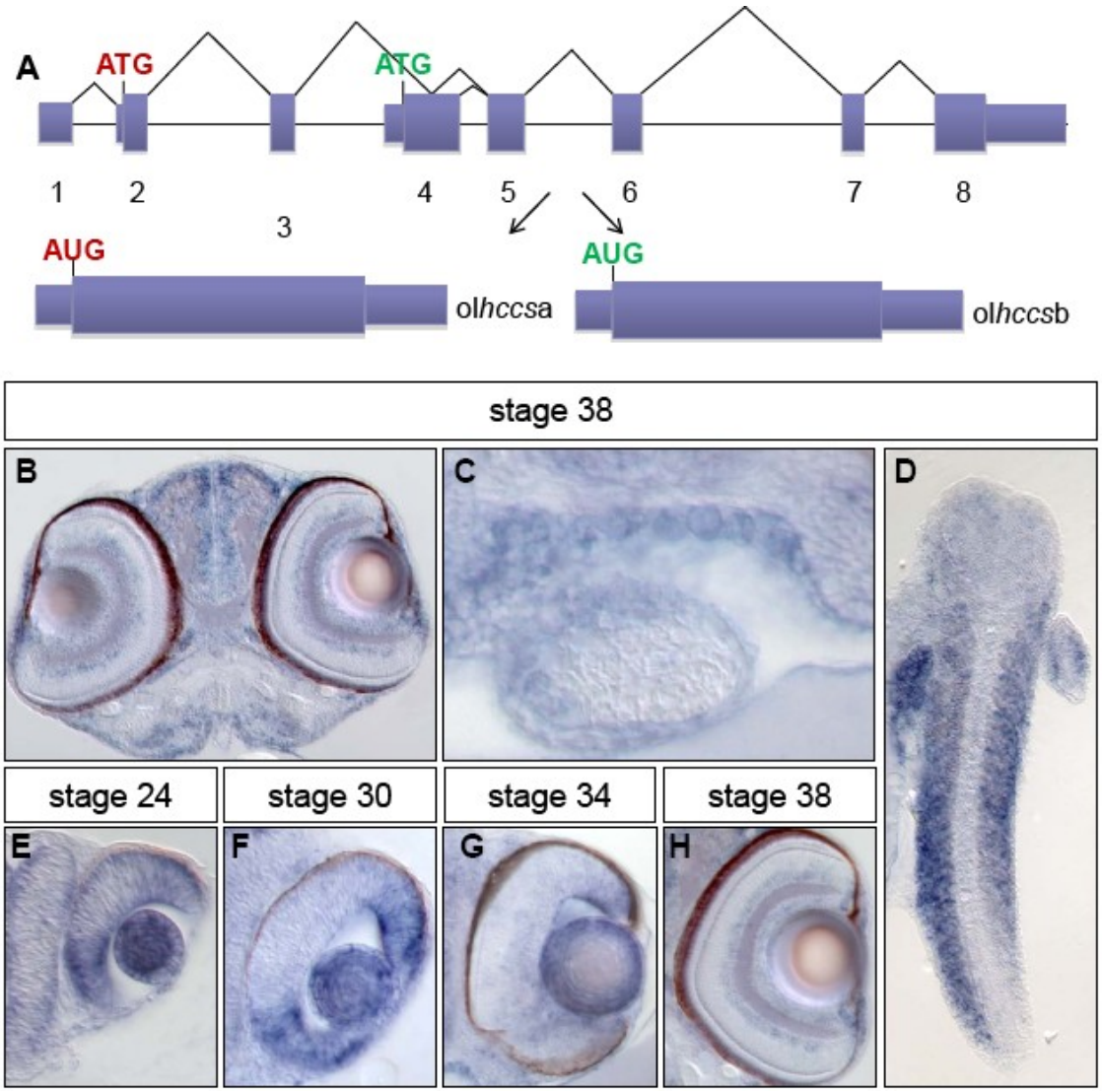

Figure 13. Structure and expression of the ol*hccs* transcripts in medaka.
(A) Structure of the olhccs transcript in medaka: exon/intron gene organization and the two alternative mRNAs identified by RT-PCR are displayed. (B-H) ISH analysis of ol*hccs* using a probe that is able to recognize both transcripts. (B,C) Frontal sections of medaka wild-type embryos at stage 38 showing a strong ol*hccs* expression in different CNS structures and in the heart, respectively. (D) Sagittal section of medaka wild-type embryos at stage 38 showing the expression in the muscles. (E-H) Frontal sections of medaka wild-type embryos at stages 24, 30, 34 and 38 showing a strong ol*hccs* expression in the different structures of the developing eye.

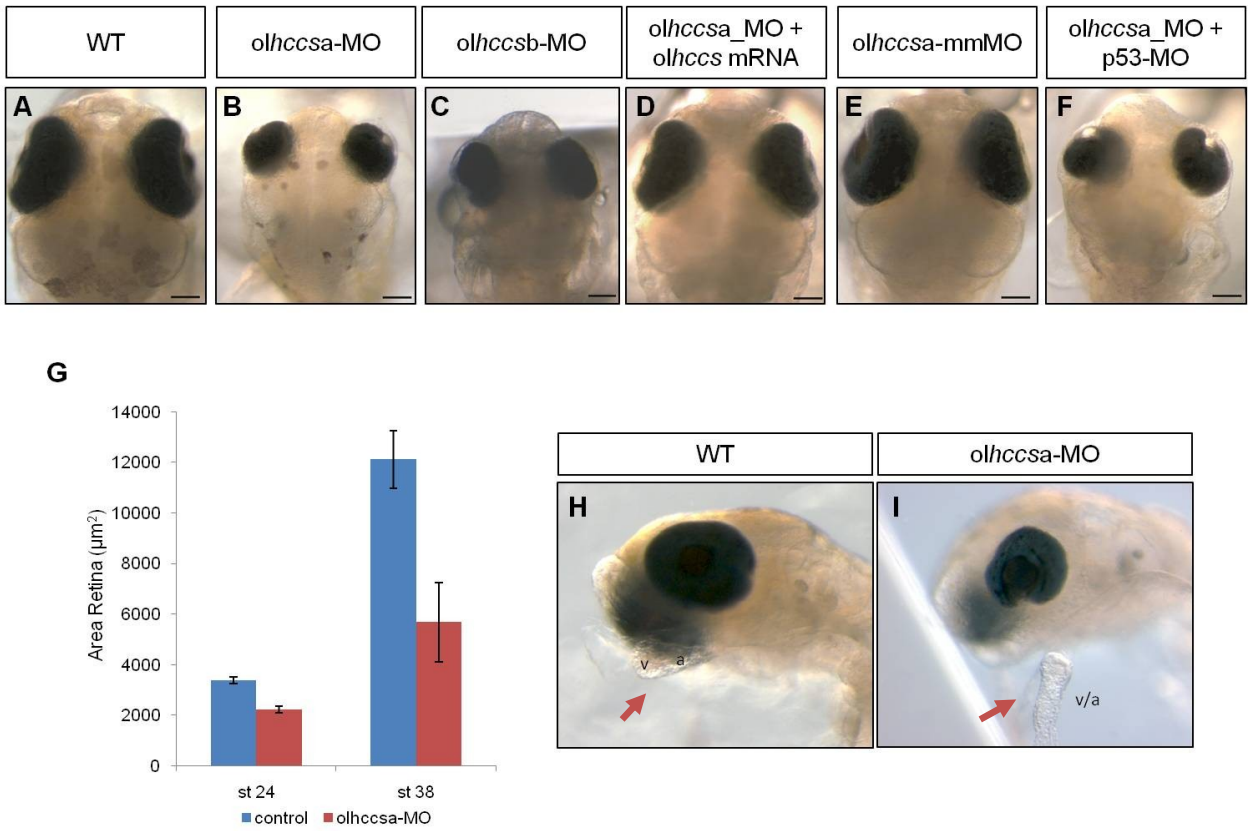

Figure 14. Effects of the morpholinos injections in medaka embryos. Bright-field stereomicroscopy images of wild-type embryos (A,H) and of ol*hccs*a-MO (B,I), ol*hccs*b-MO (C), ol*hccs*a-MO + ol*hccs*a mRNA (D), ol*hccs*a-mmMO (E), ol*hccs*a-MO + p53-MO (F) -injected medaka embryos at stage 38. A-F dorsal view. H-I lateral view. The embryos injected with morpholinos display a phenotype resembling the human MLS condition. The ocular phenotype includes microphthalmia (B,C,I), coloboma (black arrow) (I). (G) Retinal dimension analysis at stages 24 and 38. The ocular defects are associated with microcephalia (B,C,I) and cardiac defects (red arrows) (I). In wild-type embryos, the ventricle is looped behind the atrium (H). In hccs-deficient embryos the heart is not looped and is surrounded by pericardial edema (I). a, atrium; v, ventricle.

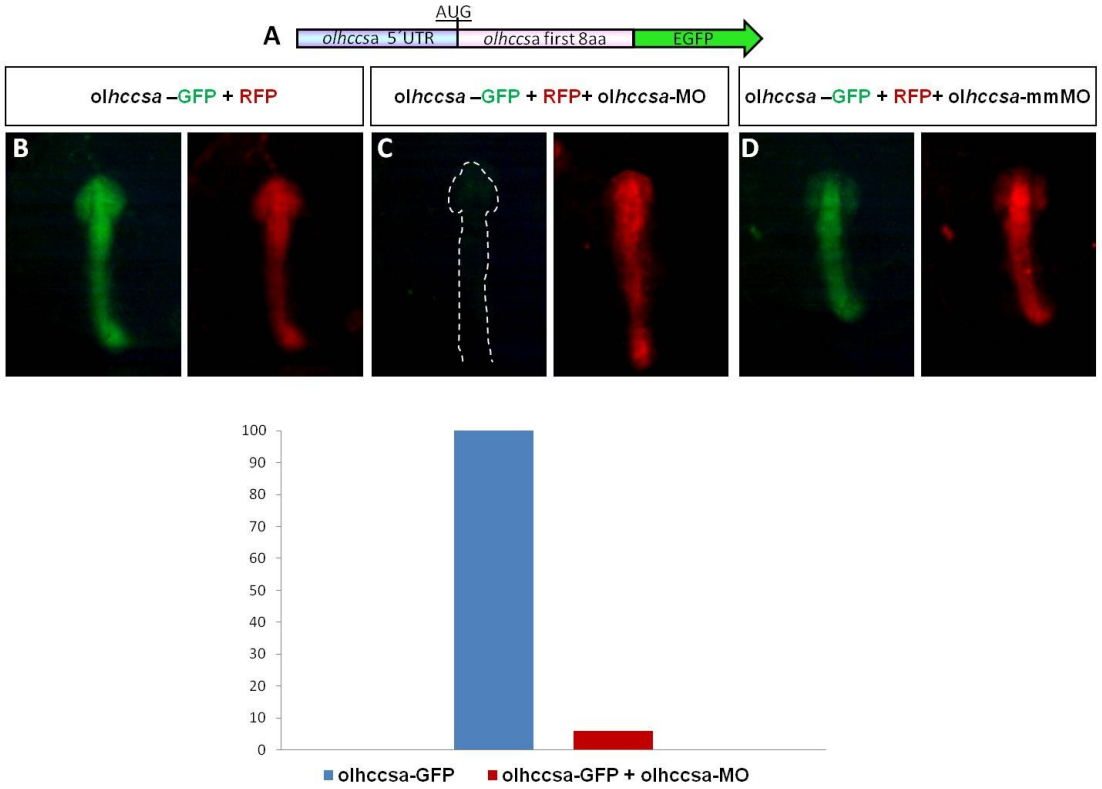

Figure 15. Morpholinos against ol*hccs*a efficiently interfere with its translation. (A) Schematic representation of the construct (ol*hccs*a-GFP) used to test the efficiency of ol*hccs*a-MO: the construct contained the 5′ portion of ol*hccs*a gene fused in frame with the GFP coding region. (B–D) Dorsal views of stage 19 embryos injected with RFP and ol*hccs*a-GFP mRNA alone (B) or in association with ol*hccs*a-MO (C), or with a control morpholino containing five mismatches with respect to the original ol*hccs*a-MO sequence (ol*hccs*a-mmMO) (D). Note how ol*hccs*a-MO but not ol*hccs*a-mmMO, significantly inhibits GFP expression. (E) Percentage of inhibition, quantified by GFP/RFP intensity using Adobe-Photoshop software.

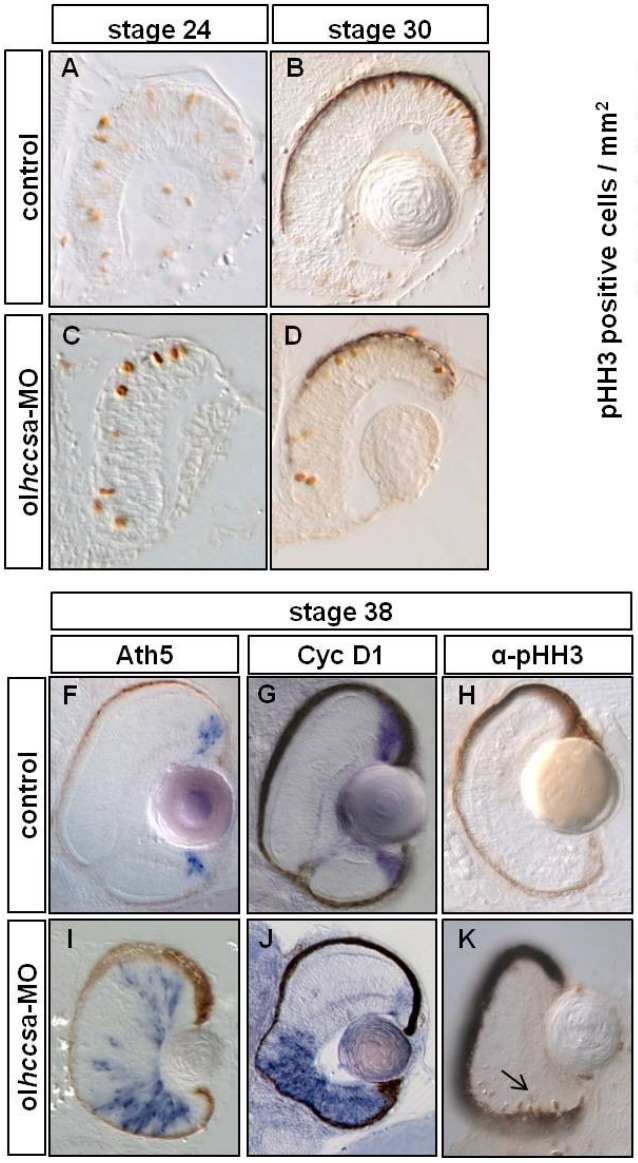

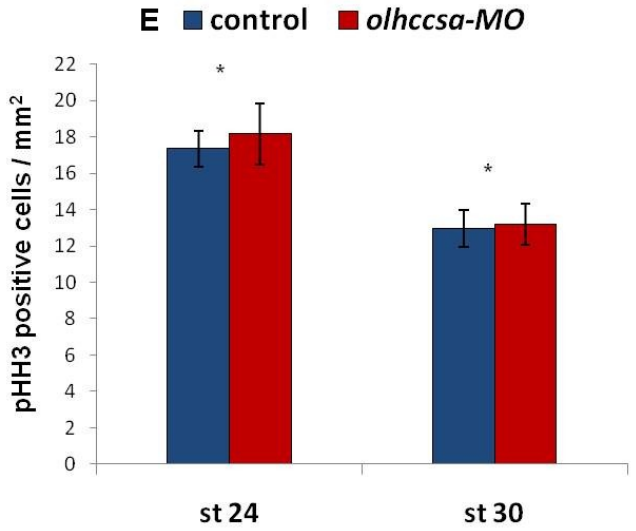

Figure 16. Analysis of cell proliferation in hccs-deficient embryos. (A-D, H, K) Immunochemistry with α-pHH3. (A,B,H) Controls. (C, D, K) Embryos injected with ol*hccs*a-MO. (E) Number of pHH3-positive cells normalized for area. At stages 24 and 30 morphant embryos do not show abnormalities in cell proliferation (n = 10 embryos per stage, * $p < 0,05$). At stage 38, contrary to what observed in control animal (H), cell in mitosis in the ventral part of the retina (arrow) can still be observed in mutant embryos (K).
(F,I G,J) *In situ* hybridization analysis of Ath5 and CycD1. (F, G) Controls. (I,J) Embryos injected with ol*hccs*a-MO show an expansion of Ath5 and CycD1 expression in the ventral retina.

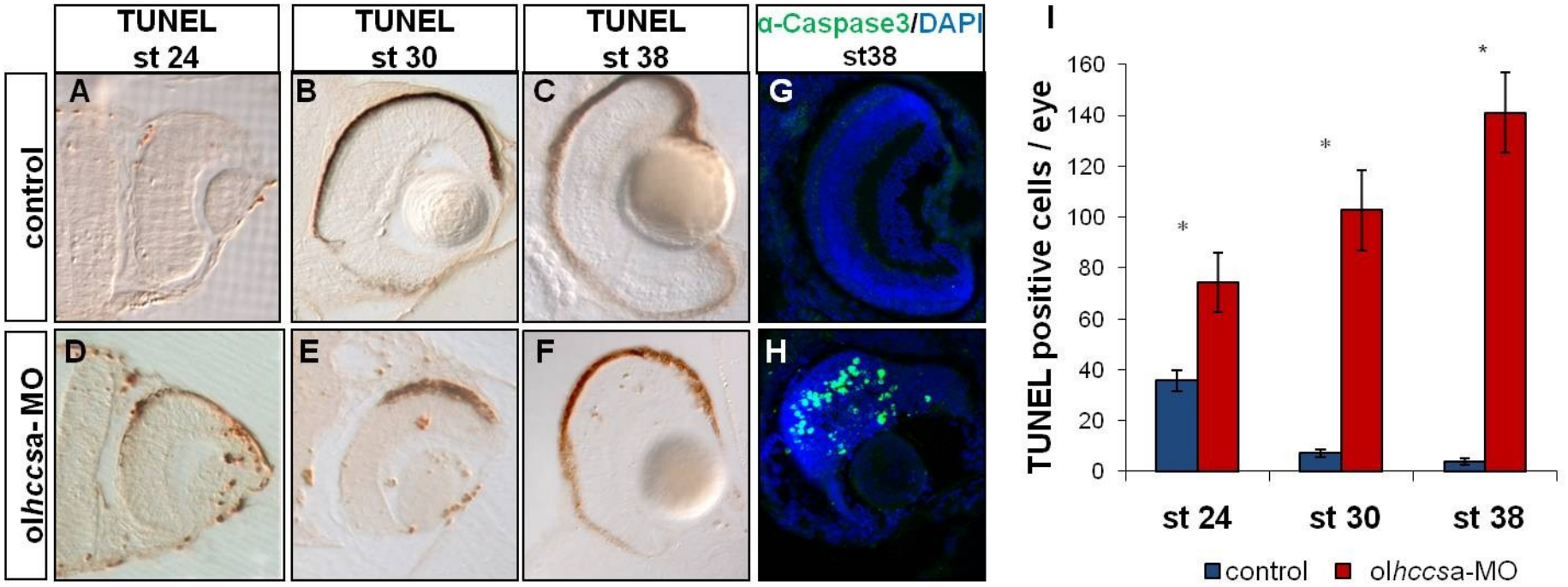

Figure 17. Increase of apoptosis in the retina of ol*hccs*-deficient embryos. (A-F) TUNEL assay. (A, B, C) Controls. (D, E, F) Embryos injected with ol*hccs*a-MO show a dramatic increase of cell death at all stages analysed. (I) Number of TUNEL-positive cells for eye (n = 10 embryos per stage, * p < 0,05). (G,H) Immunofluorescence analysis with α-active-Caspase 3 on control (G) and ol*hccs*a-MO-injected (H) embryos at stage 38.

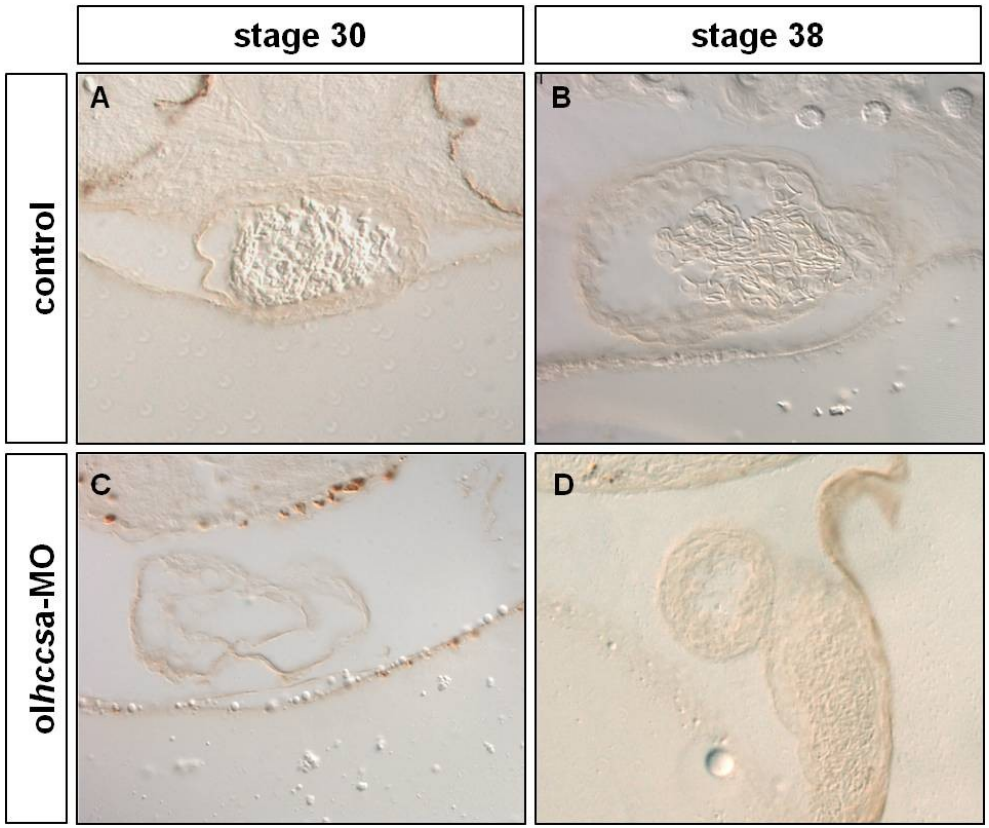

Figure 18. TUNEL assay on medaka heart. Frontal section of controls (A, B) and ol*hccs*a-MO-injected embryos (C,D) at stage 30 and 38. No alteration in programmed cell death was detected in morphant embryos.

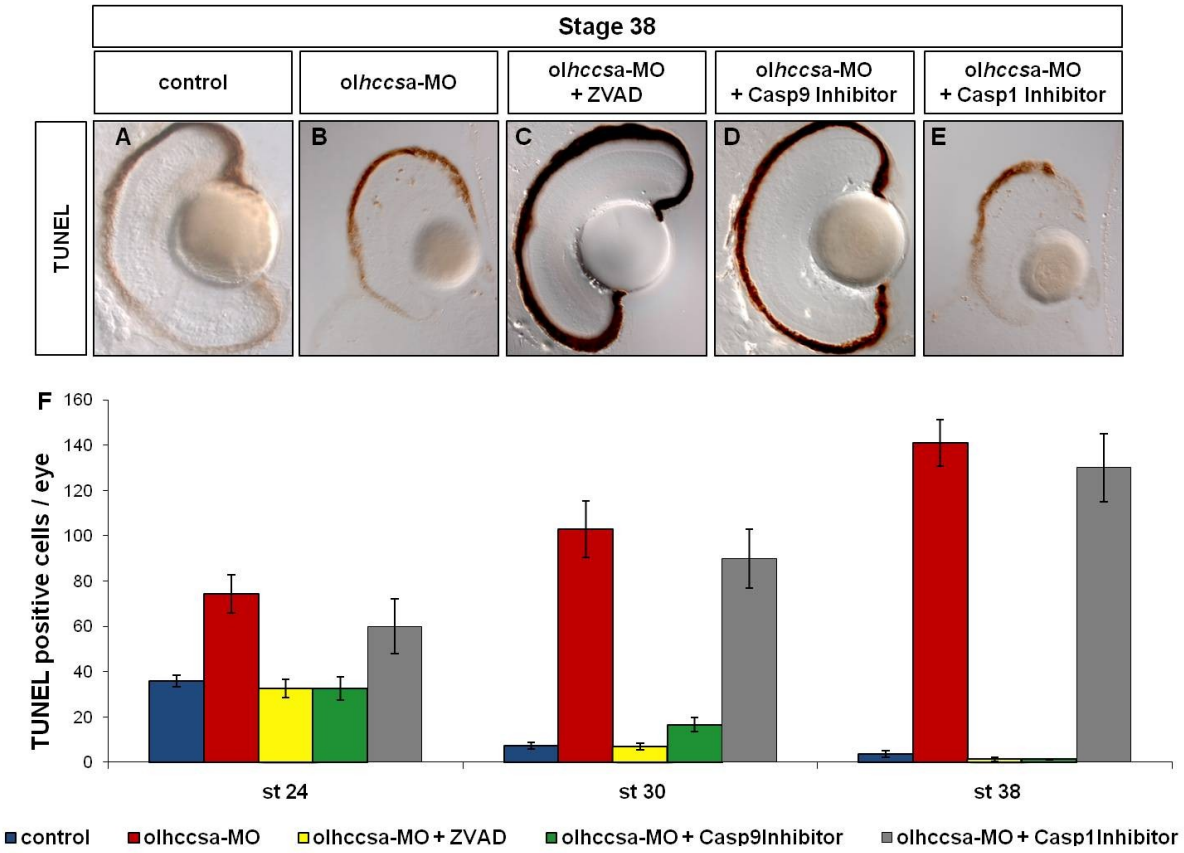

Figure 19. Coinjection of caspase inhibitors to rescue the ol*hccs*a knockdown microphthalmic phenotype. (A-E) TUNEL assay on control embryos (A) and embryos injected with ol*hccs*a-MO alone (B) or in association with a pan-Caspase inhibitor (ZVAD) (C), or with the Caspase 9 Inhibitor (D) or with the Caspase 1 Inhibitor (E) (n = 100 for each treatment). (F) Number of TUNEL-positive cells for eye (n = 10 embryos per stage). Note how only a pan-Caspase inhibitor or an inhibitor specific to Caspase 9 rescued the reduction in eye size caused by the ol*hccs*a-MO mediated increase of apoptosis.

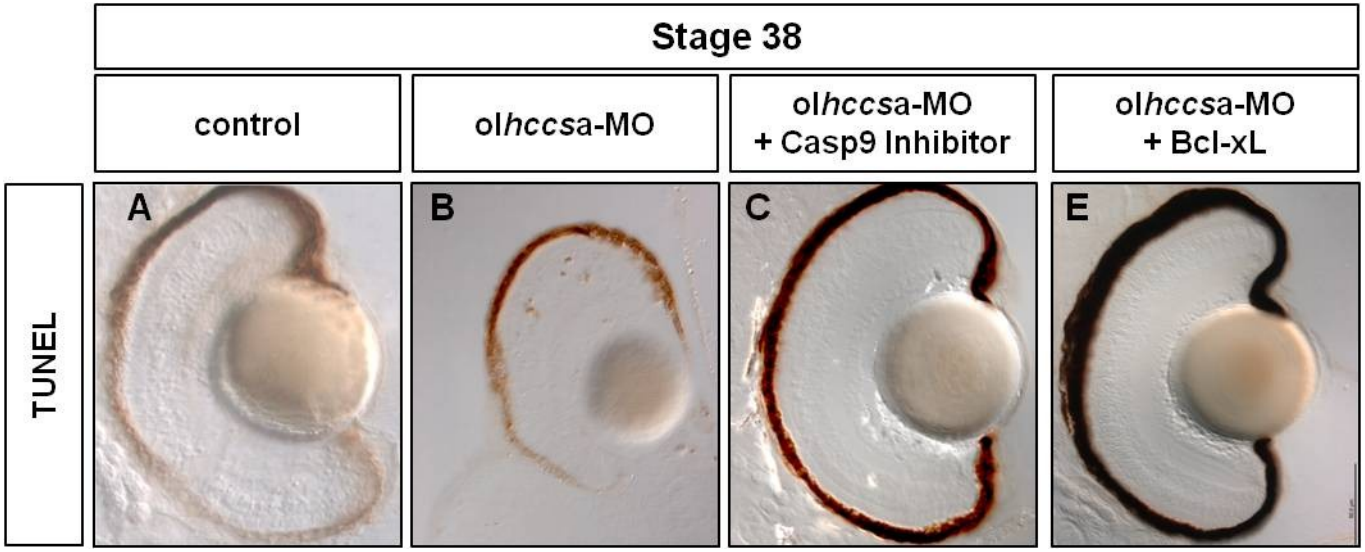

Figure 20. Involvement of Mitochondrial-Dependent cell death pathway in ol*hccs*a knockdown microphthalmic phenotype. (A-E) TUNEL assay on control embryos (A) and embryos injected with ol*hccs*a-MO alone (B) or in association with the Caspase 9 Inhibitor (C) or with the *Bcl*-xL mRNA (D) (n = 100 for each treatment).

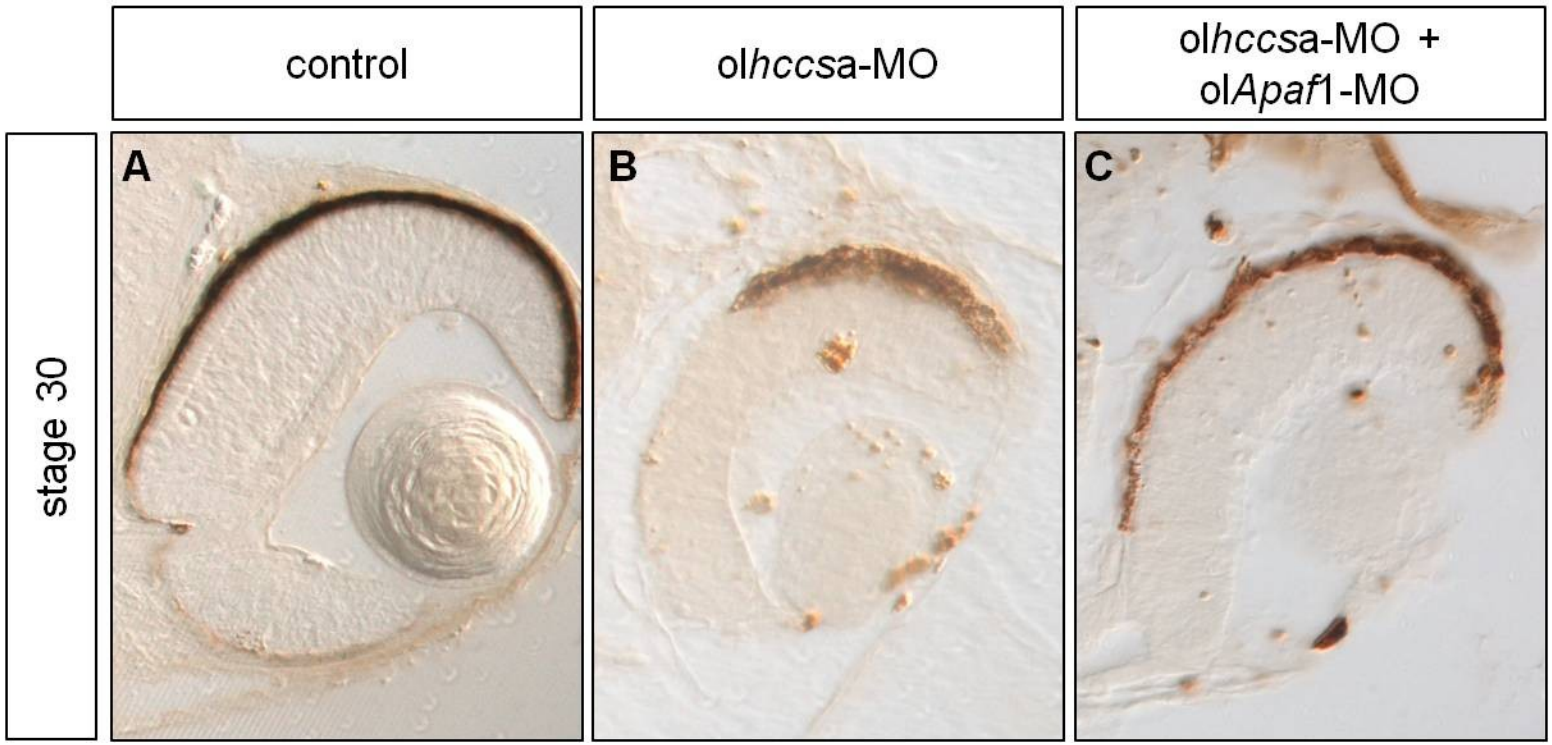

Figure 21. Apaf1-independent cell death in the retina of hccs-deficient embryos. TUNEL assay on control embryos (A) and embryos injected with ol*hccs*a-MO alone (B) or in association with ol*Apaf*1-MO. (n = 100 for each treatment).

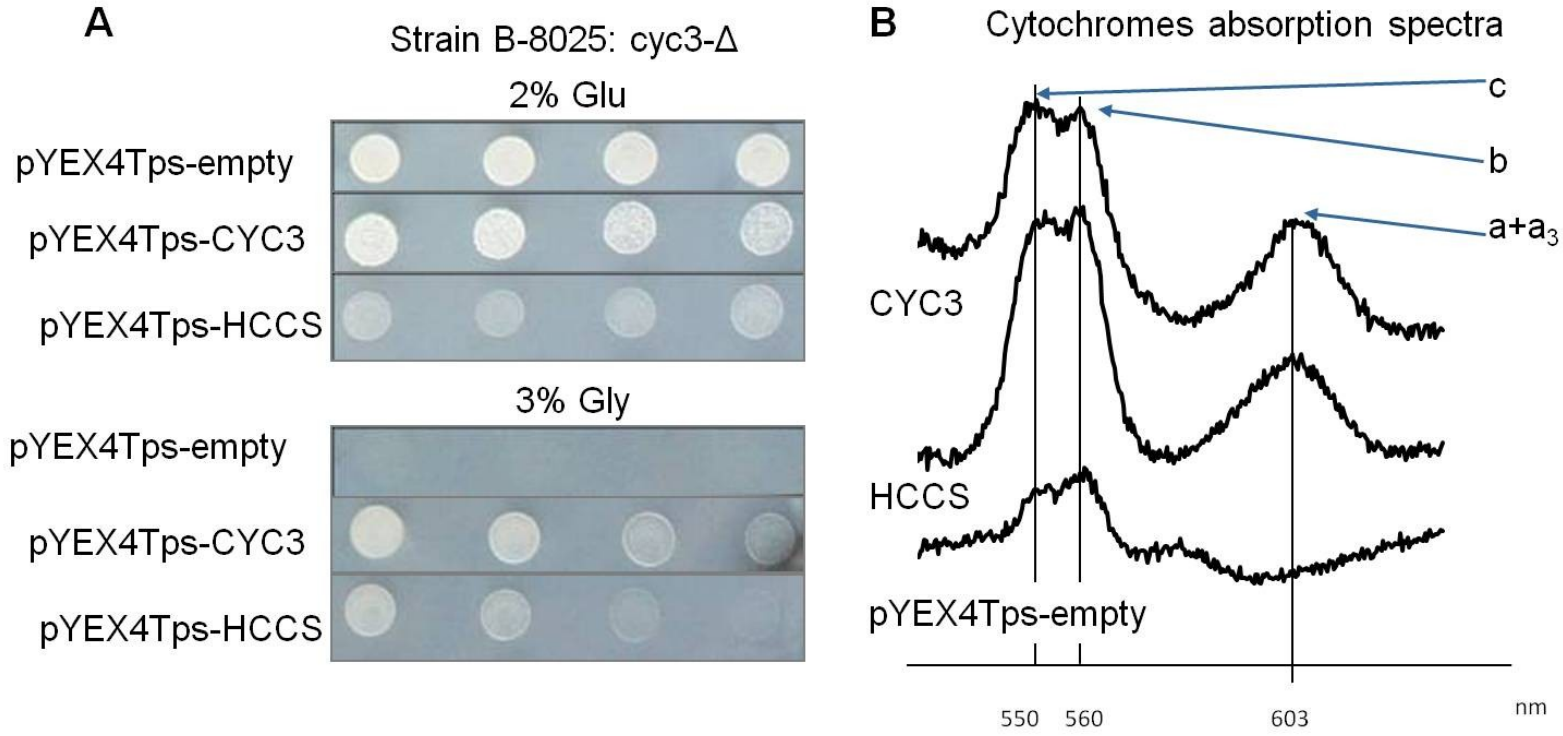

Figure 22. Impairment of mitochondrial respiratory chain in yeast. (A) The *S. cerevisiae* strain B-8025 (Cyc3Δ) was transformed with yeast CYC3, human HCCS or empty expression construct pYEX4T, and grown on fermentable (glucose) or respiratory (glycine) substrates. Note the CYC3 mutant strain is not able to grow on non-fermentable carbon sources and needs complementation to show respiratory growth. (B) Cytochrome spectra of the heme lyase mutant strain B-8025 transformed with yeast CYC3, human HCCS or empty vector. The arrows indicate the absorption maxima of the bands of cytochromes c and c1 (550 nm), b (560 nm), and $a+a_3$ (603 nm). The spectra were reduced in CYC3 mutant, indicating a block at the distal end of the respiratory chain. In collaboration Dr. I. Ferrero and Dr. P. Goffrini (University of Parma)

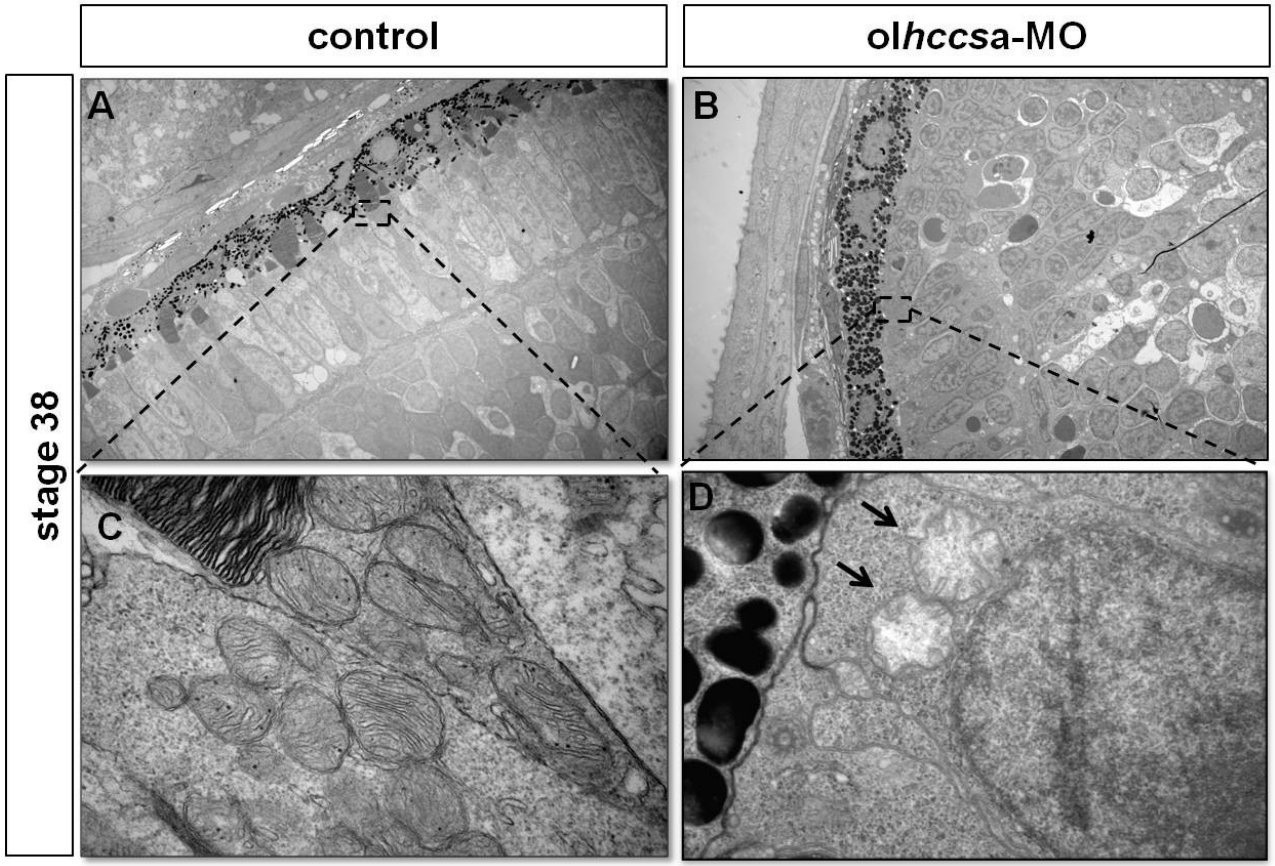

Figure 23. TEM analysis of mitochondrial morphology in hccs-deficient embryos. Retinal sections of controls (A) and ol*hccs*a-MO-injected embryos (B) at stage 38. (C,D) Magnifications showing several mitochondria in photoreceptor cells. Note the presence of abnormal mitochondria, with internal disorganization of the cristae (arrows in D) in the morphants compared to controls (C).

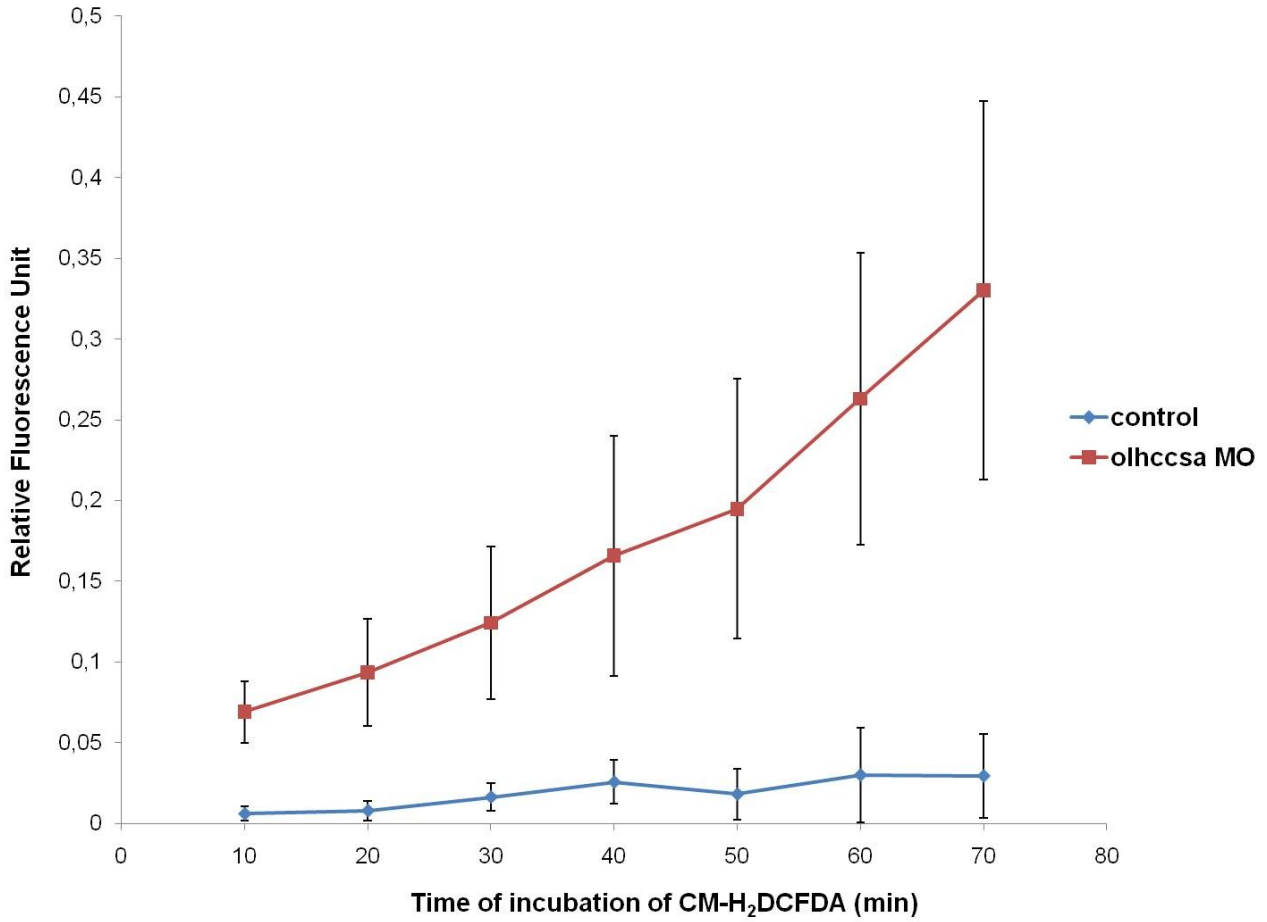

Figure 24. Detection of ROS levels in ol*hccs*a MO-injected fish. Accumulation of the CMH_2DCFDA dye, used as indicator of ROS levels, in ol*hccs*a MO-injected and control embryos at stage 24. ROS levels are increased in ol*hccs*a MO-injected fish. Values represent means of ten samples. Each sample is represented by a group of 3 fish.

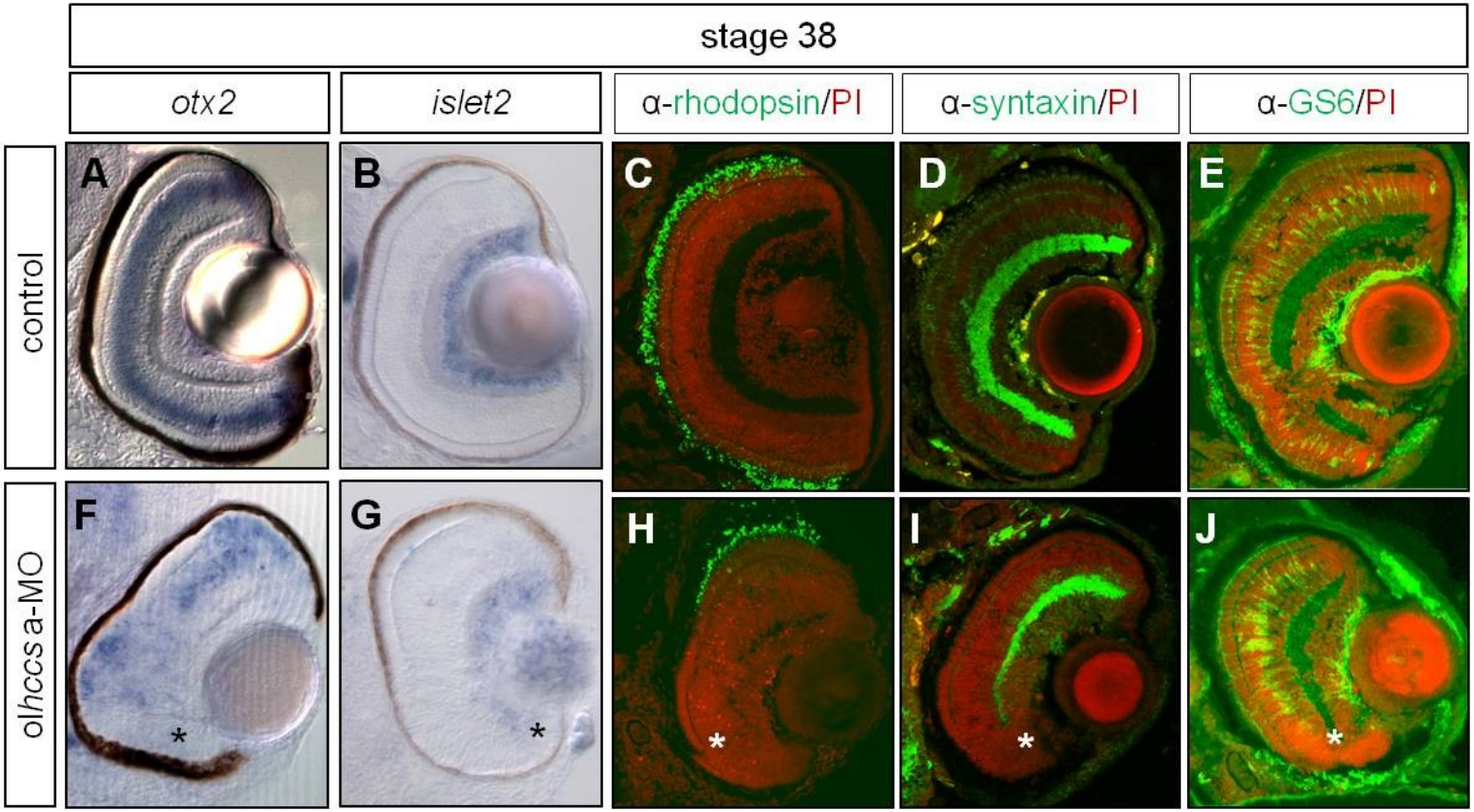

Figure 25. Analysis of retinal cells type specific markers. Retinal sections of controls (A-E) and ol*hccs*a-MO-injected embryos (F-J) at stage 38. (A,F B,G) ISH analysis to look at the expression pattern of *otx2* and *islet2*. (C,H D,I E,J) Immunofluorescence with α-rhodopsin, α-syntaxin and α-GS6 antibodies. Note the absence of all signals in the morphant ventral retina (asterisks in F-J).

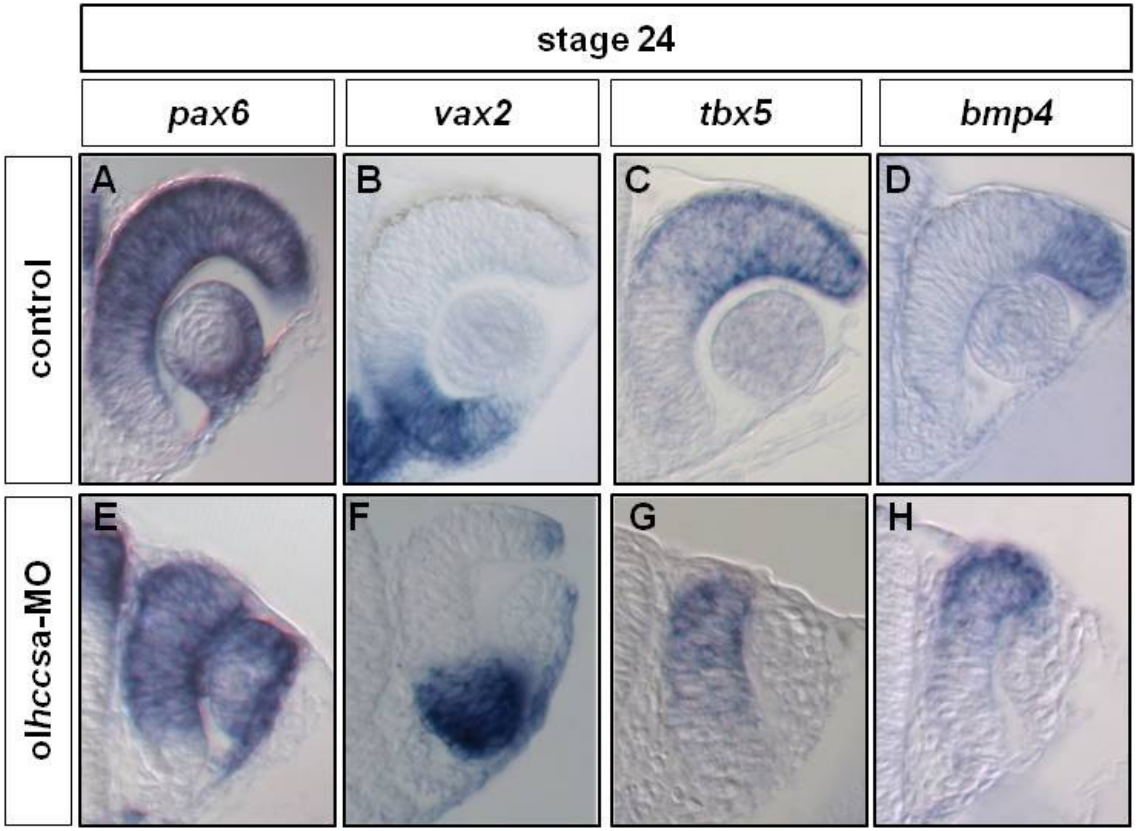

Figure 26. Analysis of dorso-ventral pattern on ol*hccs*a MO-injected fish. Retinal sections of controls (A-D) and ol*hccs*a-MO-injected embryos (E-H) at stage 24. (A,E B,F C,G D,H) ISH analysis to detect the pattern of expression of *pax6, vax2, tbx5* and *bmp4*. Injected embryos display the same pattern of expression of control embryos indicating that the dorso-ventral patterning of the retina does not seem to be perturbed.

4. DISCUSSION

Eye diseases represent one of the most common groups of genetic disorders in the human population. Over 200 different forms of ocular heritable disorders have been described and it has been estimated that about 27% of the phenotypes described in OMIM affect the eye. In the majority of conditions the pathogenetic causes of eye developmental anomalies remain very elusive. This is particularly true for Microphthalmia and Anophthalmia both characterized by major structural eye malformations. Among the genetic forms of Microphthalmia/Anophthalmia, MLS syndrome, first described in the 1990, represents one of the most puzzling genetic disorder. As fully described in chapter 1.3 MLS is a rare X-linked dominant male lethal neurodevelopmental disorder characterized by a syndromic form of microphthalmia associated to skin abnormalities (linear skin lesions), central nervous system anomalies and congenital heart defects. An high degree of intra- as well as interfamilial clinical variability has been observed in this condition possibly related to the role of X-inactivation (Franco B et al.,2006; Van den Veyver IB, 2001). In the past fifteen years, several research groups have been actively searching for the gene responsible for this disorder. The MLS critical region it has been defined by deletion mapping in the 1993 (Wapenaar et al., 1993; Wapenaar et al., 1994). However, the conclusive evidence that *HCCS* is the gene responsible for MLS syndrome have been found only in 2006 (Wimplinger et al., 2006).

HCCS encodes a mitochondrial holocytochrome c–type synthase and catalyzes the covalent attachment of heme to both apocytochrome c and c1. Functional studies demonstrated that this protein plays a critical role in mithocondrial function (Bernard et al., 2003; Schwarz and Cox, 2002)

Although mutation analysis clearly indicates a role for HCCS in the pathogenesis of this genetic condition, the molecular mechanisms underlying the developmental defects observed in the presence of HCCS dysfunction are still unknown. Previous

studies demonstrated the early lethality of *Hccs* knock-out mouse embryos (Prakash et al., 2002).

Medakafish is considered an ideal model to study developmental biology processes and in particularly the eye development (Wittbrodt et al., 2002)..

HCCS is a protein highly conserved in evolution and in particular the two proteins codified by the two transcript variants (ol*hccs*a and ol*hccs*b) identified in medaka showed, respectively, 64% and 69% of identity with the human HCCS protein. Moreover our data showed also that the *hccs* expression pattern in medaka is consistent with what has been reported concerning the expression of the HCSS transcript in human and mouse (Ramskold et al., 2009; Schaefer et al., 1996; Schwarz and Cox, 2002; Franco, unpublished data). Moreover our data, in addition to what previously reported, showed that a strong expression in the eye was evident from early stages (stage 24) and continued throughout the development. The expression become more specific, for the ganglion and amacrine cell layers, and for the ciliary marginal zone (CMZ) at later stages (stage 38), although lower level of transcripts are also detectable also in other layers. The differences in the expression of *hccs* between the different retinal cell types could be explain by a specific request in mitochondrial energy of some types of retinal cells, such as the ganglion cells in which rich accumulations of mitochondria are observed in the soma, neurofiber layer, and pre-laminar region (unmyelinated axons) (Barron et al., 2004).

Taken together this finding indicated medaka like a good model to study the hccs function and its role in the pathogenesis of MLS syndrome. We thus decided to generate a model for this disease in medakafish, where we planned to perform loss of function studies to better define the function of this gene and its role in the pathogenesis of MLS syndrome.

Moreover medaka is also a particularly amenable system model for reverse-genetic analyses. Microinjection of early embryos with either mRNA or antisense morpholino oligonucleotides results in transient gene overexpression or knockdown, respectively and allow studying a highly specific gene function, without any laborious, time and resource consuming techniques. In addition, the use of graded concentrations of specific morpholinos, directed against the alternative forms ol*hccs*a and ol*hccs*b allowed us to obtain a partial gene inactivation. Different attempts using different dose of morpholinos allowed us to establish the dose that reduces the level of *hccs* activity to a degree that impairs normal development but is not immediately lethal. This is a great advantage to study diseases, such as MLS, where the total inactivation of the gene is lethal.

Capitalizing on the characteristics of medaka, we have investigated the effects of hccs deficiency in different organ's development and function. Our results demonstrated that medaka indeed represents an informative and powerful model to study the MLS syndrome.

To determine and analyze the function of ol*hccs* during development we used three different MOs designed against the 5'UTR of the two-transcript variants ol*hccs*a and ol*hccs*b (ol*hccs*a-MO and ol*hccs*b-MO) and against the first common splice donor site (ol*hccs*-MO). Our experiments showed that the injection of the three different morpholinos resulted in a pathological phenotype, which resembles the human MLS condition: the embryos show a severe ocular phenotype with microphthalmia, alteration of retinal pigmented epithelium (RPE), and coloboma associated to microcephaly and a severe cardiovascular pathology. Not surprisingly the injection of ol*hccs*-MO, which is able to downregulate both transcripts, resulted in a very severe phenotype and about the 70% of fish die before the gastrulation stage. All suggested controls (Eisen and Smith, 2008) were employed to demonstrate that these phenotype were not secondary to injection

trauma or MO toxicity but specific to hccs deficiency. These strategy allowed as to generate an animal model which, to date, is the only animal model recapitulating the phenotype observed in MLS syndrome.

We demonstrated that HCCS, in yeast as well as in fish, is necessary for proper mitochondrial functioning and in particular that hccs-deficiency leads to a block at the distal end of the respiratory chain and to an overproduction of reactive oxidative species (ROS) which are known to be involved in oxidation of macromolecules, mtDNA mutations, aging, and cell death (Ott et al., 2007; Skulachev, 1997). These results further supprt the critical role of HCCS and expand our knowledge on the mithocondrial function of this protein. On the basis of our results we propose that MLS syndrome could be considered a mitochondrial disease. As showed in Table 3 mitochondrial diseases are a clinically heterogeneous group of disorders that display involvement of multiple organs, often with the prominent presence of clinical signs affecting the CNS and the muscles (DiMauro and Moraes, 1993). However, there are examples in which mithochondrial dysfunction affect a single organ (e.g., the eye in Leber hereditary optic neuropathy). Although neurological disorders and cardiac defects are common features of mitochondrial disorders, *HCCS* seems to be the first human gene codifying for a mitochondrial respiratory chain protein which when mutated causes microphthalmia.

We hypothesized that the eye size may be affected either by a decrease in cell proliferation or by an increase in apoptosis. Our data showed that the cell proliferation was not affected in early stages and seemed even increased in the ventral portion of the retina at later stages. In contrast our results revealed a dramatic increase in caspase-dependent apoptosis in the eye of ol*hccs*a knockdown embryos. Furthermore, the increase in apoptosis due to ol*hccs*a knockdown is evident from early stages (stage 24), and interestingly worsen

during the development of the fish along with the worsening of the microphthalmic phenotype, suggesting that deregulation of this process can underlie the onset of microphthalmia. Notably, no apoptotic cells were detected in the heart of ol*hccs*a-MO-injected embryos. These results are in accordance to what previously reported in a heart-specific conditional knockout mouse model of *Hccs* (Drenckhahn et al., 2008) and in a zebrafish model of OXPHOS deficiency (Baden et al., 2007), suggesting that the cardiac phenotype observed in ol*hccs*a-MO-injected embryos could be due to an energy failure and not to pathological changes caused by cell death.

Apoptosis is a critical process for the proper development of different organs and in particular of the CNS and the eye and is strictly connected to the pathogenesis of many human diseases, including developmental or neurodegenerative diseases (Tait and Green, 2010; Valenciano et al., 2009). Interesting, our data clearly showed that the downregulation of ol*hccs* leads to an increase of Mitochondrial mediated apoptosis. We clearly demonstrated that an activation of this pathway is the main cause of the microphtalmia in our model. Both specific inhibition of caspase 9 and overexpression of *Bcl-xL* are indeed able to block cell death in hccs deficient embryos and to completely rescue the microphthalmic phenotype observed in ol*hccs*-MO injected fish.

Activation of the initiator caspase-9 determines the induction of the mitochondrion-linked intrinsic pathway of apoptosis in response to diverse cellular stresses (Foo et al., 2005). In the original model, the formation of the ‘apoptosome’ comprising of the apoptosis protease activating factor 1 (Apaf 1), cytochrome c and procaspase-9 is assumed to be the only mechanism to convert procaspase-9 to the active form caspase-9 in the cytosol (Cain et al., 2002). Detailed studies of the mechanisms underlying intrinsic apoptosis have shown that the heme group of cytochrome c is necessary for Apaf1 activation, apoptosome formation and caspase 9 activation

(Martin and Fearnhead, 2002). However, recent data that uncouple cytochrome c, Apaf 1 and caspase-9 activation in numerous cell death models have challenged this view (Hao et al., 2005; Ho et al., 2004; Ho et al., 2007; Katoh et al., 2008; Mills et al., 2006) and suggested us that, in our model, a caspase 9 activation can occurs in a apoptosome-indipendent way.

Although the majority of studies to date have described localization of the caspase-9 enzyme within the cytosol, pro- and processed-caspase9 has also reportedly been found sequestered in the mitochondrial intermembrane space in some cell types. These molecules can then be released upon mitochondrial outer membrane permeabilization (MOMP) into the cytosol where they participate to the induction of apoptosis (Costantini et al., 2002; Ho et al., 2007; Susin et al., 1999a). To support this observation, among other data, Krajewski et al. showed the release of caspase-9 from mitochondria during neuronal apoptosis and ischemia in rat and canine models (Krajewski et al., 1999). In this conditions the caspase-9 is secluded behind the outer mitochondrial membrane and thus separated from Apaf 1, a cytosolic protein that has never been detected in the mitochondrial fraction; thus an apoptosome-independent caspase 9 activation it has been proposed. The fact that the caspase 9 may be secluded behind the outer membrane of mitochondria underlines the importance of mitochondrial membrane permeabilization as a rate limiting step of the apoptotic cascade. Anti-apoptotic members of the Bcl-2 family fully prevent the translocation of pre-processed caspase-9 from mitochondria (Costantini et al., 2002).

Interestingly, our results showed that *Apaf* 1 down-regulation was not able to block the apoptotic cascade and to rescue the microphtalmic phenotype, indicating that indeed, as we hypothesized, in our model the activation of cell death is mediated by an apoptosome-independent but Bcl-xL-dependent caspase 9 activation.

Moreover, it has been reported that requirement and coupling of caspase-9 with Apaf1 and cytochrome c are both context dependent and cell type specific (Hao et al., 2005; Ho et al., 2004; Katoh et al., 2008). This could explain the finding that the increased apoptosis is not detectable in the heart of ol*hccs*a-MO-injected embryos, but is specific for the CNS and the eyes.

Although apoptosis-inducing mechanisms distinct from the apoptosome model deserve more extensive investigation by various approaches, several possible mechanisms for caspase-9 activation without the involvement of cytochrome c and Apaf1 have been postulated: (1) the activation of a Lysosomal Cell Death Pathway (Gyrd-Hansen et al., 2006); (2) the activation of caspase-9 by endoplasmic reticulum (ER)-specific caspase-12 (Morishima et al., 2002); (3) ROS-dependent caspase-9 activation (Katoh et al., 2008; Katoh et al., 2004; Kim and Park, 2003).

The finding that overexpression of *Bcl-xL* is able to rescue the apoptotic phenotype in our model excludes the first hypothesis because activation of this pathway is bcl-independent (Gyrd-Hansen et al., 2006).

We can't completely exclude the second hypothesis because a bcl-dependent mechanism (Morishima et al., 2004) in ER-dependent apoptosis has been described (Morishima et al., 2004). Our data, however, suggested that an implication of ROS in triggering caspase 9 activation is more consistent. Indeed, in p53(-/-) mouse embryonic fibroblasts (MEFs), ER stress-induced apoptosis is almost suppressed (Li et al., 2006) while down-regulation of p53 in hccs deficient embryos does not ameliorate the microphthalmic phenotype. In addition, we observed that hccs deficient embryos displayed strongly increased levels of ROS at early stages (stage 24) and this could be directed linked to an OXPHOS impairment. It has been demonstrated that when the respiratory chain is inhibited downstream of complex III, electrons coming from succinate oxidation could also

lead to superoxide anion generation by reverse electron transport from Complex II to Complex I (Lambert and Brand, 2004; St-Pierre et al., 2002).

Moreover, it has been shown that procaspase-9 is able to homo-dimerize to gain its enzyme activity in the absence of Apaf 1 as evidenced by bacterial expression systems, *in vitro* translation and biochemical analyses (Boatright et al., 2003; Pop et al., 2006; Renatus et al., 2001; Sadhukhan et al., 2006; Srinivasula et al., 1998). In particular, procaspase-9 is dimerized by higher concentrations of kosmotropes, which are salts able to stabilize proteins, such as 1 M citrate (Boatright et al., 2003; Pop et al., 2006). Citric acid is the first product in the Krebs cycle whose reactions are controlled by the electron transfer system maintaining inner membrane potential (Δψm) for ATP synthesis. It has been showed that an hypoactive Δψm, caused by oxidative stress, leads to an accumulation of citrate, probably due to a feedback control of the Krebs cycle by the electron transfer system. The accumulation of citrate could be a cause of intra-mitochondrial caspase 9 activation (Katoh et al., 2008). Thus in this model, depicted in Figure 10, Katoh and colleagues propose that an Apaf 1-independent mitochondrial *in situ* caspase 9 activation may be caused by the major metabolic reactions (Krebs cycle) in response to physiological stresses, like the ROS overproduction. More specifically, they showed that an increased level of ROS produced from the respiratory chain can inactivate aconitase, an iron-sulfur (Fe-S) protein that catalyzes hydration of citrate at the beginning of the Krebs cycle, and thereby causes citrate accumulation in the matrix (Katoh et al., 2008).

This model could well describe what occur in hccs deficient model in which there is a constitutive block of mitochondrial respiratory chain.

Furthemore, many mitochondrial disease have been linked to ROS overproduction and this is particularly true for diseases with severe involving of CNS and eyes (Biousse et al., 2002; Liu et al., 2009; Quinzii et al., 2010; Wallace and Fan, 2009).

To clearly demonstrate that on overproduction of ROS underlie the activation of apoptosis we are currently testing the effect of same known antioxidant compounds (such as N-acetylcysteine, tyoredoxin) on the microphthalmic phenotype. Moreover tacking advantage of the fish model it should be possible to screen chemical libraries to search for new compounds with antioxidant activity.

We investigated also if the downregulation of *hccs* can influence the proper retinogenesis and the differentiation of specific retinal cell types during eye development since our data showed that high level of apoptosis occur in crucial stages of retina development. Our results indicate that in the morphants, although all retinal cell types are present, there is a differentiation defect of cells of the ventral retina. Since the increased apoptosis due to *hccs* down-regulation is not specific for the ventral part of the retina we investigated if *hccs* down-regulation could affects the dorsal-ventral pattern duing eye development. However our analysis indicate that in ol*hccs*-deficient embryos the dorsal-ventral pattern is not affected and further experiments will be necessary to explain the developmental defect observed in the ventral retina.

Conclusions

We have generated an animal model for Microphthalmia with linear skin lesions syndrome by taking advantage of the chracteristics of the medaka model. Our results revealed that the fish with downregulation of the *hccs* gene reproduce the phenotype observed in the human disease and that this model represent an informative and powerful tool to study the MLS syndrome and the effects of hccs deficiency on organ development and function. To date, this is the only animal model recapitulating the phenotype observed in MLS condition. Characterization of morphants revealed that *hccs* down-regulation results in impairment of

mitochondrial functions, overproduction of reactive oxygen species (ROS) and a strong increase of apoptosis mediated by activation of Mitochondrial-Dependent cell death pathway in the CNS and in the eyes, indicating that HCCS plays a critical role in mitochondria and that MLS could be considered a mitochondrial disease. Interestingly, our data showed that, in our model, the mitochondrial dependent apoptosis is triggered by caspase 9 activation and occur in a Bcl-dependent but apoptosome-independent manner suggesting that at least in some tissues the apoptosis can happen in a non-canonical way. Our data support the evidence of an apoptosome-independent activation of caspase 9 and suggest the possibility that this event might be tissue specific. Finally our model provides strong evidences that mitochondrial mediated apoptotic events underlie microphtalmia providing new insights into the mechanisms of this developmental defect.

5. ACKNOWLEDGEMENTS

I wish to thank Dr. Ivan Conte for scientific and technical support, Dr. Marinella Pirozzi for confocal microscopy, Dr. Rosarita Tatè for TEM analysis, the Institute of Genetics and Biophysics CNR, Naples and the Telethon Institute of Genetics and Medicine (TIGEM), Naples. I wish to thank the Company of Biologists for the Development travelling fellowship and the European Molecular Biology Organization for EMBO short term fellowship spent in the laboratory of Dr. Paola Bovolenta, Institute Cajal-CSIC Madrid, Spain. I wish to thank in particular my tutor Prof. Brunella Franco, my internal supervisor Prof. Sandro Banfi and my external supervisor Prof. Paola Bovolenta.

6. REFERENCES

al-Gazali, L.I., Mueller, R.F., Caine, A., Antoniou, A., McCartney, A., Fitchett, M., and Dennis, N.R. (1990). Two 46,XX,t(X;Y) females with linear skin defects and congenital microphthalmia: a new syndrome at Xp22.3. J Med Genet *27*, 59-63.

Altshuler, D., Lo Turco, J.J., Rush, J., and Cepko, C. (1993). Taurine promotes the differentiation of a vertebrate retinal cell type in vitro. Development *119*, 1317-1328.

Austin, C.P., Feldman, D.E., Ida, J.A., Jr., and Cepko, C.L. (1995). Vertebrate retinal ganglion cells are selected from competent progenitors by the action of Notch. Development *121*, 3637-3650.

Baden, K.N., Murray, J., Capaldi, R.A., and Guillemin, K. (2007). Early developmental pathology due to cytochrome c oxidase deficiency is revealed by a new zebrafish model. J Biol Chem *282*, 34839-34849.

Barron, M.J., Griffiths, P., Turnbull, D.M., Bates, D., and Nichols, P. (2004). The distributions of mitochondria and sodium channels reflect the specific energy requirements and conduction properties of the human optic nerve head. Br J Ophthalmol *88*, 286-290.

Beebe, D.C. (1986). Development of the ciliary body: a brief review. Trans Ophthalmol Soc U K *105 (Pt 2)*, 123-130.

Belecky-Adams, T., Cook, B., and Adler, R. (1996). Correlations between terminal mitosis and differentiated fate of retinal precursor cells in vivo and in vitro: analysis with the "window-labeling" technique. Dev Biol *178*, 304-315.

Belliveau, M.J., and Cepko, C.L. (1999). Extrinsic and intrinsic factors control the genesis of amacrine and cone cells in the rat retina. Development *126*, 555-566.

Belliveau, M.J., Young, T.L., and Cepko, C.L. (2000). Late retinal progenitor cells show intrinsic limitations in the production of cell types and the kinetics of opsin synthesis. J Neurosci *20*, 2247-2254.

Bernard, D.G., Gabilly, S.T., Dujardin, G., Merchant, S., and Hamel, P.P. (2003). Overlapping specificities of the mitochondrial cytochrome c and c1 heme lyases. J Biol Chem *278*, 49732-49742.

Biousse, V., Pardue, M.T., Wallace, D.C., and Newman, N.J. (2002). The eyes of mito-mouse: mouse models of mitochondrial disease. J Neuroophthalmol *22*, 279-285.

Boatright, K.M., Renatus, M., Scott, F.L., Sperandio, S., Shin, H., Pedersen, I.M., Ricci, J.E., Edris, W.A., Sutherlin, D.P., Green, D.R.*, et al.* (2003). A unified model for apical caspase activation. Mol Cell *11*, 529-541.

Bramblett, D.E., Pennesi, M.E., Wu, S.M., and Tsai, M.J. (2004). The transcription factor Bhlhb4 is required for rod bipolar cell maturation. Neuron *43*, 779-793.

Brown, N.L., Patel, S., Brzezinski, J., and Glaser, T. (2001). Math5 is required for retinal ganglion cell and optic nerve formation. Development *128*, 2497-2508.

Burmeister, M., Novak, J., Liang, M.Y., Basu, S., Ploder, L., Hawes, N.L., Vidgen, D., Hoover, F., Goldman, D., Kalnins, V.I.*, et al.* (1996). Ocular retardation mouse caused by Chx10 homeobox null allele: impaired retinal progenitor proliferation and bipolar cell differentiation. Nat Genet *12*, 376-384.

Cain, C.C., Saul, D., Attanasio, L., Oehler, E., Hamosh, A., Blakemore, K., and Stetten, G. (2007). Microphthalmia with linear skin defects (MLS) syndrome evaluated by prenatal karyotyping, FISH and array comparative genomic hybridization. Prenat Diagn *27*, 373-379.

Cain, K., Bratton, S.B., and Cohen, G.M. (2002). The Apaf-1 apoptosome: a large caspase-activating complex. Biochimie *84*, 203-214.

Cape, C.J., Zaidman, G.W., Beck, A.D., and Kaufman, A.H. (2004). Phenotypic variation in ophthalmic manifestations of MIDAS syndrome (microphthalmia, dermal aplasia, and sclerocornea). Arch Ophthalmol *122*, 1070-1074.

Carter-Dawson, L.D., and LaVail, M.M. (1979). Rods and cones in the mouse retina. II. Autoradiographic analysis of cell generation using tritiated thymidine. J Comp Neurol *188*, 263-272.

Cepko, C.L., Austin, C.P., Yang, X., Alexiades, M., and Ezzeddine, D. (1996). Cell fate determination in the vertebrate retina. Proc Natl Acad Sci U S A *93*, 589-595.

Chipuk, J.E., and Green, D.R. (2005). Do inducers of apoptosis trigger caspase-independent cell death? Nat Rev Mol Cell Biol *6*, 268-275.

Chow, R.L., and Lang, R.A. (2001). Early eye development in vertebrates. Annu Rev Cell Dev Biol *17*, 255-296.

Conte, I., Carrella, S., Avellino, R., Karali, M., Marco-Ferreres, R., Bovolenta, P., and Banfi, S. (2010a). miR-204 is required for lens and retinal development via Meis2 targeting. Proc Natl Acad Sci U S A *107*, 15491-15496.

Conte, I., Marco-Ferreres, R., Beccari, L., Cisneros, E., Ruiz, J.M., Tabanera, N., and Bovolenta, P. (2010b). Proper differentiation of photoreceptors and amacrine cells depends on a regulatory loop between NeuroD and Six6. Development *137*, 2307-2317.

Costantini, P., Bruey, J.M., Castedo, M., Metivier, D., Loeffler, M., Susin, S.A., Ravagnan, L., Zamzami, N., Garrido, C., and Kroemer, G. (2002). Pre-processed caspase-9 contained in mitochondria participates in apoptosis. Cell Death Differ *9*, 82-88.

Cvekl, A., and Piatigorsky, J. (1996). Lens development and crystallin gene expression: many roles for Pax-6. Bioessays *18*, 621-630.

Debatin, K.M., and Krammer, P.H. (2004). Death receptors in chemotherapy and cancer. Oncogene *23*, 2950-2966.

Del Bene, F., Ettwiller, L., Skowronska-Krawczyk, D., Baier, H., Matter, J.M., Birney, E., and Wittbrodt, J. (2007). In vivo validation of a computationally predicted conserved Ath5 target gene set. PLoS Genet *3*, 1661-1671.

DiMauro, S., and Moraes, C.T. (1993). Mitochondrial encephalomyopathies. Arch Neurol *50*, 1197-1208.

Drenckhahn, J.D., Schwarz, Q.P., Gray, S., Laskowski, A., Kiriazis, H., Ming, Z., Harvey, R.P., Du, X.J., Thorburn, D.R., and Cox, T.C. (2008). Compensatory growth of healthy cardiac cells in the presence of diseased cells restores tissue homeostasis during heart development. Dev Cell *15*, 521-533.

Drygas, M.E., Lambowitz, A.M., and Nargang, F.E. (1989). Cloning and analysis of the Neurospora crassa gene for cytochrome c heme lyase. J Biol Chem *264*, 17897-17906.

Dumont, M.E., Ernst, J.F., Hampsey, D.M., and Sherman, F. (1987). Identification and sequence of the gene encoding cytochrome c heme lyase in the yeast Saccharomyces cerevisiae. EMBO J *6*, 235-241.

Dyer, M.A., Livesey, F.J., Cepko, C.L., and Oliver, G. (2003). Prox1 function controls progenitor cell proliferation and horizontal cell genesis in the mammalian retina. Nat Genet *34*, 53-58.

Eisen, J.S., and Smith, J.C. (2008). Controlling morpholino experiments: don't stop making antisense. Development *135*, 1735-1743.

Esteve, P., Lopez-Rios, J., and Bovolenta, P. (2004). SFRP1 is required for the proper establishment of the eye field in the medaka fish. Mech Dev *121*, 687-701.

Ezzeddine, Z.D., Yang, X., DeChiara, T., Yancopoulos, G., and Cepko, C.L. (1997). Postmitotic cells fated to become rod photoreceptors can be respecified by CNTF treatment of the retina. Development *124*, 1055-1067.

Farrar, G.J., Kenna, P.F., and Humphries, P. (2002). On the genetics of retinitis pigmentosa and on mutation-independent approaches to therapeutic intervention. EMBO J *21*, 857-864.

Ferda Percin, E., Ploder, L.A., Yu, J.J., Arici, K., Horsford, D.J., Rutherford, A., Bapat, B., Cox, D.W., Duncan, A.M., Kalnins, V.I.*, et al.* (2000). Human microphthalmia associated with mutations in the retinal homeobox gene CHX10. Nat Genet *25*, 397-401.

Fitzpatrick, D.R., and van Heyningen, V. (2005). Developmental eye disorders. Curr Opin Genet Dev *15*, 348-353.

Foo, R.S., Mani, K., and Kitsis, R.N. (2005). Death begets failure in the heart. J Clin Invest *115*, 565-571.

Franco, B., and Ballabio, A. (2006). X-inactivation and human disease: X-linked dominant male-lethal disorders. Curr Opin Genet Dev *16*, 254-259.

Fuhrmann, S., Levine, E.M., and Reh, T.A. (2000). Extraocular mesenchyme patterns the optic vesicle during early eye development in the embryonic chick. Development *127*, 4599-4609.

Furukawa, T., Mukherjee, S., Bao, Z.Z., Morrow, E.M., and Cepko, C.L. (2000). rax, Hes1, and notch1 promote the formation of Muller glia by postnatal retinal progenitor cells. Neuron *26*, 383-394.

Galluzzi, L., Blomgren, K., and Kroemer, G. (2009). Mitochondrial membrane permeabilization in neuronal injury. Nat Rev Neurosci *10*, 481-494.

Gearhart, M.D., Corcoran, C.M., Wamstad, J.A., and Bardwell, V.J. (2006). Polycomb group and SCF ubiquitin ligases are found in a novel BCOR complex that is recruited to BCL6 targets. Mol Cell Biol *26*, 6880-6889.

Giacomello, M., Drago, I., Pizzo, P., and Pozzan, T. (2007). Mitochondrial Ca2+ as a key regulator of cell life and death. Cell Death Differ *14*, 1267-1274.

Glaser, T., Jepeal, L., Edwards, J.G., Young, S.R., Favor, J., and Maas, R.L. (1994). PAX6 gene dosage effect in a family with congenital cataracts, aniridia, anophthalmia and central nervous system defects. Nat Genet *7*, 463-471.

Glucksmann, A. (1965). Cell death in normal development. Arch Biol (Liege) *76*, 419-437.

Graw, J. (1996). Genetic aspects of embryonic eye development in vertebrates. Dev Genet *18*, 181-197.

Guillemot, F., and Cepko, C.L. (1992). Retinal fate and ganglion cell differentiation are potentiated by acidic FGF in an in vitro assay of early retinal development. Development *114*, 743-754.

Gyrd-Hansen, M., Farkas, T., Fehrenbacher, N., Bastholm, L., Hoyer-Hansen, M., Elling, F., Wallach, D., Flavell, R., Kroemer, G., Nylandsted, J.*, et al.* (2006). Apoptosome-independent activation of the lysosomal cell death pathway by caspase-9. Mol Cell Biol *26*, 7880-7891.

Hao, Z., Duncan, G.S., Chang, C.C., Elia, A., Fang, M., Wakeham, A., Okada, H., Calzascia, T., Jang, Y., You-Ten, A.*, et al.* (2005). Specific ablation of the

apoptotic functions of cytochrome C reveals a differential requirement for cytochrome C and Apaf-1 in apoptosis. Cell *121*, 579-591.

Happle, R., Daniels, O., and Koopman, R.J. (1993). MIDAS syndrome (microphthalmia, dermal aplasia, and sclerocornea): an X-linked phenotype distinct from Goltz syndrome. Am J Med Genet *47*, 710-713.

Harris, W.A. (1997). Cellular diversification in the vertebrate retina. Curr Opin Genet Dev *7*, 651-658.

Hatakeyama, J., and Kageyama, R. (2004). Retinal cell fate determination and bHLH factors. Semin Cell Dev Biol *15*, 83-89.

Hill, M.M., Adrain, C., Duriez, P.J., Creagh, E.M., and Martin, S.J. (2004). Analysis of the composition, assembly kinetics and activity of native Apaf-1 apoptosomes. EMBO J *23*, 2134-2145.

Ho, A.T., Li, Q.H., Hakem, R., Mak, T.W., and Zacksenhaus, E. (2004). Coupling of caspase-9 to Apaf1 in response to loss of pRb or cytotoxic drugs is cell-type-specific. EMBO J *23*, 460-472.

Ho, A.T., Li, Q.H., Okada, H., Mak, T.W., and Zacksenhaus, E. (2007). XIAP activity dictates Apaf-1 dependency for caspase 9 activation. Mol Cell Biol *27*, 5673-5685.

Holt, C.E., Bertsch, T.W., Ellis, H.M., and Harris, W.A. (1988). Cellular determination in the Xenopus retina is independent of lineage and birth date. Neuron *1*, 15-26.

Hu, M., and Easter, S.S. (1999). Retinal neurogenesis: the formation of the initial central patch of postmitotic cells. Dev Biol *207*, 309-321.

Inoue, T., Hojo, M., Bessho, Y., Tano, Y., Lee, J.E., and Kageyama, R. (2002). Math3 and NeuroD regulate amacrine cell fate specification in the retina. Development *129*, 831-842.

Ishikawa, Y. (2000). Medakafish as a model system for vertebrate developmental genetics. Bioessays *22*, 487-495.

Iwamatsu, T. (2004). Stages of normal development in the medaka Oryzias latipes. Mech Dev *121*, 605-618.

Jiang, X., and Wang, X. (2004). Cytochrome C-mediated apoptosis. Annu Rev Biochem *73*, 87-106.

Johnson, C.R., and Jarvis, W.D. (2004). Caspase-9 regulation: an update. Apoptosis *9*, 423-427.

Kapur, R., Tu, E.Y., Toyran, S., Shah, P., Vangveeravong, S., Lloyd, W.C., 3rd, and Edward, D.P. (2008). Corneal pathology in microphthalmia with linear skin defects syndrome. Cornea *27*, 734-738.

Katoh, I., Sato, S., Fukunishi, N., Yoshida, H., Imai, T., and Kurata, S. (2008). Apaf-1-deficient fog mouse cell apoptosis involves hypo-polarization of the mitochondrial inner membrane, ATP depletion and citrate accumulation. Cell Res *18*, 1210-1219.

Katoh, I., Tomimori, Y., Ikawa, Y., and Kurata, S. (2004). Dimerization and processing of procaspase-9 by redox stress in mitochondria. J Biol Chem *279*, 15515-15523.

Kelley, M.W., Turner, J.K., and Reh, T.A. (1994). Retinoic acid promotes differentiation of photoreceptors in vitro. Development *120*, 2091-2102.

Kim, J.Y., and Park, J.H. (2003). ROS-dependent caspase-9 activation in hypoxic cell death. FEBS Lett *549*, 94-98.

Kobayashi, M., Kiyosawa, M., Toyoura, T., and Tokoro, T. (1998). An XX male with microphthalmos and sclerocornea. J Pediatr Ophthalmol Strabismus *35*, 122-124.

Kondoh, H., Uchikawa, M., and Kamachi, Y. (2004). Interplay of Pax6 and SOX2 in lens development as a paradigm of genetic switch mechanisms for cell differentiation. Int J Dev Biol *48*, 819-827.

Korshunov, S.S., Skulachev, V.P., and Starkov, A.A. (1997). High protonic potential actuates a mechanism of production of reactive oxygen species in mitochondria. FEBS Lett *416*, 15-18.

Krajewski, S., Krajewska, M., Ellerby, L.M., Welsh, K., Xie, Z., Deveraux, Q.L., Salvesen, G.S., Bredesen, D.E., Rosenthal, R.E., Fiskum, G., *et al.* (1999). Release of caspase-9 from mitochondria during neuronal apoptosis and cerebral ischemia. Proc Natl Acad Sci U S A *96*, 5752-5757.

La Vail, M.M., Rapaport, D.H., and Rakic, P. (1991). Cytogenesis in the monkey retina. J Comp Neurol *309*, 86-114.

Lambert, A.J., and Brand, M.D. (2004). Inhibitors of the quinone-binding site allow rapid superoxide production from mitochondrial NADH:ubiquinone oxidoreductase (complex I). J Biol Chem *279*, 39414-39420.

Lassus, P., Opitz-Araya, X., and Lazebnik, Y. (2002). Requirement for caspase-2 in stress-induced apoptosis before mitochondrial permeabilization. Science *297*, 1352-1354.

Li, J., Lee, B., and Lee, A.S. (2006). Endoplasmic reticulum stress-induced apoptosis: multiple pathways and activation of p53-up-regulated modulator of apoptosis (PUMA) and NOXA by p53. J Biol Chem *281*, 7260-7270.

Li, K., Li, Y., Shelton, J.M., Richardson, J.A., Spencer, E., Chen, Z.J., Wang, X., and Williams, R.S. (2000). Cytochrome c deficiency causes embryonic lethality and attenuates stress-induced apoptosis. Cell *101*, 389-399.

Li, L.Y., Luo, X., and Wang, X. (2001). Endonuclease G is an apoptotic DNase when released from mitochondria. Nature *412*, 95-99.

Li, S., Mo, Z., Yang, X., Price, S.M., Shen, M.M., and Xiang, M. (2004). Foxn4 controls the genesis of amacrine and horizontal cells by retinal progenitors. Neuron *43*, 795-807.

Lieschke, G.J., and Currie, P.D. (2007). Animal models of human disease: zebrafish swim into view. Nat Rev Genet *8*, 353-367.

Lillien, L., and Wancio, D. (1998). Changes in Epidermal Growth Factor Receptor Expression and Competence to Generate Glia Regulate Timing and Choice of Differentiation in the Retina. Mol Cell Neurosci *10*, 296-308.

Lindsay, E.A., Grillo, A., Ferrero, G.B., Roth, E.J., Magenis, E., Grompe, M., Hulten, M., Gould, C., Baldini, A., Zoghbi, H.Y., *et al.* (1994). Microphthalmia with

linear skin defects (MLS) syndrome: clinical, cytogenetic, and molecular characterization. Am J Med Genet *49*, 229-234.

Liu, C.Y., Lee, C.F., and Wei, Y.H. (2009). Role of reactive oxygen species-elicited apoptosis in the pathophysiology of mitochondrial and neurodegenerative diseases associated with mitochondrial DNA mutations. J Formos Med Assoc *108*, 599-611.

Liu, X., Kim, C.N., Yang, J., Jemmerson, R., and Wang, X. (1996). Induction of apoptotic program in cell-free extracts: requirement for dATP and cytochrome c. Cell *86*, 147-157.

Livesey, F.J., and Cepko, C.L. (2001). Vertebrate neural cell-fate determination: lessons from the retina. Nat Rev Neurosci *2*, 109-118.

Loosli, F., Koster, R.W., Carl, M., Krone, A., and Wittbrodt, J. (1998). Six3, a medaka homologue of the Drosophila homeobox gene sine oculis is expressed in the anterior embryonic shield and the developing eye. Mech Dev *74*, 159-164.

Marquardt, T., Ashery-Padan, R., Andrejewski, N., Scardigli, R., Guillemot, F., and Gruss, P. (2001). Pax6 is required for the multipotent state of retinal progenitor cells. Cell *105*, 43-55.

Marquardt, T., and Gruss, P. (2002). Generating neuronal diversity in the retina: one for nearly all. Trends Neurosci *25*, 32-38.

Martin, A.G., and Fearnhead, H.O. (2002). Apocytochrome c blocks caspase-9 activation and Bax-induced apoptosis. J Biol Chem *277*, 50834-50841.

Martinez-Morales, J.R., Rodrigo, I., and Bovolenta, P. (2004). Eye development: a view from the retina pigmented epithelium. Bioessays *26*, 766-777.

Mathers, P.H., Grinberg, A., Mahon, K.A., and Jamrich, M. (1997). The Rx homeobox gene is essential for vertebrate eye development. Nature *387*, 603-607.

Mills, K., Daish, T., Harvey, K.F., Pfleger, C.M., Hariharan, I.K., and Kumar, S. (2006). The Drosophila melanogaster Apaf-1 homologue ARK is required for most, but not all, programmed cell death. J Cell Biol *172*, 809-815.

Moraes, C.T., Diaz, F., and Barrientos, A. (2004). Defects in the biosynthesis of mitochondrial heme c and heme a in yeast and mammals. Biochim Biophys Acta *1659*, 153-159.

Morishima, N., Nakanishi, K., Takenouchi, H., Shibata, T., and Yasuhiko, Y. (2002). An endoplasmic reticulum stress-specific caspase cascade in apoptosis. Cytochrome c-independent activation of caspase-9 by caspase-12. J Biol Chem *277*, 34287-34294.

Morishima, N., Nakanishi, K., Tsuchiya, K., Shibata, T., and Seiwa, E. (2004). Translocation of Bim to the endoplasmic reticulum (ER) mediates ER stress signaling for activation of caspase-12 during ER stress-induced apoptosis. J Biol Chem *279*, 50375-50381.

Morleo, M., and Franco, B. (2008). Dosage compensation of the mammalian X chromosome influences the phenotypic variability of X-linked dominant male-lethal disorders. J Med Genet *45*, 401-408.

Morleo, M., Pramparo, T., Perone, L., Gregato, G., Le Caignec, C., Mueller, R.F., Ogata, T., Raas-Rothschild, A., de Blois, M.C., Wilson, L.C.*, et al.* (2005). Microphthalmia with linear skin defects (MLS) syndrome: clinical, cytogenetic, and molecular characterization of 11 cases. Am J Med Genet A *137*, 190-198.

Morrison, D., FitzPatrick, D., Hanson, I., Williamson, K., van Heyningen, V., Fleck, B., Jones, I., Chalmers, J., and Campbell, H. (2002). National study of microphthalmia, anophthalmia, and coloboma (MAC) in Scotland: investigation of genetic aetiology. J Med Genet *39*, 16-22.

Morrow, E.M., Furukawa, T., Lee, J.E., and Cepko, C.L. (1999). NeuroD regulates multiple functions in the developing neural retina in rodent. Development *126*, 23-36.

Ng, D., Thakker, N., Corcoran, C.M., Donnai, D., Perveen, R., Schneider, A., Hadley, D.W., Tifft, C., Zhang, L., Wilkie, A.O.*, et al.* (2004). Oculofaciocardiodental and Lenz microphthalmia syndromes result from distinct classes of mutations in BCOR. Nat Genet *36*, 411-416.

Nguyen, M., and Arnheiter, H. (2000). Signaling and transcriptional regulation in early mammalian eye development: a link between FGF and MITF. Development *127*, 3581-3591.

Ogata, T., Wakui, K., Muroya, K., Ohashi, H., Matsuo, N., Brown, D.M., Ishii, T., and Fukushima, Y. (1998). Microphthalmia with linear skin defects syndrome in a mosaic female infant with monosomy for the Xp22 region: molecular analysis of the Xp22 breakpoint and the X-inactivation pattern. Hum Genet *103*, 51-56.

Oppenheim, R.W. (1991). Cell death during development of the nervous system. Annu Rev Neurosci *14*, 453-501.

Ott, M., Gogvadze, V., Orrenius, S., and Zhivotovsky, B. (2007). Mitochondria, oxidative stress and cell death. Apoptosis *12*, 913-922.

Ow, Y.P., Green, D.R., Hao, Z., and Mak, T.W. (2008). Cytochrome c: functions beyond respiration. Nat Rev Mol Cell Biol *9*, 532-542.

Papadopoulou, L.C., Sue, C.M., Davidson, M.M., Tanji, K., Nishino, I., Sadlock, J.E., Krishna, S., Walker, W., Selby, J., Glerum, D.M.*, et al.* (1999). Fatal infantile cardioencephalomyopathy with COX deficiency and mutations in SCO2, a COX assembly gene. Nat Genet *23*, 333-337.

Pop, C., Timmer, J., Sperandio, S., and Salvesen, G.S. (2006). The apoptosome activates caspase-9 by dimerization. Mol Cell *22*, 269-275.

Prakash, S.K., Cormier, T.A., McCall, A.E., Garcia, J.J., Sierra, R., Haupt, B., Zoghbi, H.Y., and Van Den Veyver, I.B. (2002). Loss of holocytochrome c-type synthetase causes the male lethality of X-linked dominant microphthalmia with linear skin defects (MLS) syndrome. Hum Mol Genet *11*, 3237-3248.

Prakash, S.K., Paylor, R., Jenna, S., Lamarche-Vane, N., Armstrong, D.L., Xu, B., Mancini, M.A., and Zoghbi, H.Y. (2000). Functional analysis of ARHGAP6, a novel GTPase-activating protein for RhoA. Hum Mol Genet *9*, 477-488.

Quaderi, N.A., Schweiger, S., Gaudenz, K., Franco, B., Rugarli, E.I., Berger, W., Feldman, G.J., Volta, M., Andolfi, G., Gilgenkrantz, S.*, et al.* (1997). Opitz G/BBB syndrome, a defect of midline development, is due to mutations in a new RING finger gene on Xp22. Nat Genet *17*, 285-291.

Quinzii, C.M., Lopez, L.C., Gilkerson, R.W., Dorado, B., Coku, J., Naini, A.B., Lagier-Tourenne, C., Schuelke, M., Salviati, L., Carrozzo, R., *et al.* (2010). Reactive oxygen species, oxidative stress, and cell death correlate with level of CoQ10 deficiency. FASEB J *24*, 3733-3743.

Ragge, N.K., Brown, A.G., Poloschek, C.M., Lorenz, B., Henderson, R.A., Clarke, M.P., Russell-Eggitt, I., Fielder, A., Gerrelli, D., Martinez-Barbera, J.P., *et al.* (2005). Heterozygous mutations of OTX2 cause severe ocular malformations. Am J Hum Genet *76*, 1008-1022.

Ragge, N.K., Subak-Sharpe, I.D., and Collin, J.R. (2007). A practical guide to the management of anophthalmia and microphthalmia. Eye (Lond) *21*, 1290-1300.

Ramskold, D., Wang, E.T., Burge, C.B., and Sandberg, R. (2009). An abundance of ubiquitously expressed genes revealed by tissue transcriptome sequence data. PLoS Comput Biol *5*, e1000598.

Renatus, M., Stennicke, H.R., Scott, F.L., Liddington, R.C., and Salvesen, G.S. (2001). Dimer formation drives the activation of the cell death protease caspase 9. Proc Natl Acad Sci U S A *98*, 14250-14255.

Robu, M.E., Larson, J.D., Nasevicius, A., Beiraghi, S., Brenner, C., Farber, S.A., and Ekker, S.C. (2007). p53 activation by knockdown technologies. PLoS Genet *3*, e78.

Ruiz, J.M., Rodriguez, J., and Bovolenta, P. (2009). Growth and differentiation of the retina and the optic tectum in the medaka fish requires olSfrp5. Dev Neurobiol *69*, 617-632.

Sadhukhan, R., Leone, J.W., Lull, J., Wang, Z., Kletzien, R.F., Heinrikson, R.L., and Tomasselli, A.G. (2006). An efficient method to express and refold a truncated human procaspase-9: a caspase with activity toward Glu-X bonds. Protein Expr Purif *46*, 299-308.

Saka, Y., and Smith, J.C. (2001). Spatial and temporal patterns of cell division during early Xenopus embryogenesis. Dev Biol *229*, 307-318.

Sakane, A., Manabe, S., Ishizaki, H., Tanaka-Okamoto, M., Kiyokage, E., Toida, K., Yoshida, T., Miyoshi, J., Kamiya, H., Takai, Y., *et al.* (2006). Rab3 GTPase-

activating protein regulates synaptic transmission and plasticity through the inactivation of Rab3. Proc Natl Acad Sci U S A *103*, 10029-10034.

Samali, A., Cai, J., Zhivotovsky, B., Jones, D.P., and Orrenius, S. (1999). Presence of a pre-apoptotic complex of pro-caspase-3, Hsp60 and Hsp10 in the mitochondrial fraction of jurkat cells. EMBO J *18*, 2040-2048.

Sanyanusin, P., Schimmenti, L.A., McNoe, L.A., Ward, T.A., Pierpont, M.E., Sullivan, M.J., Dobyns, W.B., and Eccles, M.R. (1995). Mutation of the PAX2 gene in a family with optic nerve colobomas, renal anomalies and vesicoureteral reflux. Nat Genet *9*, 358-364.

Satow, T., Bae, S.K., Inoue, T., Inoue, C., Miyoshi, G., Tomita, K., Bessho, Y., Hashimoto, N., and Kageyama, R. (2001). The basic helix-loop-helix gene hesr2 promotes gliogenesis in mouse retina. J Neurosci *21*, 1265-1273.

Schaefer, L., Ballabio, A., and Zoghbi, H.Y. (1996). Cloning and characterization of a putative human holocytochrome c-type synthetase gene (HCCS) isolated from the critical region for microphthalmia with linear skin defects (MLS). Genomics *34*, 166-172.

Schaefer, L., Prakash, S., and Zoghbi, H.Y. (1997). Cloning and characterization of a novel rho-type GTPase-activating protein gene (ARHGAP6) from the critical region for microphthalmia with linear skin defects. Genomics *46*, 268-277.

Schafer, Z.T., and Kornbluth, S. (2006). The apoptosome: physiological, developmental, and pathological modes of regulation. Dev Cell *10*, 549-561.

Schluth, C., Cossee, M., Girard-Lemaire, F., Carelle, N., Dollfus, H., Jeandidier, E., and Flori, E. (2007). Phenotype in X chromosome rearrangements: pitfalls of X inactivation study. Pathol Biol (Paris) *55*, 29-36.

Schwarz, Q.P., and Cox, T.C. (2002). Complementation of a yeast CYC3 deficiency identifies an X-linked mammalian activator of apocytochrome c. Genomics *79*, 51-57.

Scorrano, L., Ashiya, M., Buttle, K., Weiler, S., Oakes, S.A., Mannella, C.A., and Korsmeyer, S.J. (2002). A distinct pathway remodels mitochondrial cristae and mobilizes cytochrome c during apoptosis. Dev Cell *2*, 55-67.

Sharma, V.M., Ruiz de Luzuriaga, A.M., Waggoner, D., Greenwald, M., and Stein, S.L. (2008). Microphthalmia with linear skin defects: a case report and review. Pediatr Dermatol *25*, 548-552.

Shaw, G.M., Carmichael, S.L., Yang, W., Harris, J.A., Finnell, R.H., and Lammer, E.J. (2005). Epidemiologic characteristics of anophthalmia and bilateral microphthalmia among 2.5 million births in California, 1989-1997. Am J Med Genet A *137*, 36-40.

Sisodiya, S.M., Ragge, N.K., Cavalleri, G.L., Hever, A., Lorenz, B., Schneider, A., Williamson, K.A., Stevens, J.M., Free, S.L., Thompson, P.J.*, et al.* (2006). Role of SOX2 mutations in human hippocampal malformations and epilepsy. Epilepsia *47*, 534-542.

Skulachev, V.P. (1997). Membrane-linked systems preventing superoxide formation. Biosci Rep *17*, 347-366.

Srinivasula, S.M., Ahmad, M., Fernandes-Alnemri, T., and Alnemri, E.S. (1998). Autoactivation of procaspase-9 by Apaf-1-mediated oligomerization. Mol Cell *1*, 949-957.

St-Pierre, J., Buckingham, J.A., Roebuck, S.J., and Brand, M.D. (2002). Topology of superoxide production from different sites in the mitochondrial electron transport chain. J Biol Chem *277*, 44784-44790.

Stiemke, M.M., and Hollyfield, J.G. (1995). Cell birthdays in Xenopus laevis retina. Differentiation *58*, 189-193.

Susin, S.A., Lorenzo, H.K., Zamzami, N., Marzo, I., Brenner, C., Larochette, N., Prevost, M.C., Alzari, P.M., and Kroemer, G. (1999a). Mitochondrial release of caspase-2 and -9 during the apoptotic process. J Exp Med *189*, 381-394.

Susin, S.A., Lorenzo, H.K., Zamzami, N., Marzo, I., Snow, B.E., Brothers, G.M., Mangion, J., Jacotot, E., Costantini, P., Loeffler, M.*, et al.* (1999b). Molecular characterization of mitochondrial apoptosis-inducing factor. Nature *397*, 441-446.

Tait, S.W., and Green, D.R. (2010). Mitochondria and cell death: outer membrane permeabilization and beyond. Nat Rev Mol Cell Biol *11*, 621-632.

Taranova, O.V., Magness, S.T., Fagan, B.M., Wu, Y., Surzenko, N., Hutton, S.R., and Pevny, L.H. (2006). SOX2 is a dose-dependent regulator of retinal neural progenitor competence. Genes Dev *20*, 1187-1202.

Temple, I.K., Hurst, J.A., Hing, S., Butler, L., and Baraitser, M. (1990). De novo deletion of Xp22.2-pter in a female with linear skin lesions of the face and neck, microphthalmia, and anterior chamber eye anomalies. J Med Genet *27*, 56-58.

Tomita, K., Moriyoshi, K., Nakanishi, S., Guillemot, F., and Kageyama, R. (2000). Mammalian achaete-scute and atonal homologs regulate neuronal versus glial fate determination in the central nervous system. EMBO J *19*, 5460-5472.

Torres, M., Gomez-Pardo, E., and Gruss, P. (1996). Pax2 contributes to inner ear patterning and optic nerve trajectory. Development *122*, 3381-3391.

Turner, D.L., and Cepko, C.L. (1987). A common progenitor for neurons and glia persists in rat retina late in development. Nature *328*, 131-136.

Turner, D.L., Snyder, E.Y., and Cepko, C.L. (1990). Lineage-independent determination of cell type in the embryonic mouse retina. Neuron *4*, 833-845.

Twiddy, D., Brown, D.G., Adrain, C., Jukes, R., Martin, S.J., Cohen, G.M., MacFarlane, M., and Cain, K. (2004). Pro-apoptotic proteins released from the mitochondria regulate the protein composition and caspase-processing activity of the native Apaf-1/caspase-9 apoptosome complex. J Biol Chem *279*, 19665-19682.

Valenciano, A.I., Boya, P., and de la Rosa, E.J. (2009). Early neural cell death: numbers and cues from the developing neuroretina. Int J Dev Biol *53*, 1515-1528.

Van den Veyver, I.B. (2001). Skewed X inactivation in X-linked disorders. Semin Reprod Med *19*, 183-191.

Van den Veyver, I.B. (2002). Microphthalmia with linear skin defects (MLS), Aicardi, and Goltz syndromes: are they related X-linked dominant male-lethal disorders? Cytogenet Genome Res *99*, 289-296.

Van den Veyver, I.B., Subramanian, S., and Zoghbi, H.Y. (1998). Genomic structure of a human holocytochrome c-type synthetase gene in Xp22.3 and mutation analysis in patients with Rett syndrome. Am J Med Genet *78*, 179-181.

Vecino, E., Hernandez, M., and Garcia, M. (2004). Cell death in the developing vertebrate retina. Int J Dev Biol *48*, 965-974.

Verma, A.S., and Fitzpatrick, D.R. (2007). Anophthalmia and microphthalmia. Orphanet J Rare Dis *2*, 47.

Voronina, V.A., Kozhemyakina, E.A., O'Kernick, C.M., Kahn, N.D., Wenger, S.L., Linberg, J.V., Schneider, A.S., and Mathers, P.H. (2004). Mutations in the human RAX homeobox gene in a patient with anophthalmia and sclerocornea. Hum Mol Genet *13*, 315-322.

Walker, J.C., and Harland, R.M. (2009). microRNA-24a is required to repress apoptosis in the developing neural retina. Genes Dev *23*, 1046-1051.

Wallace, D.C. (2005). A mitochondrial paradigm of metabolic and degenerative diseases, aging, and cancer: a dawn for evolutionary medicine. Annu Rev Genet *39*, 359-407.

Wallace, D.C., and Fan, W. (2009). The pathophysiology of mitochondrial disease as modeled in the mouse. Genes Dev *23*, 1714-1736.

Wallis, D.E., Roessler, E., Hehr, U., Nanni, L., Wiltshire, T., Richieri-Costa, A., Gillessen-Kaesbach, G., Zackai, E.H., Rommens, J., and Muenke, M. (1999). Mutations in the homeodomain of the human SIX3 gene cause holoprosencephaly. Nat Genet *22*, 196-198.

Wang, J., Wilhelmsson, H., Graff, C., Li, H., Oldfors, A., Rustin, P., Bruning, J.C., Kahn, C.R., Clayton, D.A., Barsh, G.S.*, et al.* (1999). Dilated cardiomyopathy and atrioventricular conduction blocks induced by heart-specific inactivation of mitochondrial DNA gene expression. Nat Genet *21*, 133-137.

Wapenaar, M.C., Bassi, M.T., Schaefer, L., Grillo, A., Ferrero, G.B., Chinault, A.C., Ballabio, A., and Zoghbi, H.Y. (1993). The genes for X-linked ocular albinism (OA1) and microphthalmia with linear skin defects (MLS): cloning and characterization of the critical regions. Hum Mol Genet *2*, 947-952.

Wapenaar, M.C., Schiaffino, M.V., Bassi, M.T., Schaefer, L., Chinault, A.C., Zoghbi, H.Y., and Ballabio, A. (1994). A YAC-based binning strategy facilitating

the rapid assembly of cosmid contigs: 1.6 Mb of overlapping cosmids in Xp22. Hum Mol Genet *3*, 1155-1161.

Wimplinger, I., Morleo, M., Rosenberger, G., Iaconis, D., Orth, U., Meinecke, P., Lerer, I., Ballabio, A., Gal, A., Franco, B.*, et al.* (2006). Mutations of the mitochondrial holocytochrome c-type synthase in X-linked dominant microphthalmia with linear skin defects syndrome. Am J Hum Genet *79*, 878-889.

Wimplinger, I., Shaw, G.M., and Kutsche, K. (2007). HCCS loss-of-function missense mutation in a female with bilateral microphthalmia and sclerocornea: a novel gene for severe ocular malformations? Mol Vis *13*, 1475-1482.

Wistow, G.J., and Piatigorsky, J. (1988). Lens crystallins: the evolution and expression of proteins for a highly specialized tissue. Annu Rev Biochem *57*, 479-504.

Wittbrodt, J., Shima, A., and Schartl, M. (2002). Medaka--a model organism from the far East. Nat Rev Genet *3*, 53-64.

Wride, M.A. (1996). Cellular and molecular features of lens differentiation: a review of recent advances. Differentiation *61*, 77-93.

Young, R.W. (1985). Cell differentiation in the retina of the mouse. Anat Rec *212*, 199-205.

Yu-Wai-Man, P., Griffiths, P.G., Hudson, G., and Chinnery, P.F. (2009). Inherited mitochondrial optic neuropathies. J Med Genet *46*, 145-158.

Zamzami, N., Susin, S.A., Marchetti, P., Hirsch, T., Gomez-Monterrey, I., Castedo, M., and Kroemer, G. (1996). Mitochondrial control of nuclear apoptosis. J Exp Med *183*, 1533-1544.

Zhang, X.M., and Yang, X.J. (2001). Regulation of retinal ganglion cell production by Sonic hedgehog. Development *128*, 943-957.

Zhu, Z., Yao, J., Johns, T., Fu, K., De Bie, I., Macmillan, C., Cuthbert, A.P., Newbold, R.F., Wang, J., Chevrette, M.*, et al.* (1998). SURF1, encoding a factor involved in the biogenesis of cytochrome c oxidase, is mutated in Leigh syndrome. Nat Genet *20*, 337-343.

Zollner, A., Rodel, G., and Haid, A. (1992). Molecular cloning and characterization of the Saccharomyces cerevisiae CYT2 gene encoding cytochrome-c1-heme lyase. Eur J Biochem *207*, 1093-1100.

Zou, H., Li, Y., Liu, X., and Wang, X. (1999). An APAF-1.cytochrome c multimeric complex is a functional apoptosome that activates procaspase-9. J Biol Chem *274*, 11549-11556.

Zvulunov, A., Kachko, L., Manor, E., Shinwell, E., and Carmi, R. (1998). Reticulolinear aplasia cutis congenita of the face and neck: a distinctive cutaneous manifestation in several syndromes linked to Xp22. Br J Dermatol *138*, 1046-1052.